Université de Montréal

The Independence of CXCR4's Pathways, Gαi and β-Arrestin2, and Their Modulation by AMD3100 and TC14012

par
Nassr Nama

Département de Microbiologie, Infectiologie et Immunologie
Faculté de Médecine

Mémoire présenté à la Faculté de Médecine
en vue de l'obtention du grade de maîtrise
en microbiologie et immunologie

Septembre, 2014

RÉSUMÉ

CXCR4 est un récepteur de chimiokines impliqué dans les métastases et la mobilisation des cellules souches hématopoïétiques. Il signale par deux voies: Gαi et β-arrestin2. La β-arrestine2 termine la signalisation des protéines G et cible le récepteur vers l'endocytose.

Un des objectifs du projet était d'étudier l'effet de certaines mutations de CXCR4 sur la signalisation et la localisation du récepteur. À l'aide de la technique BRET, nous avons confirmé que le mutant N119S est constitutivement actif sur la voie de signalisation Gαi. De plus, nous avons constaté que le mutant R134A était dépourvu de signalisation par les protéines G, mais qu'il recrutait constitutivement la β-arrestine2.

Nous souhaitions également étudier la dépendance du recrutement de la β-arrestine2 sur l'activité de Gαi. En utilisant la toxine de la coqueluche, un inhibiteur de la voie Gαi, le recrutement constitutif de la β-arrestine2 à R134A et N119S était maintenu. Ces résultats démontrent que, pour le récepteur CXCR4, le recrutement de la β-arrestine2 est indépendant de l'activation de Gαi.

Finalement, nous avons investigué la capacité de recrutement de la β-arrestine2 induite par deux ligands synthétiques de CXCR4, soit AMD3100 et TC14012. À noter, AMD3100 est un médicament déjà approuvé pour la transplantation des cellules souches. Par contre, il démontre des effets secondaires considérables. D'un côté, nous avons constaté qu'AMD3100 était un antagoniste sur les deux voies de signalisation, soit Gαi et β-arrestine2. De l'autre côté, TC14012 a démontré l'effet d'agoniste inverse sur la voie Gαi, mais d'antagoniste sur la voie β-arrestine2. À la lumière de ces résultats, TC14012 pourrait être plus approprié dans des cas cliniques puisqu'il réduirait toute activité basale de Gαi sans affecter le recrutement de la β-arrestine2. Enfin, ces résultats suggèrent que le ligand TC14012 pourrait être utilisé dans des essais cliniques visant la mobilisation des cellules souches.

Mots-clés: CXCR4, RCPG, AMD3100, Plerixafor, TC14012, CAM, CIM, motif DRY, N3.35

SUMMARY

CXCR4, a chemokine receptor involved in metastasis and homing of hematopoietic stem cells, signals through two major pathways: Gαi and β-arrestin2. β-arrestin2 terminates G-protein signaling and targets the receptor to endocytosis.

This project proposed to study the effect of a previously described set of CXCR4 mutants on both these signaling pathways, as well as their localization. These mutants were assayed by different Bioluminescence Resonance Energy Transfer (BRET) systems. Using these systems, we confirmed that N119S is a constitutively active mutant (CAM), spontaneously activating Gαi. As well, we found that R134A is a constitutively inactive mutant (CIM), devoided of G-protein signaling, but spontaneously recruiting β-arrestin2.

In addition, we studied the dependency of β-arrestin2 recruitment on the Gαi activity. By targeting R134A and N119S with pertussis toxin, an inhibitor of the Gαi activation, we showed efficient blocking of the Gαi pathway, while maintaining the constitutive recruitment of β-arrestin2. This demonstrated that for CXCR4, β-arrestin2 recruitment is independent of the Gαi pathway.

Finally, two synthetic ligands of CXCR4, AMD3100 and TC14012 were tested for their ability to recruit β-arrestin2. AMD3100 is a clinically approved drug used for stem cell transplantation, with considerable side effects. We found it to be an antagonist on both Gαi and β-arrestin2 recruitment. On the other hand, TC14012 was found to be an inverse agonist on Gαi and an antagonist on β-arrestin2 recruitment. Based on this finding, it would be preferable to use of TC14012 as it will further reduce any basal Gαi activity, without affecting β-arrestin2 recruitment. These results support the development of TC14012 for stem cell mobilization trials.

Keywords: CXCR4, GPCR, AMD3100, Plerixafor, TC14012, CAM, CIM, DRY motif, N3.35

ABBREVIATIONS

A	Alanine
AC	Adenylate Cyclase
ALL	Acute Lymphoblastic Leukemia
AML	Acute Myeloid Leukemia
AngII	Angiotensin II
ANOVA	Analysis Of Variance
$AT_{1A}R$	Angiotensin II type 1A Receptor
B.N.U	BRET Net Unit
B.U	BRET Unit
BRET	Bioluminescence Resonance Energy Transfer
C-terminal	Carboxy-Terminal
Ca^{2+}	Calcium ions
CAM	Constitutively Active Mutant
cAMP	Cyclic Adenosine Monophosphate
CCV	Clathrin-Coated Vesicles
CI	Confidence Interval
CIM	Constitutively Inactive Mutant
D	Aspartic acid
DNA	Deoxyribonucleic Acid
EC50	Half maximal effective concentration
Epac	Exchange protein directly activated by cAMP
ERK	Extracellular Signal Regulated Kinases
FDA	Food and Drug Administration
FRAP	Fluorescence Recovery After Photobleaching
G-CSF	Granulocyte-Colony Stimulating Factor
GAP	GTPase Activating Protein
GDP	Guanosine Diphosphate
GEF	Guanine Exchange Factor
GFP^{10}	Green Fluorescent Protein 10
GPCR	G-Protein Coupled Receptor
GRK	GPCR Kinase
GTP	Guanosine Triphosphate

GTPγS	Guanosine 5'-O-[Gamma-Thio] Triphosphate
HEK	Human Embryonic Kidney cells
HSC	Hematopoietic Stem Cell
K	Lysine
M1 AChR	Muscarinic acetylcholine receptor M1
MAPK	Mitogen-Activated Protein Kinase
mRFP	Monomeric Red Fluorescent Protein
MVB	Multivesicular Bodies
N	Asparagine
N-terminal	Amino-Terminal
PKC	Protein Kinase C
PLC	Phospholipase C
PTHR	Parathyroid Hormone Receptor
PTX	Pertussis Toxin
R	Arginine
RGS	Regulator of G-Protein Signaling
Rluc3	*Renilla* Luciferase 3
S	Serine
SDF-1α	CXCL12, Stromal Cell Derived Factor-1α
SEM	Standard Error of the Mean
TM	Transmembrane Helix
$V_{1a}R$	Vasopressin 1a receptor
V2R	Vasopressin Type II Receptor
VSMC	Vascular Smooth Muscle Cell
wt	Wildtype
Y	Tyrosine
YFP	Yellow Fluorescent Protein
α_{1B}-AR	α1B-Adrenoceptor
α_{2A}-AR	α2A-Adrenoceptor
β2-AR	β_2-Adrenoceptor

TABLE OF CONTENTS

LIST OF TABLES

LIST OF FIGURES

ACKNOWLEDGMENTS

I would like to thank Dr. Nikolaus Heveker for his constant enthusiasm to teaching, his motivational encouragement and his amazing support throughout the whole project.

As well, I want to thank all of the lab members; Nicolas Montpas and Stéphanie Gravel for their outstanding teaching and supervision, François Guité-Vinet for being a constant source of motivation, Guillaume Sylvain-Drolet for developing CXCR4 mutants, as well as Genevieve St-Onge, Marilou Lefrançois and Julien Bonneterre.

Also, I would like to express my appreciation to Dr. Gilles Hickson and his laboratory. They have offered me the possibility to work with them and learn from their microscopy expertise.

Thank you to Tyler James, Thinh Nguyen and Richard Hae for proofreading this thesis.

Finally, a special thanks to the Mach-Gaensslen Foundation of Canada and the Canadian Institutes for Health Research for funding this study.

1. INTRODUCTION

1.1. G-protein Coupled Receptors (GPCRs)

The seven-transmembrane domain receptors, more commonly known as G-protein coupled receptors (GPCRs), are the largest family of integral membrane proteins on the cell surface (1), and are found only in eukaryotic cells (2). This family of receptors modulates several important physiological responses, such as cardiovascular and renal functions, as well as neurotransmission. With their central implication in the functioning of several systems, there is no surprise in the significance of their deregulation (3). The importance of these receptors is demonstrated by the fact that 30–40% of prescribed drugs target this family (4). The ligands of these receptors are diverse ranging from amino acids, proteins, hormones, peptides, nucleotides to odorant molecules and even some ions (1).

The name of these receptors comes from their structure, consisting of seven transmembrane alpha helices (TMs). These hydrophobic structures are separated by three intracellular loops and three extracellular ones (Fig. 1) (5). The extracellular surface is composed of the N-terminal tail with the extracellular loops, which forms the binding surface of the receptors' ligands. On the other hand, the three intracellular loops and the C-terminus form the site of interaction with the proteins that regulate the activity of the receptors, such as the G-proteins.

Classes: The GPCRs are stratified according to the GRAFS classification system (6). This acronym stands for the five families of receptors: Glutamate, Rhodopsin, Adhesion, Frizzles/taste2, and Secretin.

The chief interest of this project is a chemokine receptor, CXCR4, belonging to the rhodopsin-like family. This family will, therefore, be discussed in more detail. It is the largest family of receptors containing almost 700 members. Most of these show a conserved E/DRY motif in the second intracellular loop, next to third transmembrane helix (TM III) (Fig. 1). Among the members of this family, we distinguish the adrenergic, the chemokine, and the opioid receptors (6).

1.2. Signaling

The GPCRs exert their signaling mainly by coupling with the heterotrimeric G protein family (7). However, it is clear now that the GPCRs can signal through mechanisms independent of the G proteins, mainly through beta-arrestins (β-arrestins).

G-proteins: The heterotrimeric G proteins are the main intracellular effectors associated with GPCRs. They belong to the family of proteins called GTPases and are composed of three distinct proteins called alpha, beta, and gamma (α, β, and γ) (1). In its inactive form, the Gα subunit is bound to a guanosine diphosphate (GDP), thus enabling the Gα subunit to bind noncovalently to the Gβγ complex.

The binding of a GPCR ligand induces conformational changes within this receptor, leading to the activation of the heterotrimeric G proteins. The activated receptor plays the role of a guanine exchange factor (GEF), which means that it induces the exchange of the GDP attached to the α subunit with a guanosine triphosphate (GTP) (1,8). The activated G-proteins lead to the subsequent activation of the downstream effectors. The Gα subunit has an intrinsic GTPase activity, leading to the eventual hydrolysis of GTP to GDP and the termination of the signaling process. This GTPase activity could be accelerated by a GTPase-accelerating protein (GAP), such as the regulators of G-protein signaling (RGS) (1,1,8,9).

Sixteen Gα genes have been identified so far, and alternative splicing can generate twenty Gα proteins. On the basis of their sequence, they can be grouped into four families: Gαs, Gαi/o, Gαq, and Gα12/13 (Fig. 2) (1). The Gαs family regroups the different Gα subunits that stimulate adenylate cyclase (AC), while the Gαi/o family contains the Gα subunits capable of inhibiting this enzyme, Gαi and Gαo. The Gαq family includes those that activate phospholipase C (PLC), such as Gαq and Gα11. Finally, the Gα12/13 family regulates the cytoskeletal assembly through its two effectors Gα12 and Gα13 (10).

Previously the general assumption was that each GPCR is coupled to one type of Gα subunit. However, it is now widely accepted that it could be coupled with different ones, depending on the tissue expression and the cellular localization (11).

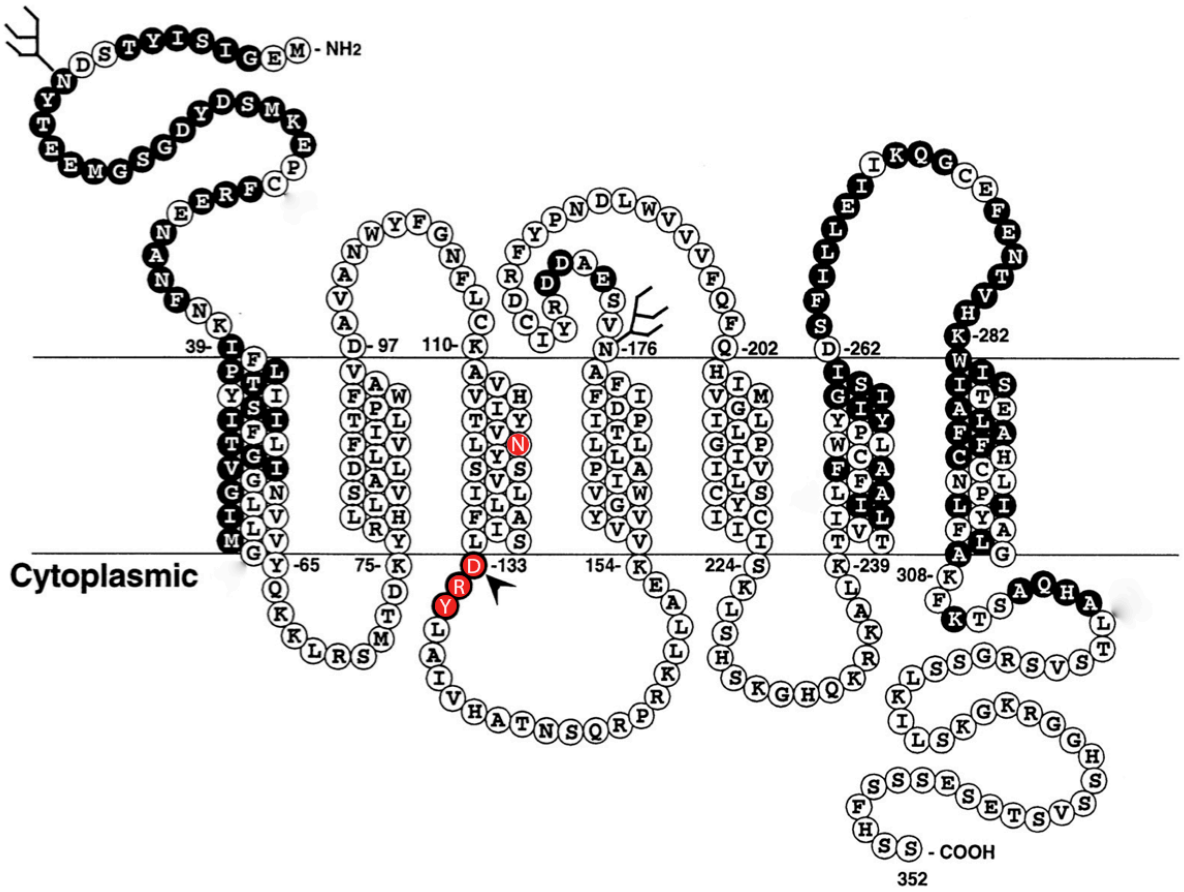

Figure 1. Schema of CXCR4 amino acids. CXCR4 receptor portrayed as a chain of amino acids. Seven transmembrane helices, three intracellular loops, three extracellular loops, an N-terminal and a C-terminal compose the receptor. The DRY motif and the conserved Asparagine N119 are highlighted in red. The residues highlighted in black are important for ligand binding and signaling. Modified from Doranz 1999 (8).

G protein-coupled receptor kinases (GRKs): Following stimulation, the GPCRs are phosphorylated by GPCR kinases (12). The GRKs 1-7 phosphorylate residues on the C-terminal of the GPCRs or the third intracellular loop. This phosphorylation is one of the mechanisms used to terminate G-protein signaling. However, its role is more complex as it induces a second wave of signaling independently of the G-proteins (13). The roles of these different GRKs are not purely redundant. Different GRKs exhibit different functions, by phosphorylating different residues of the GPCR. For instance, GRK5/6 activates β-arrestin

signaling, associated with vasopressin type II receptor (V2R) and β_2-adrenoceptors (β2-AR) (14-16). On the other hand, phosphorylation by GRK2/3 negatively regulates this signaling pathway.

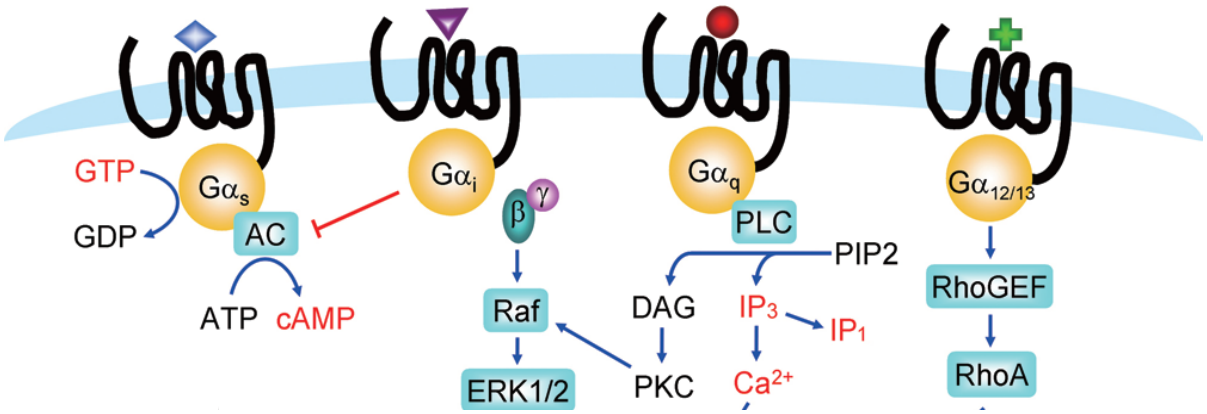

Figure 2. The four families of Gα-proteins. The Gαs, and the Gαi stimulates or inhibits the Adenylate Cyclase (AC) respectively, thus affecting the levels of cAMP. Gαq activates Phospholipase C (PLC), leading to the activation of Protein Kinase C (PKC), and Ca^{2+} release. Gα12/13 activates RhoGEF, leading to the activation of RhoA. Finally, the activated complex Gβγ activates Raf, and the ERK1/2 pathway. Modified from Zhang 2012 (17).

β-arrestin: β-arrestin proteins (1 and 2) bind to the phosphorylated receptors and shut off signal transduction in a process called desensitization. They then target the desensitized receptor to clathrin-coated pits and endocytosis. Recruitment of β-arrestin to the activated receptor allows assembly of the endocytic machinery and targeting of the receptor to the clathrin-coated vesicles (CCVs) (18). At the same time, β-arrestin functions as a scaffolding protein by recruiting several interacting proteins such as E3 ubiquitin ligases or Mitogen-Activated Protein Kinases (MAPKs) (19,20).

The two isoforms of the β-arrestin share a common sequence of 78% (21). Even if the functions of the two β-arrestins are often interchangeable, the presence of at least one of them is crucial, as knocking out both is lethal in animal models (22). Nevertheless, they are not always functionally redundant. For example, the internalization of the β2-Adrenoreceptor (β-2AR) is dependent on β-arrestin2, while that of proteinase-activated receptor 1 (PAR1)

depends on β-arrestin1. The preferential association of a GPCR to one of the two β-arrestins depends on a GPCR classification that is discussed later, in the '1.3. Trafficking' section. According to this classification system, Class A receptors show a preference for β-arrestin2 over β-arrestin1, while class B receptors have equivalent affinities for both (18).

The recruitment modalities of β-arrestin include the affinity between the two proteins, the distance between the two, the conformation of the interaction, as well as kinetics along with the dynamics of the binding. Recruitment of β-arrestin can occur in various conformations (23). β-arrestin acts as a scaffolding protein and recruits different proteins depending on its conformation. While some conformations may be more compatible with the recruitment of the endocytic machinery, others may be more efficient to activate the MAPKs. This shows that even the recruitment of β-arrestin can be regulated, leading to the activation of various signaling pathways. The recruitment of β-arrestins is dependent on two factors, the change in the receptor conformation induced by the agonist and the phosphorylation of specific sites in the receptor's C-terminus (24). The differential modalities observed here might be due to either of these two factors. The phosphorylation of the C-terminus generates a barcode that is different, depending on the phosphorylation sites. This differential phosphorylation leads to recruitment of β-arrestins in various conformations, thus affecting its biological functions (24).

Mitogen-activated protein kinase (MAPK): Several pathways are recruited by β-arrestins and MAPK is the best understood one. The MAPK family includes several members, such as the extracellular-signal-regulated kinases (ERK) 1 and 2. These pathways have an impact on target gene transcription, cell-cycle progression, and apoptosis (22,25). The ERK1/2 pathway consists of MAPK kinase kinases (Raf), MAPK kinases (MEK1/2), and finally the MAPKs (ERK1/2). As a scaffolding protein, β-arrestin ensures an efficient arrangement of the complex of these three proteins (18). Thus, activation of the GPCR by its ligand leads to the recruitment of β-arrestin, and also the following activation of the preformed complex Raf-MEK-ERK on this protein (25,26). This activation requires that β-arrestin is in a conformation capable of recruiting these proteins, and their subsequent activation. As β-arrestin can be recruited in various conformations, not all are compatible with the activation of the MAPK.

1.3. Trafficking

Endocytosis of the GPCRs is a complex process. It starts mainly with the phosphorylation by GRKs, the recruitment of β-arrestins and is followed by clathrin-mediated endocytosis. Although this process was first regarded as a means to desensitize the stimulated receptor, it is now clear that it involves G-independent signaling pathways.

As mentioned earlier, the phosphorylation of the GPCR by a GRK and the recruitment of β-arrestin to the activated receptor allow the assembly of the endocytic machinery and the internalization of the complex in the clathrin-coated vesicles (CCVs) (19). These vesicles proceed to form endosomes containing the activated receptor bound to β-arrestin. Once in these endosomes, the GPCRs can either recycle to the plasma membrane or be directed for degradation in the lysosomes (27). Depending on the stability of the interaction of GPCR-β-arrestin, two patterns of trafficking can be observed, and the GPCRs can be organized in two classes (A or B) (Fig. 3) (18,22).

First, the Class A receptors show a high affinity for β-arrestin2 compared to β-arrestin1 (28). They interact transiently with β-arrestin2 and form complexes that dissociate quickly after being internalized (29). This rapid dissociation of β-arrestin permits the receptor to recycle to the cell membrane. This is the case for the β2-AR, which upon stimulation with its endogenous ligand is rapidly desensitized, dephosphorylated, and recycled to the cellular surface (18,30).

In contrast, the class B receptors have a stronger interaction with β-arrestin, leading to a slower desensitization process (18). The receptors and their β-arrestins form a strong complex that can even be observed on the endosomes. This higher affinity slows down receptor recycling and directs the majority of the receptors toward degradation.

Ubiquitination: The trafficking and sorting of the GPCRs after endocytosis is closely dependent on their ubiquitination (31). β-arrestin2 plays an important role in this ubiquitination, as it is likely to function as an adaptor for E3 ligase, the third enzyme of the ubiquitination process (32,33). This ubiquitination will determine the receptor's final fate,

degradation or membrane recycling. Monoubiquitination of a receptor is associated with its internalization (34), while its polyubiquitination acts as a lysosomal sorting signal (35,36). The CXCR4 receptor follows this pattern of ubiquitination. Lysine residues on the C-terminal of the receptor are ubiquitinated and the receptor is directed to degradation (37).

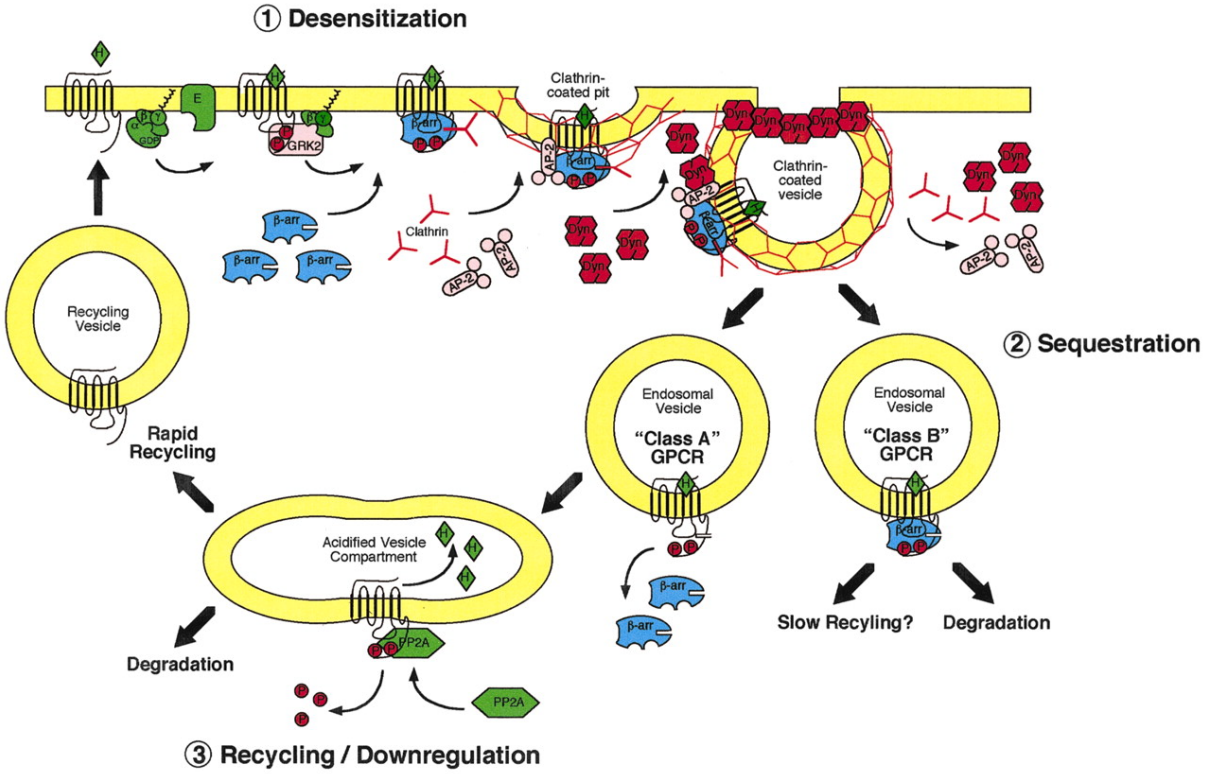

Figure 3. Trafficking of GPCRs. After activation of the GPCR, the GPCR kinase (GRK) phosphorylates the C-terminal of the receptor, leading to the recruitment of β-arrestin, and the endocytic machinery. After endocytosis, receptors follow one of two patterns, class A receptors lose the β-arrestin and are either rapidly recycled or degraded, while class B receptors are mainly directed to degradation. Modified from Luttrell 2002 (38).

1.4. Chemokines

Chemokines are a family of cytokines displaying a chemotactic activity and orienting the cells throughout the organism. They are small basic proteins consisting of 70 to 130 amino acids, varying between 8kDa and 12kDa in size (39,40). Chemokines exhibit their main functions by signaling through GPCRs. Initially, chemokines had been associated with inflammatory responses, given their role in leukocyte migration (41). Furthermore, some are equally involved in cellular survival and growth (42). On the basis of their function, chemokines can be divided into two groups: constitutive chemokines and inflammatory ones. The former group comprises chemokines constitutively expressed and involved in the development and homing of stem cells. The latter group contains proinflammatory cytokines, whose expression is induced during an inflammatory response (41).

The diversity of the functional roles of chemokines makes their receptors attractive therapeutic targets (41). The Food and Drug Administration (FDA) has approved two such therapeutics drugs, Maraviroc, and Mozobil, targeting CCR5 and CXCR4, respectively (25). The major problems facing the development of new therapeutic molecules are the promiscuity and the redundancy of chemokines (40,41). Promiscuity is due to the binding of one chemokine to more than one receptor, while redundancy is related to the similar physiological functions exhibited by various chemokines (40).

More than 50 different chemokines have been identified so far, and they are organized in four different classes (Fig. 4) (40). This system of classification depends on a conserved two-cysteine motif in their N-terminal: CXC, CC, C, and CX3C, where the letter X denotes any amino acid. On the basis of this system of classification, each chemokine is identified by the class to which it belongs, the letter ‘L’ for the ligand, and a number based on their chronological order of discovery. For example, the chemokine SDF-1 belongs to the family CXC and, therefore, it is identified as CXCL12. The receptor’s nomenclature follows the chemokine it binds to, by adding the letter ‘R’ for receptor and a number that is not necessarily related to the chemokine number (43). Despite the introduction of this classification system, the old nomenclature is widely used (44).

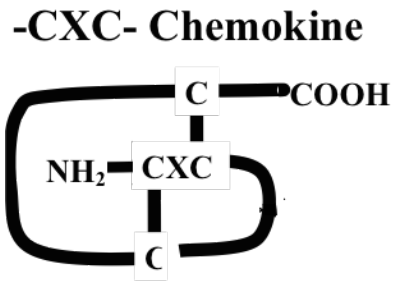

Figure 4. The CXC chemokine family. Chemokines are classified depending on four conserved cysteines, into four families CXC, CC, C, and CX3C. X represents any amino acid. Modified from Townson 2003 (45).

1.5. Chemokine Receptors

Chemokine receptors are GPCRs (46). Twenty receptors belonging to this family have been identified (40). They are involved in the body's homeostasis, as well as in the coordination of the two branches of the immune response — the innate and acquired immune responses. Deregulation of proper chemokine functions leads to serious immunological problems. This results in an inefficient immune system either failing to respond adequately to infections or becoming overly responsive to exogenous substances, as in asthma, or one's own-self, as in rheumatoid arthritis (RA) (41).

Chemokine receptors belong to the Rhodopsin-like family. They share 25–80% of their amino acid sequence identity, as well as several other characteristics (40). Indeed, chemokine receptors have a highly conserved DRY motif in the second intracellular loop, and a cysteine residue in each extracellular loop, enabling them to form disulfide bridges, ensuring the proper folding of the receptor and stabilizing the surface of interaction with the ligand (47).

The expression of chemokine receptors is not specific to immune cells. Chemokine receptors are also found on epithelial cells, endothelial cells, neurons and glial cells (40).

1.6. CXCR4

CXCR4 is a GPCR (48), which binds one endogenous chemokine ligand, CXCL12 (Fig. 1). CXCL12 is a constitutive chemokine, implicated in cellular migration during various stages of development, such as organogenesis and hematopoiesis (48,49). During adult life, CXCR4 plays a pivotal role in hematopoietic stem cell homing and their retention in the bone marrow (50). CXCR4 is equally involved in different pathologies including tumors, metastasis, and inflammatory diseases (49). As well, it serves as a secondary co-receptor for some strains of HIV (51). Therefore, we can assume that CXCR4 is a valid potential target for several pathologies.

CXCR4 has only one physiological ligand, CXCL12. CXCL12 is a peptide of 68 amino-acids that assumes a tertiary structure of a compact core and a flexible N-terminus (52). CXCL12 binds to the external domains of CXCR4 (53). This binding leads to conformational changes in CXCR4, and thus, its activation (52-55). After activation by CXCL12, CXCR4 signals through two major pathways: Gαi and β-arrestin (Fig.5)

1) G-proteins: Upon agonist binding, CXCR4 activates Gαi (56). Gαi inhibits AC, which is responsible for generating cyclic adenosine monophosphate (cAMP). The β/γ complex on the other hand activates PLC-β, Phosphatidylinositol 3'-Kinase (PI3K) and Protein Kinase C (PKC). These pathways result in a cytosolic Ca^{2+} influx and activation of the MAPK (48), leading to regulation of gene transcription and cell migration. In addition, CXCR4 activates small G-proteins such as Rho, Rac, and Cdc42, the central regulators of actin polymerization and chemotaxis (57). This signaling pathway is sensitive to the pertussis toxin (PTX). This toxin inhibits Gαi signaling by ADP-ribosylating the α subunit (58). Although Gαi is the main G-protein activated by CXCR4, it is not the only one. Several reports have identified Gαq/11 (59-61), and Gα12/13 (60,62) as pathways activated by CXCR4 and both are necessary for chemotaxis.

2) β-arrestin: After stimulation with CXCL12, CXCR4 is phosphorylated by GPCR kinases (GRKs), such as GRK2, 3, 5, and 6 (12). The β-arrestin proteins (1 and 2) bind to the phosphorylated receptors and shut off signal transduction in a process called

desensitization (12). β-arrestins target the desensitized receptor to clathrin-coated pits and endocytosis. Following internalization, CXCR4 may be slightly recycled back to the membrane, but it is mainly targeted for degradation by the lysosomes. β-arrestins are also able to induce signaling effects by activating the ERK pathway leading to enhanced chemotaxis and cellular survival (63).

As mentioned earlier, the roles of various GRKs are not merely redundant. For CXCR4, phosphorylation by GRK2 and 6 leads to the recruitment of β-arrestin1 and the termination of Gαi signaling, while phosphorylation by GRK3 and 6 induces the recruitment of β-arrestin2 and the subsequent activation of the ERK pathway (14).

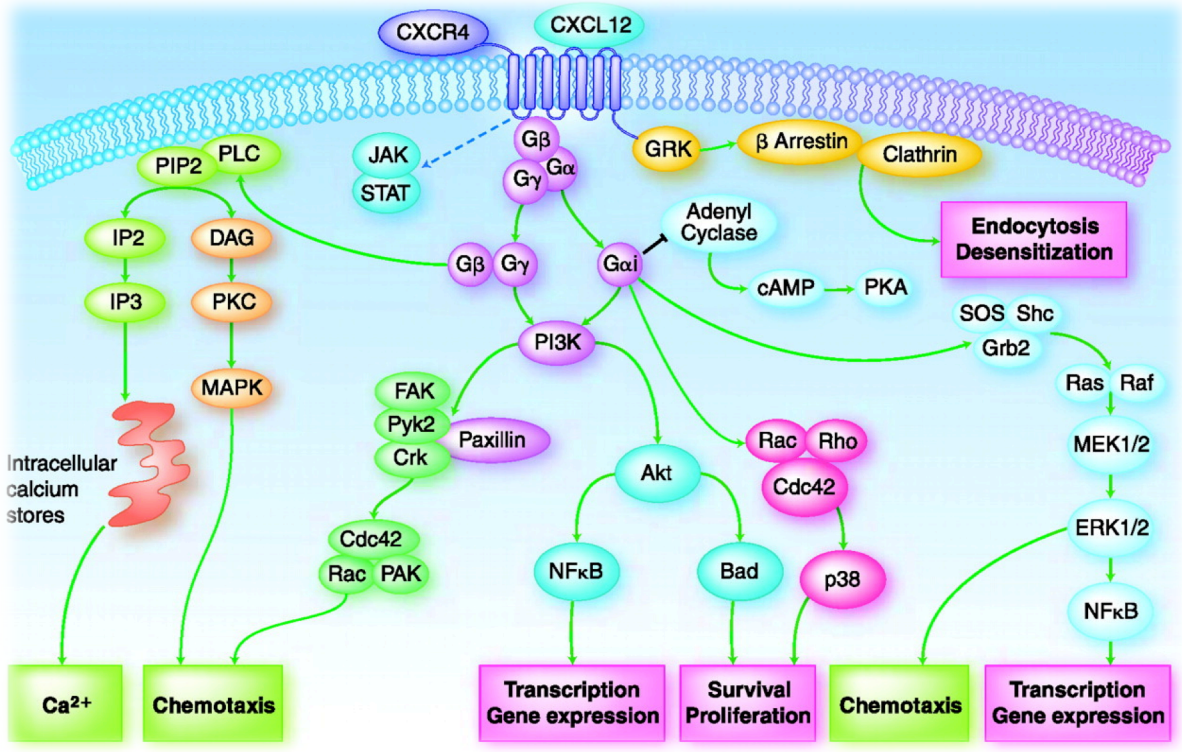

Figure 5. CXCR4 signaling pathways. Activation of CXCR4 by its ligand CXCL12 leads to the activation of Gαi, and β-arrestin pathways. These lead to the activation of the different proteins illustrated in the figure. Figure taken from Teicher 2010 (64).

Physiological functions of CXCR4: The CXCL12–CXCR4 axis is functionally prominent. As mentioned earlier, it is implicated in hematopoiesis and in the immune response. The importance of this axis is demonstrated in the knockout animal models. Mice lacking the two genetic copies of either CXCR4 or CXCL12 die perinatally due to defects in the development of the heart and brain, GI tract vascularization, hematopoiesis and B-cell lymphopoiesis (1).

Mobilization and homing of hematopoietic stem cells: Homing is the process of migration of hematopoietic stem cells (HSCs) through the blood stream, toward various organs or the bone marrow (Fig. 6). In the opposite process, mobilization involves the recruitment of HSCs from the marrow to the blood stream (50,65). Both processes are modulated through CXCL12 and its receptor CXCR4 (66). Signaling through CXCR4 induces the homing of the HSCs and their retention in the bone marrow (67,68), while the interruption of this pathway leads to the mobilization of HSCs into the bloodstream (50). In the bone marrow, HSCs play an active role by self-renewing and having the potential to repopulate the blood cells (67,69). These HSCs are preserved in a microenvironment (niche) composed of stromal cells secreting CXCL12 (70). The commonly used name for this chemokine is SDF-1, which stands for the Stromal Cell-Derived Factor (69). Since this chemokine is secreted in the bone marrow niches, they contain its highest concentration. Diffusion of CXCL12 leads to the generation of a gradient capable of attracting the HSCs to populate these niches. Even though the low concentration of CXCL12 in the periphery promotes proliferation and migration of cells, the high doses present in the bone marrow niches induce cellular survival and quiescence (71).

Cancer and Metastasis: CXCR4 is the most widely expressed chemokine receptor on cancer cells (72), where it is highly expressed on several tumors of the breast, prostate, ovaries, and melanoma. This level of expression is correlated with tumor malignancy or its ability to metastasize (73). CXCR4 signaling induces proliferation and cell survival in some types of tumors (72). Also, the receptor has been proposed as a prognostic marker, and its inhibition by gene targeting or antibody blocking has stopped tumor growth and metastasis in several preclinical animal models.

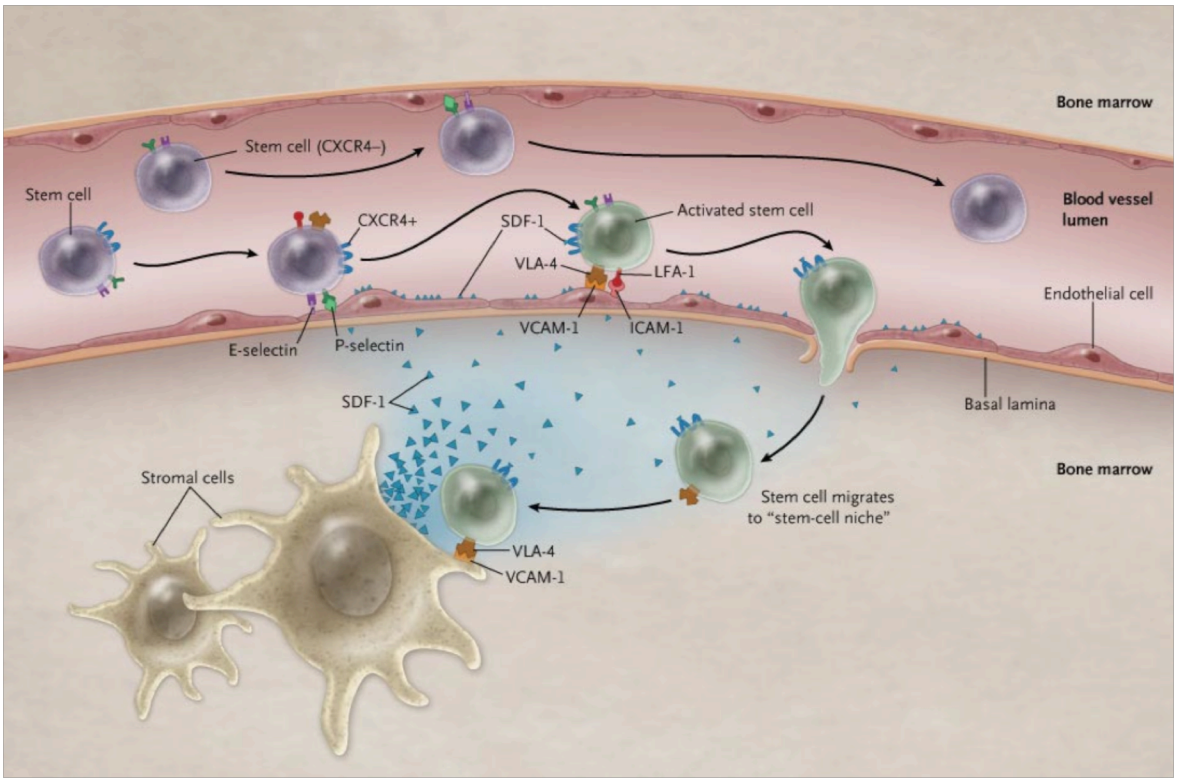

Figure 6. Homing of hematopoietic stem cells. Stem cells in the blood stream are expressing CXCR4 (blue receptor). CXCL12 (SDF-1) is expressed by the stromal cells of the bone marrow, released, diffuses from its source and is present on the surface of the endothelial cells. Activation of stem cells by CXCL12 leads to their direction to the bone marrow. Different integrins play important roles in the interaction between the stem cells and the endothelial wall. Figure taken from Homan 2011 (74).

Metastasis is the major cause of mortality in cancer (75). It arises as a spread of the primary tumor and formation of secondary metastatic tumors. Detection of cancer in patients early, before the metastatic process, allows for an increased chance of treatment by chemotherapy, radiotherapy or surgery (76). As the tumor spreads throughout the body, the prognosis of the patient decreases dramatically, due to the difficulty of controlling and treating all the cancerous foyers. Therefore, it is primordial to understand the process of the metastatic spread and the mechanisms that contribute to it, to be able to predict its targets and to develop specific drugs to obstruct it.

Metastatic dissemination is extremely regulated in the process of cancer spread. Metastatic cells tend to co-opt chemokine signals that are usually used for leukocyte trafficking (73). While CXCR4 is significant in primary tumor development, it is also essential in directing the migration of cancer cells invading the secondary organs (48,73). Activation of CXCR4 leads to the stimulation of signaling pathways required for migration (77). In addition, CXCL12 dictates the profile of metastasis in the CXCR4 expressing breast cancers (Fig. 7) (73). For example, the cancerous cells that express CXCR4 tend to migrate to organs with a high level of expression of this receptor's ligand, CXCL12 (73), such as the lungs, the liver and the bone marrow (78).

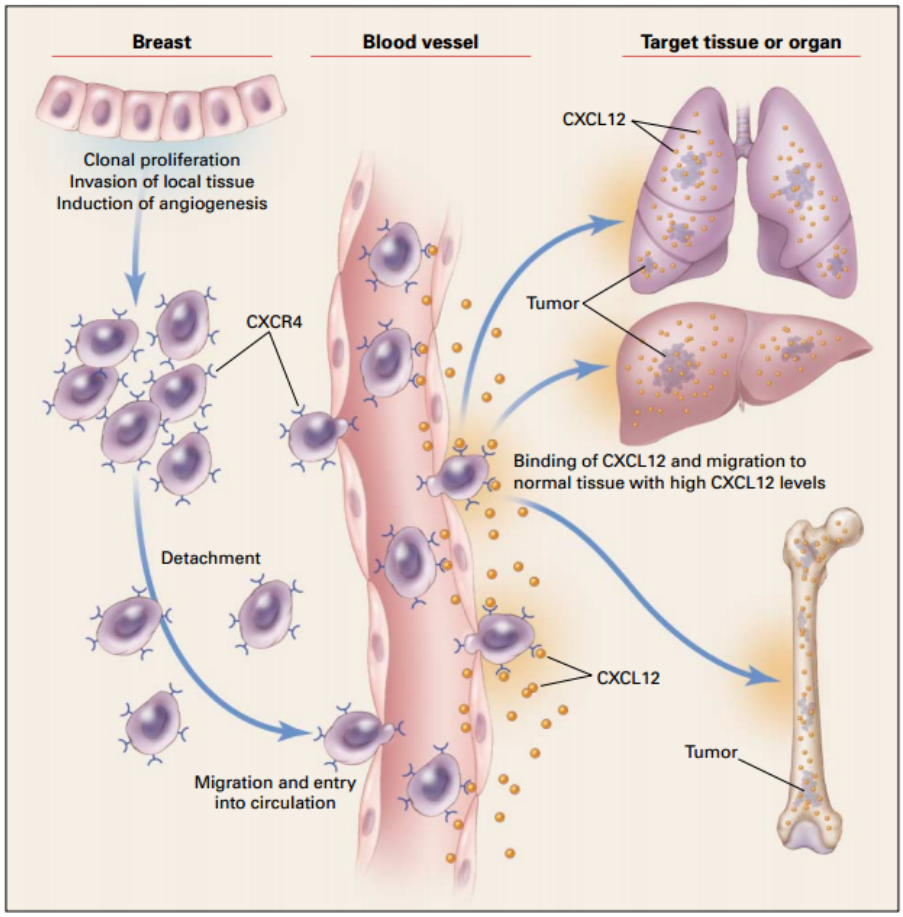

Figure 7. Implication of CXCR4 in metastasis. Cancer cells from the primary breast tumor expressing CXCR4 lose attachment and enter the circulation. In the blood vessels CXCR4 interacts with CXCL12 present on the endothelial cell surface leading to their exit from the circulation and migration towards the organs expressing high levels of CXCL12, such as lungs, liver, and bone marrow. Figure taken from Murphy 2001 (75).

1.7. The Conserved DRY Motif

The DRY-motif is situated in TMIII, at the 3.49 position (Fig. 1). This is according to the Ballesteros–Weinstein nomenclature, where the first number reflects the transmembrane helix and the most conserved residue in this helix is given the number 50 (79). The DRY-motif is the most conserved motif in GPCRs and it has been reported to interact directly with the Gα proteins (80). To highlight the importance of this motif, Arginine 3.50 is conserved among 100% of the chemokine receptors. As well, in 95% of these GPCRs, the position 3.51 is occupied by an aromatic residue and a negatively charged residue at 3.49 (81). In the inactive form, the aspartic acid residue (D 3.49) and the arginine one (R 3.50) interact together (79). This interaction is interrupted during activation, leading to the release of arginine and its interaction with the Gα proteins. The importance of R3.50 in the activation and functioning of the chemokine receptors has been demonstrated after studying the DRY motif mutants (82). This residue has been revealed to be primordial to the G-protein signaling of several receptors, such as Muscarinic acetylcholine receptor M1 (M1 AChR) and Vasopressin 1a receptor ($V_{1a}R$) (82). In these receptors, as well as in CXCR4, the arginine of the DRY motif is involved in the direct coupling of the receptor to the G-proteins and the conformational changes induced by their respective agonists.

Mutating residues of the DRY-motif leads to two types of functionally variant mutants, the constitutively active ones (CAMs) and the constitutively inactive ones (CIMs). The CAMs spontaneously activate G-protein signaling (82,83), while the CIMs constitutively recruit β-arrestin and are deprived of G-protein signaling. Today, CXCR4 CAMs have been identified, but no CIM has yet been described.

Berchiche et al. had previously studied the DRY mutants for CXCR4 (84). Mutating the D3.49 to asparagine (D133N) or the Y3.51 to alanine (Y135A) gave a signaling pattern similar to that of the wild-type receptor. Arginine mutation (R134A) led to a receptor unable to activate the G-proteins. Nevertheless, it was not clear whether this mutant could demonstrate any signaling activity at all. The expression of these mutants on the cell surface was found comparable to the wild-type receptor (84). Both D133N and R134A had a slight decrease in

cell surface expression, which could be explained by several mechanisms: decrease in receptor's stability, increase in internalization, or even a decrease in the receptor's delivery to the cell surface by the trafficking machinery.

While these mutants have been tested with several techniques, neither the Gαi pathway nor β-arrestin2 recruitment have been studied specifically. The previous two reports studying this motif in CXCR4 focused on the recruitment of guanosine 5'-O-[gamma-thio] triphosphate (GTPγS), calcium influx, and gene transcription, all of which are shared among the G-proteins, without being specifically related to the Gαi subunit.

1.8. The Asparagine N3.35

The asparagine residue N3.35 is conserved among chemokine receptors (25). This residue is essential in the conformational changes induced during the activation of these receptors (85). Zhang et al. studied this amino acid in the chemokine receptor CXCR4 (85). Changing asparagine N119 to alanine or serine generated CAMs on the G-protein pathway. In this study, both mutants were able to constitutively activate a galactose gene reporter, recruit GTPγS to the plasmic membrane, induce a calcium influx and confer a constitutive phosphorylation to the C-terminus of the receptor (84,85). Furthermore, this constitutive activity was sensitive to pertussis toxin (PTX) indicating that it was associated with the Gαi pathway. Other mutations had different signaling patterns. The mutant N119D showed a similar activity to the wild-type in all three pathways mentioned above, which were related to the G-proteins. Surprisingly, the mutant N119K had no G-protein signaling. Nevertheless, all these mutants were adequately expressed on the cell surface (84), and their binding to the CXCL12 did not vary significantly (85).

Similar to what was mentioned for the DRY motif, this residue has not been studied for its role in specifically recruiting β-arrestin2.

1.9. Pharmacology

Several pharmacological parameters are used in this thesis and are, therefore, introduced here.

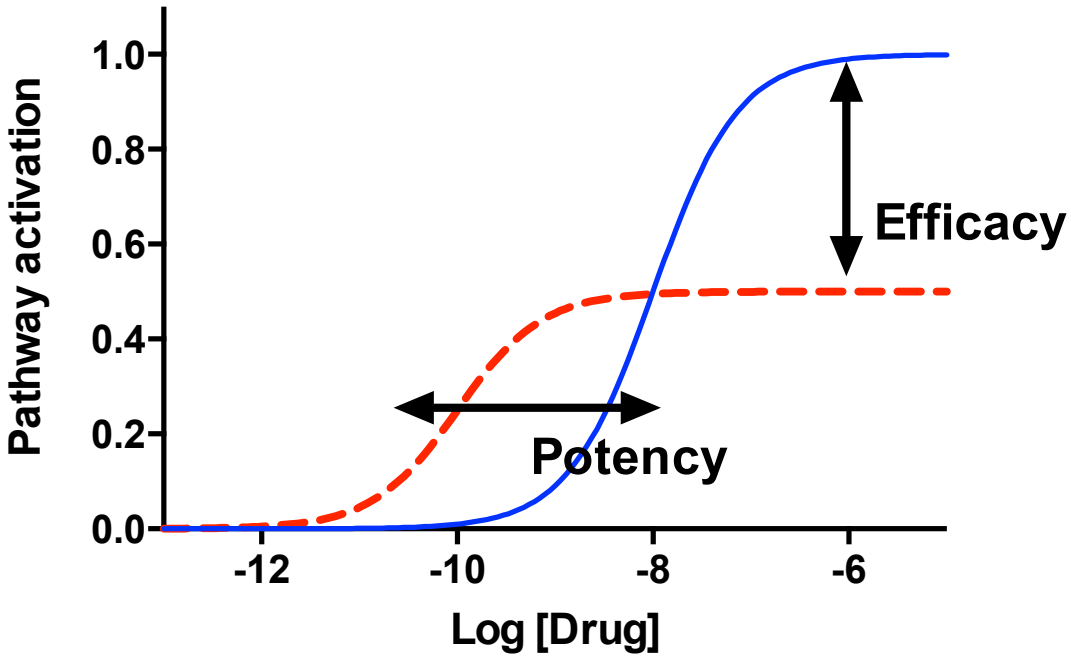

Figure 8. Pharmacology of GPCR activity. Schematic representation of the activity on one pathway as a function of the drug's concentration. The concentration is presented on a logarithmic scale. Potency represents the concentration of a drug required to induce a response while efficacy represents the maximal response induced.

Affinity: The affinity describes the strength of interaction between the ligand and its receptor or two proteins (86). This strength depends on the chemical forces resulting in the interaction. Several types of forces stabilize this interaction, such as electrostatic, hydrophobic, hydrogen bonds or Van der Waals. This affinity can be measured by radio-binding assays. Here, the study focuses on the effect of different ligands on the relative affinity between CXCR4 and β-arrestin2, and a BRET titration assay is used for that. Although this type of assay does not provide quantifiable data on the affinity of the interaction, it permits comparison of the affinity among different conditions.

Efficacy: Efficacy is a measure of the capacity of a ligand to induce a physiological effect (Fig. 8). It represents the maximal response that this ligand can induce on a pathway. Efficacy is measured using dose-response sigmoidal curves. With saturating concentrations of the ligand, the observed effect attains a plateau that represents the efficacy of this ligand (86).

Potency: Potency represents the concentration of a ligand required to induce a response (86). It is usually measured as EC50, the concentration of the ligand required to produce 50% of the maximal response (the efficacy). The lower the EC50 is, the more potent the ligand, meaning that even a small concentration of it can induce a response.

1.10. Agonist, Antagonist and Inverse Agonist

A receptor's ligand is defined as a molecule with an affinity for the receptor. Still, its effect on receptor signaling can vary. Endogenous or synthetic ligands of a GPCR are classified as agonists, antagonists, or inverse agonists.

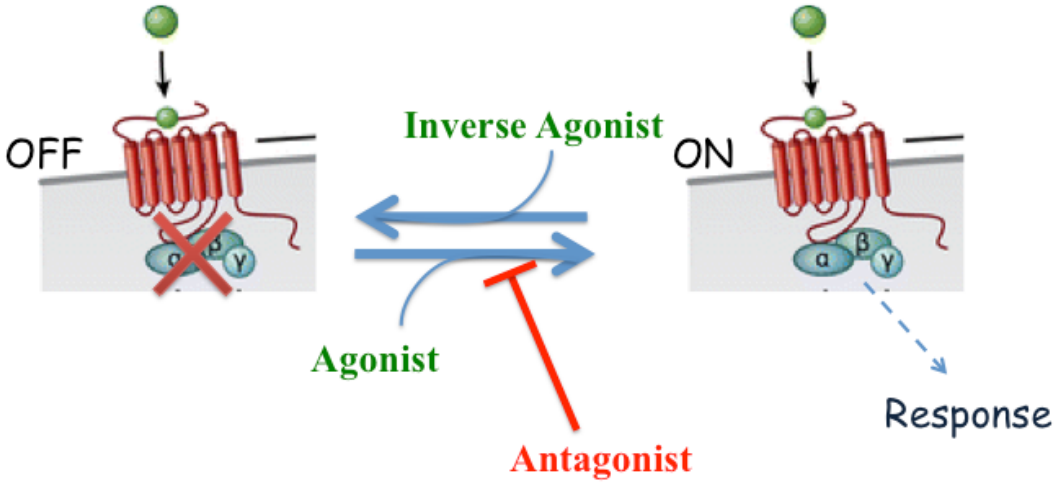

Figure 9. Agonist, antagonist and inverse agonist. A receptor represented as it has two states, an inactive (off) state, and an active (on) one giving a response. The equilibrium between the two is affected by the type of the ligand bound to the receptor. An agonist drives the equilibrium towards the active form; the inverse agonist changes it in the opposite way, while an antagonist blocks the receptor in its basal state. Modified from Zhang 2012 (17).

Agonist: An agonist is a ligand capable of inducing a response and also increasing the basal signaling of the receptor (Fig. 9) (87). It favors a transition to the activated conformation of a receptor, in respect to a particular pathway. The degree of agonism depends on the ligand and it can vary between a full agonist effect with a maximal response or a partial one. Often, endogenous ligands are those that show a maximal response. This difference in efficacy of agonism does not depend on the concentration of the ligand, as receptors are saturated with either ligand when measuring its efficacy. Rather, it is the intrinsic capacity of the ligand that dictates its maximal response.

Antagonist: An antagonist is a ligand capable of binding the receptor, and causing a block in its conformation without activating a signaling pathway (86,87). As it has no intrinsic activity, its effect can be observed when combined with an agonist. In this context, the antagonist would decrease the effect induced by the agonist on a particular pathway, either by competing with this latter for the binding site (Orthosteric Antagonist) or by allosterically modifying its activity (Allosteric Antagonist). An antagonist may or may not be competitive. A competitive antagonist sterically competes with the agonist and, by increasing the agonist's concentration, can rescue its activity on this pathway. However, with a non-competitive antagonist, such as an allosteric one, adding increasing amounts of the agonist will not be able to counteract the antagonist effect.

Inverse Agonist: Finally, a ligand can also act as an inverse agonist. The inverse agonists reduce the basal signaling of a receptor in respect to a signaling pathway (88). Observing this activity requires a receptor with a basal constitutive activity (CAM) on this pathway, in the absence of any ligand. Stimulating these receptors with an inverse agonist demonstrates its negative efficacy (89,90). In the absence of such a constitutive activity, the inverse agonist acts as a mere antagonist.

1.11. Functional Selectivity

Biased signaling: A central aspect in the pharmacology of GPCRs is the concept of biased signaling (91), where a receptor state is not merely on or off, but the on/off must be used in terms of a particular pathway. A receptor's ligand may be an agonist on one pathway, but not on the other (92).

Previously, the activation of the receptor has been explained by using the two-state model. This theory affirms that a receptor is in equilibrium between two states, an active state (on) and an inactive one (off). A ligand may affect this equilibrium by favoring one conformation over the other. For example, an agonist is any ligand that stabilizes the active conformation further.

After detailed studies and accumulating evidences, it is now accepted that this process is more complex. The receptor, as a protein, does not have one or two definite conformations, but it is represented as an energy landscape (93). The activation of any pathway is associated with several conformations that increase the binding of the signaling complexes. After binding a ligand, the receptor traverses to a new energy landscape and different ligands induce different landscapes, thus stabilizing different conformations and exhibiting a preference for different signaling complexes.

Angiotensin type 1A receptor ($AT_{1A}R$), for example, when stimulated with its endogenous ligand angiotensin II (Ang II) fails to activate G-protein signaling, while showing a recruitment of β-arrestin2 and activation of ERK1/2 (94).

Another example of the functional selectivity concept is propranolol, which is an inverse agonist on Gαs through the β1-AR, even when it is an agonist activating the MAPK pathway, independent of the G proteins (95).

Previous classifications of ligands as agonists or antagonists have often not taken the potential bias for a particular pathway into account, and assessment of each of these pathways remains to be done. For example, if a ligand can activate the Gα pathway through its receptor,

it is wrong to assume that it can induce the recruitment of β-arrestin as well. Each pathway must be assessed separately to determine the ligand's effect on each.

With the introduction of functional selectivity, the concept of redundancy has changed. While two distinct ligands can bind the same receptor, they may not activate the same pathways. Although, they might share some physiological functions, they would differ in their signaling capacities.

Biological Implications of Biased Signaling: The importance of biased signaling in the therapeutic field is tremendous. As stated earlier, more than 30% of the prescribed drugs act on GPCRs. It may be beneficial for the treatment of several pathologies, to activate or inhibit only one pathway associated with the targeted receptor and not the others. For example, the μ-opioid receptor is the target of several opioids, such as morphine, which acts as an analgesic through its G-protein activity (96-98). However, activation of β-arrestin by these agonists is associated with respiratory depression. Ideally, we are interested to look at an opioid agonist that is deprived of the ability to recruit the β-arrestin to the receptor.

Another example is the angiotensin receptor and its implication in arterial pressure and cardiovascular diseases. Losartan, an antagonist of this receptor on both Gαq and β-arrestin reduces arterial pressure and cardiac performance. On the other hand, the synthetic biased antagonist TRV120027 on the Gαq activates β-arrestin, leading to several advantages, such as preservation of heart stroke volume and an increase in cardiac performance, giving increased efficiency to the treatment of these patients (99).

Biased Trafficking: Different ligands can lead to a differential phosphorylation by the GRKs (100), which would affect the recruitment of β-arrestin, force, affinity, and duration. As described earlier, β-arrestin plays a role in: (i) the ubiquitination of the receptor, (ii) the assembly of endocytic vesicles, (iii) the trafficking of the receptor and (iv) the initiation of G-independent signaling. Taking that into account, it would be tempting to hypothesize that differential β-arrestin recruitment would lead to biased trafficking of the receptor and subsequent biased signaling through the pathways recruited on the scaffolding protein β-arrestin.

1.12. AMD3100

CXCR4 antagonist AMD3100 or Plerixafor is a drug that is used to block the retention of HSCs in the bone marrow and thus mobilize them into the blood stream (101). AMD3100 binds CXCR4 and blocks the effect of the endogenous ligand CXCL12. This molecule is a synthetic one, with a bicyclam structure (Fig. 10) (102). It was first developed to inhibit the HIV 1/2 envelope protein, Gp120, and its cellular entry via the HIV co-receptor (103). During its preclinical evaluation as a potential antiretroviral drug, a significant side effect was observed in otherwise healthy patients (104). Patients receiving intravenous injections of AMD3100 showed abnormally elevated white blood cell counts. As AMD3100 blocks the interaction between CXCR4 and CXCL12, it induces the release of the stem cells in the peripheral blood (105). After the observation of this side effect, research on the medical use of AMD3100 was refocused on another therapeutic indication. Administering AMD3100 in combination with granulocyte-colony stimulating factor (G-CSF) induced rapid mobilization of stem cells into the peripheral circulation (106).

AMD3100 or Plerixafor is currently approved by the FDA for this therapeutic use (72). It is administered to a bone marrow donor, to be able to mobilize HSCs and collect them from the periphery. This is mostly used for autologous stem-cell transplantation in patients with multiple myelomas or non-Hodgkin's lymphomas (107,108). Prior to the discovery of AMD3100, G-CSF was the standard of care for these patients. For this reason, clinical trials studied the effect of adding AMD3100 to the G-CSF regimen (108).

In addition, Plerixafor is currently used in clinical trials to improve the efficiency of chemotherapy for patients with acute lymphoblastic leukemia (ALL) or acute myeloid leukemia (AML) (109,110). During chemotherapy, cancerous stem cells tend to lodge in the bone marrow environment. This niche, with its stromal cells, provides drug resistance to these cells, which may lead to future relapse (107). Administering Plerixafor is believed to mobilize these cells, and increase their sensitivity to chemotherapy.

Although mobilizing cancer cells from the bone marrow is beneficial in the context of sensitizing them to chemotherapy, inducing the release of cancer cells from their primary

origin increases the risk of metastasis. It has been demonstrated that Plerixafor shows a weak activation on CXCR4. As this receptor is the most widely expressed chemokine receptor on cancer cells (72), this compound activates the migration of these cancer cells. This outcome is devastating as it causes metastatic migration of tumor cells, as well as the contamination of peripheral blood by the cancer cells, leading to subsequent relapse after auto-transplantation with the stem cells (111). For this reason, a thorough understanding of the mechanisms of action of AMD3100 and its effects on CXCR4 signaling is necessary.

Even though AMD3100 is believed to be a neutral antagonist, Zhang et al. have suggested that it can be a partial agonist on the Gαi pathway (85). They have based their deduction after observing that AMD3100 induces GTPγS recruitment to the membrane and a Ca^{2+} influx, as well as an activation of a galactose gene reporter. Interestingly, these last two pathways are activated by the Gβγ complex rather than the Gαi (112). As discussed earlier, Gαi is the principal α subunit activated by CXCR4, although not the only one. As the complex βγ is shared between different Gα proteins, the activation of any of these can explain the effects observed. For example, activation of Gαq can lead to similar consequences (60). To answer this question, we should assay the signaling effects of Gαi specifically, by observing its effect on the activity of adenylate cyclase (AC).

β-arrestin is a major pathway associated with migration, chemotaxis, and metastasis. Due to the concept of functional selectivity, we cannot deduce the impact of AMD3100 on this pathway based on the previously described experiment. To further understand the role of Plerixafor on cancer metastasis, the effect of this drug on the activation of Gαi and the recruitment of β-arrestin should be studied and is one of the aims of this project.

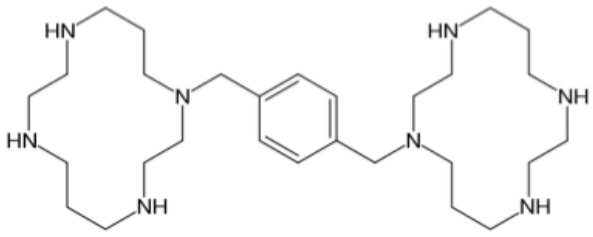

Figure 10. AMD3100

1.13. TC14012

As mentioned earlier, CXCR4 is an HIV co-receptor. Similar to AMD3100, the peptide T140 was developed specifically as a CXCR4 inhibitor, to exhibit an antiretroviral activity (113). T140 is a peptide of fourteen amino acids, and is derived from self-defense peptides called polyphemusins, which are used by the horseshoe crab (114,115). T140 has shown an anti-HIV activity by antagonizing the cellular entry of the HIV-1 X4-tropic strain (116). T140 showed a high cytotoxicity (115) and was unstable in bovine serum (111). For these two reasons, TC14012 has been developed to increase its pharmacological efficiency (Fig. 11) (117). Two residues of the peptide T140 have been substituted by Citrulline and Deoxy-Citrulline, respectively (111), leading to a decrease in the cytotoxicity of the peptide. Also, the C-terminal of the compound has been amidated to enhance its stability in the serum (115).

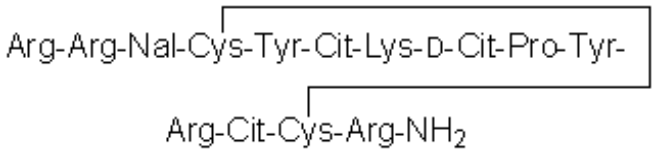

Figure 11. TC14012

Analogs of T140 showed several clinical potentials in the treatment of arthritis, cancer, and leukemia (115). One of these analogs, 4F-benzoyl-TN14003 showed anti-metastatic properties by decreasing the migration of breast cancer cells, MDA-MB-231 (118).

The peptide TC14012 was identified to be a CXCR4 inverse agonist on the G-protein pathway (85). This was demonstrated through the same experiments discussed earlier, which implied that AMD3100 be a partial agonist. Nevertheless, inverse agonism effects were not specifically observed on the Gαi pathway, and again its effect on β-arrestin recruitment remains to be elucidated. These two questions are among the aims of this study.

Being an inverse agonist, TC14012 may be more advantageous than AMD3100. As partial agonists like AMD3100 have the capacity to activate and promote the migration of cancer cells expressing the CXCR4 receptor, inverse agonists will demonstrate a clinical advantage by limiting the adverse effects discussed above (115).

2. OBJECTIVES

The main aim of this project is to study the relationship between β-arrestin2 and Gαi on the receptor CXCR4. To achieve this we used previously described mutants affecting the conserved DRY motif and the asparagine 119. Specifically, we had six questions that we wanted to assess in this project:

1. These mutants have only been studied for their capacity to activate the G-proteins in general. Here, we wanted to measure a parameter that is specific to the Gαi activity, such as the concentration of cAMP.
2. Some mutants were previously known to be unable to activate the G-proteins. Whether they were able to activate a G-independent pathway has not been tested. Here, the capacity to recruit β-arrestin2 is assayed and the conformation of this recruitment is compared between the mutants.
3. Signaling and trafficking are interrelated. Keeping in mind that these mutants have a different pattern of signaling, we wanted to assess their respective localization, to find out whether this differential signaling is leading to a differential trafficking.
4. CXCR4 can both activate the Gαi pathway, and recruit β-arrestin2. The concept of functional selectivity states that a ligand can activate one pathway without the other. We wanted to verify if this is true for CXCR4 and determine if β-arrestin2 is dependent on Gαi. This was performed by inhibiting the Gαi pathway with pertussis toxin, while testing for the effect of this inhibition on β-arrestin2 recruitment.
5. To differentiate between an antagonist and an inverse agonist effects, a receptor showing constitutive activity on the pathway is required. N119S has been previously identified as a CAM on Gαi pathway. Yet, no mutant is known to constitutively recruit β-arrestin2 and we aimed to identify such a mutant.
6. The effect of the two synthetic CXCR4 ligands, AMD3100 and TC14012 on CXCR4 signaling has only been studied on the G-proteins pathway. Here we wanted to assay their role on the Gαi signaling specifically, and the recruitment of β-arrestin2, and to differentiate if they were partial agonist, neutral antagonist, or inverse agonist on each of the two pathways.

3. MATERIAL AND METHODS

3.1. Materials and Plasmids

HEK293E cells (Invitrogen, Carlsbad, CA) were cultured in DMEM (4.5 g/L D-Glucose) (Gibco®, Grand Island, NY), FBS (WisEnt, Rocklin, CA), Penicillin/Streptomycin (Invitrogen), G-418 sulfate (WisEnt), and Plasmocin (Invivogen, San Diego, CA). For transfections, OptiMEM (Invitrogen) was used in combination with Polyethylenimine (Polysciences, Warrington, PA). The BRET experiments were conducted in BRET 96-well microplates (PerkinElmer, Waltham, MA) that are coated with 0.1% Poly-D-Lysine (Sigma-Aldrich, St. Louis, MO). BRET tampon contained BSA Fraction V (WisEnt), and the Luciferase substrate Coelenterazine H (Nanolight technology, Pinetop, AZ). Imaging was performed in 8-well chambered coverglass dishes (Labtek, Nunc). Five ligands were used: forskolin (Sigma), Pertussis Toxin (Calbiochem, San Diego, CA), recombined CXCL12 (PeproTech, Rocky Hill, NJ), AMD3100 (Sigma), and synthesized TC14012, a gift from Nobutaka Fujii (111).

Mutants of CXCR4 were developed by the Kunkel method and were previously described (84).

3.2. Cell Culture and Transfection

HEK293E cells were cultured at 37˚C, and 5% CO_2 in Dulbecco's modified Eagle's medium (DMEM) supplemented with 10% fetal bovine serum (FBS), 200µg/mL G-418 sulfate, 2.5µg/mL plasmocyin and 100units/mL penicillin/streptomycin. Transfection was conducted on the cells in 6-well plates, 24h after plating 800,000 cells in each well, and a total DNA amount of 2µg was added. The transfection protocol, using polyethyleneimine, has been previously described (119).

3.3. cAMP Biosensor BRET^2 Assay

GFP^{10}-Epac-Rluc3 was used as a BRET^2 reporter for cAMP reduction (119). Live HEK293E cells were transiently cotransfected with 0.04µg of the Epac plasmid and 1µg of the CXCR4-myc wild-type or mutant. The Epac protein contained both the BRET^2 donor and acceptor. 24 hours post-transfection, cells were transferred to white, 96-well, clear-bottom microplates coated with poly-D-Lysine hydrobromide. 36-48 hours post-transfection, the cell medium was changed to BRET buffer (PBS, 0.5mM $MgCl_2$ and 0.01% BSA). Level of fluorescence was measured by Mithras LB940 instrument (Berthold Technologies) using an excitation filter of 400nm and an emission filter of 515nm. Rluc3 substrate, coelenterazine 400A was added to a concentration of 5µM. Cells were stimulated with 20µM of forskolin, with the different doses of ligand for 10min at room temperature before measurements. Total luminescence was equally taken by Mithras LB940 immediately before the BRET^2 measurements. Raw BRET^2 was calculated as the ratio of emission of GFP^{10} at 515nm to the emission of Rluc3 at 400nm (17).

3.4. β-Arrestin2 Recruitment BRET^2 Assay

β-arrestin2 recruitment to the CXCR4 receptors was measured using a BRET^2 assay (120). The experiment was conducted similarly to the Epac reporter, while cotransfecting with 0.05µg of each CXCR4 mutant or wild-type tagged with the BRET^2 donor *Renilla* Luciferase 3, and 1µg of β-arrestin2 tagged with GFP^{10}, the BRET^2 acceptor. Cells were incubated with the ligands for 5 min at 37˚C and 10 min at room temperature before measurements. Values were corrected by subtracting a background ratio detected when the CXCR4-Rluc3 was transfected alone, giving the BRET^2 net values.

3.5. Titration Assays

Similar to the β-arrestin2 recruitment assays, cells were cotransfected with 0.05µg of CXCR4-Rluc3, wild-type, R134A, or N119S with a varying quantity of β-arrestin2-GFP10, between 0.05µg and 1.95µg. 48h post-transfection, cells were stimulated with a saturating

dose of CXCL12, 200nM. Values were corrected by subtracting a background ratio detected when the CXCR4-Rluc3 was transfected alone, giving the $BRET^2$ net values.

3.6. Imaging of CXCR4 Using Spinning Disc Confocal Microscopy

HEK293E cells were transfected with 1µg of CXCR4-YFP, wild-type or mutants, in a pcDNA3 plasmid 48h before imaging. After 24h, cells were transferred to 8-well chambered coverglass dishes. Live cell imaging of transfected cells was performed at 37°C and 5% CO_2 using an Ultra view Vox spinning disc confocal system (Perkin Elmer), and an Orca-R2 CCD camera (Hamamatsu). This was combined to a Leica DMI6000B inverted microscope equipped with a motorized piezo-electric stage (Applied Scientific Instrumentation), and using a scanning unit CSU-X1 (Yokogawa) as described earlier (121).

Volocity 5 software (Improvision/PerkinElmer) was used for image acquisition, quantitation, and analysis. Imaging was performed using a Plan Apo 40x (0.85 NA) air objective and a camera binning of 2x2. The YFP tag is observed at 488nm.

3.7. Data Analysis

Collected data were analyzed using Prism 6.0 software (GraphPad Software, San Diego, CA). For the Gαi activation and the β-arrestin2 recruitment, data were fitted with a sigmoidal dose-response curve to determine the potency and the efficiency. Michaelis-Menten curve was used for the titration experiments and the maximum association and the affinity were determined. Differences between the ligands were analyzed using a non-matched one-way ANOVA, followed by a Dunnett's posttest.

3.8. The Principle of Bioluminescence Resonance Energy Transfer (BRET)

Bioluminescence Resonance Energy Transfer or BRET is a method used to study protein–protein interactions in a live cell medium (122). It can also reflect changes in the intramolecular conformation. This energy transfer is not radioactive, and it occurs between two electromagnetic dipoles, one belonging to the energy donor bioluminescent molecule and the other to the receptor fluorescent molecule (123). However, for this transfer to occur, the two molecules need to be close to each other, with a distance less than 100 Å (124). In addition, some compatibility between the two molecules is required. The emission spectrum of the donor must somewhat overlap the excitation spectrum of the second molecule. Thus, the efficacy of this transfer and intensity of the BRET signal depends on the distance separating the two molecules, as well as the angle between them (122).

One widely used bioluminescent donor is the enzyme *Renilla luciferase*. This enzyme belongs to the animal *Renilla reniformis*, a sea animal that has a natural capacity for bioluminescence (123). For the experiments described here a variation of this enzyme, Rluc3, is used. This enzyme contains three specific mutations, A55T, C124A, and M185V enhancing its stability and its light output (119,125). This enzyme generates a wavelength of 400 nm by oxidizing its substrate Bisdeoxycoelenterazine (coelenterazine-400a), formally called DeepBlueC. This emission can be transferred to the $BRET^2$ acceptor GFP^{10}, a variation of the Green Fluorescent Protein. If the two tags are in proximity an efficient transfer of energy can occur and the $BRET^2$ acceptor tag will fluorescence at 515 nm (101).

The BRET technique can demonstrate an intramolecular conformation change, the binding of two proteins or the change of conformation of this interaction (126). The ability to identify intramolecular conformational changes by BRET was used here in the Epac experiment (Fig. 12). The two BRET tags, Rluc3 and GFP^{10} are both fused to the same protein, Exchange protein directly activated by cAMP (Epac), one on the N-terminal and the other on the C-terminal, respectively. The conformation changes of this protein induce changes in distance and angle between the two tags, which translate into $BRET^2$ value changes (127,128). This protein changes its conformation depending on the cAMP concentration. In its

basal state, the two $BRET^2$ tags are close enough to generate a signal. However, the binding of cAMP induces a conformational change leading to the separation of the $BRET^2$ tags and the attenuation of the BRET signal.

Furthermore, to study the interaction between two proteins, a BRET signal is perceived when the two proteins, fused with the BRET tags, come into proximity of a distance of less than 100 Å (Fig. 13) (72). Here, the CXCR4 mutants have been fused with Rluc3 and β-arrestin2 with GFP^{10}. In principle, these two proteins do not interact in a cell without a specific stimulation. However, after stimulation with CXCL12, a specific interaction occurs between the two proteins and a BRET signal is generated.

BRET measures resulting from a specific interaction are quantifiable. To achieve this, the ratio of the concentrations of GFP^{10} over Rluc3 should be controlled. In the case of an unspecific interaction, the signal results from random collisions between the two BRET tags, and an increase in either concentration would increase the chance of such collisions. Based on this, the relation between the BRET signal and the ratio GFP^{10}/RLuc3 follows a straight line (129).

On the other hand, if a specific interaction occurs between the two proteins, BRET signal increases with the GFP^{10} concentration, when the Rluc3 concentration is held constant (Fig. 14) (111). Still on higher ratios of GFP^{10}/RLuc3, the signal saturates and attains a maximum. This plateau corresponds to a point where all the BRET donor proteins tagged with Rluc3 interact specifically with the BRET acceptor tagged with GFP^{10}. Adding more BRET acceptor proteins will not increase the signal, due to saturation of BRET donors. Thus, this maximal BRET signal, $BRET_{max}$, depends on the number of maximum specific interactions that can be formed.

The $BRET_{50}$ can be defined as the ratio of GFP^{10}/Rluc3 required to give a BRET signal that is 50% of $BRET_{max}$. This parameter represents the affinity between the two proteins. On the other hand, $BRET_{max}$ depends mostly on the distance separating the two BRET tags and the angle between them (130).

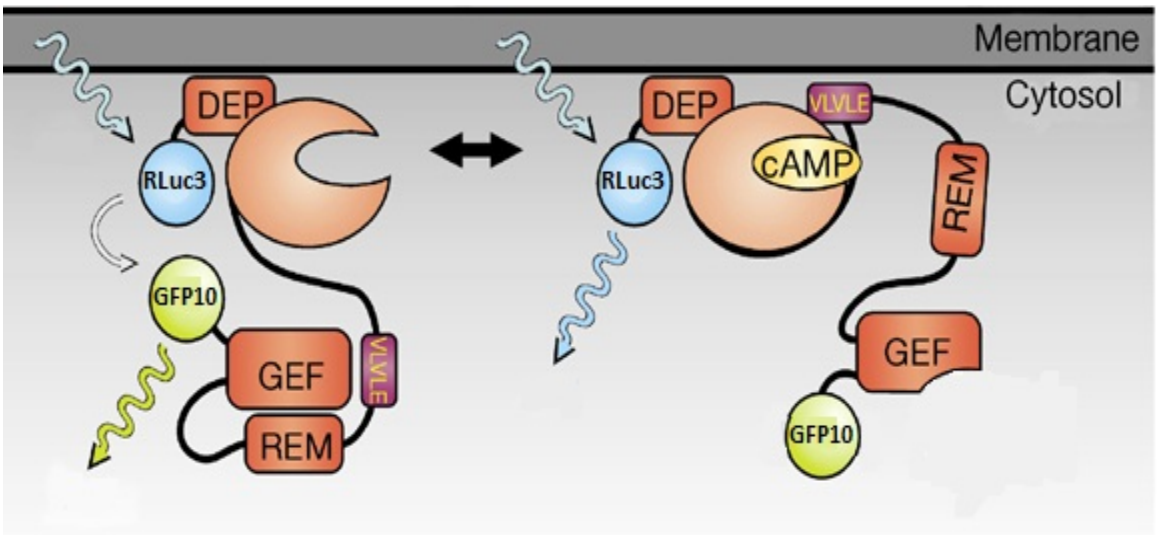

Figure 12. Assaying cAMP levels using Epac reporter. An Epac-based BRET^2 assay where an inactive mutant of human Epac-1 is integrated between GFP10 and Rluc3. Binding of cAMP to this protein induces conformational changes that decrease the BRET^2 signal. Modified from Ponsioen, 2004 (131).

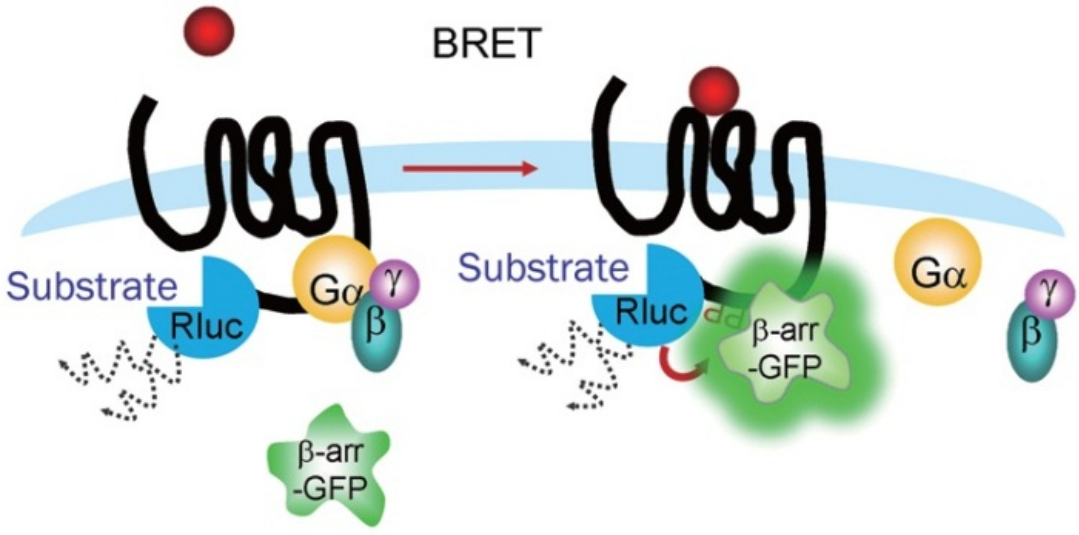

Figure 13. β-arrestin recruitment assay. A) BRET^2 assay, in which CXCR4 is tagged with RLuc3 and β-arrestin, is tagged with GFP10. Rluc3, when stimulated with a substrate, luminesces. Upon recruitment, the two tags come to proximity and give a fluorescent BRET^2 signal. Modified from Zhang, 2012 (17).

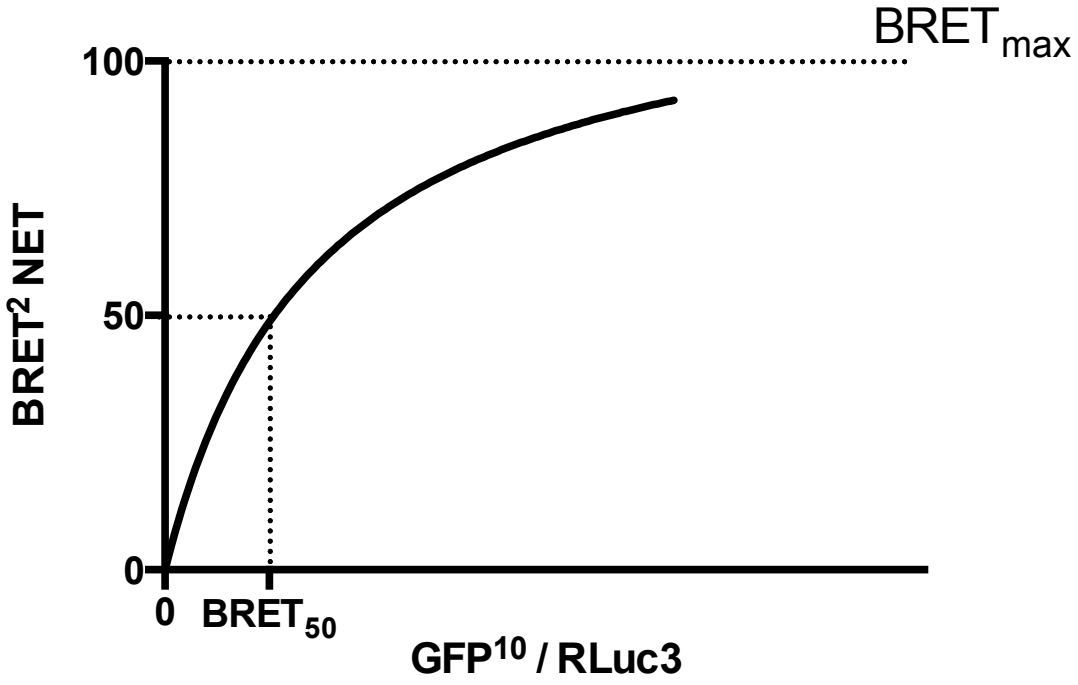

Figure 14. Analysis of a titration experiment. Varying the ratio of the two $BRET^2$ tags, GFP^{10} and Rluc3 leads to a hyperbole if there is a specific interaction between the two proteins. The $BRET_{50}$ represents the ratio required to attain a $BRET^2$ value half of the maximal one, and it is indicative of the affinity between the two proteins. $BRET_{max}$ represents the maximal achievable $BRET^2$ value, and it is indicative of the distance and the conformation between the two tags.

4. RESULTS

4.1. Gαi Activity of CXCR4 Mutants

First, we wanted to assess the capacity of the CXCR4 mutants to activate the Gαi pathway, and to compare these results with the previously published ones (84,85). These mutants have only been tested on the activation of G-proteins in general and not the Gαi specifically.

The activation of Gαi is assessed indirectly by using a reporter sensor. Epac-1 is a human protein that is activated by its binding to the cAMP. An Epac-based $BRET^2$ assay can be used to monitor the level of cAMP in the cells (119). Binding of cAMP to this protein induces conformational changes that reduce the $BRET^2$ signal. Gαi inhibits AC and decreases the concentration of the cAMP. As the levels of this are already low in a non-stimulated state, they fall below the detection range of this method. To bypass this technical difficulty, we need to pre-stimulate the cells with forskolin, an activator of AC, which leads to high basal levels of cAMP (132). The Gαi activity will then be measured by the decrease in this high concentration of cAMP, or the counteracting of the forskolin effect.

The activation of Gαi by the CXCR4 wild-type or one of its mutants was assayed by this method. The HEK293E cells were transfected with plasmids of the CXCR4 receptor, wild-type or mutant, with the Epac reporter. The experiment was designed as a dose-response, where the level of the chemokine CXCL12 was increased between 10^{-12}M and 10^{-7}M. On the basis of the previous experiments this high level of ligand was able to attain a plateau in the receptor activity. The experiment was carried out in triplicate, and was repeated at least three independent times.

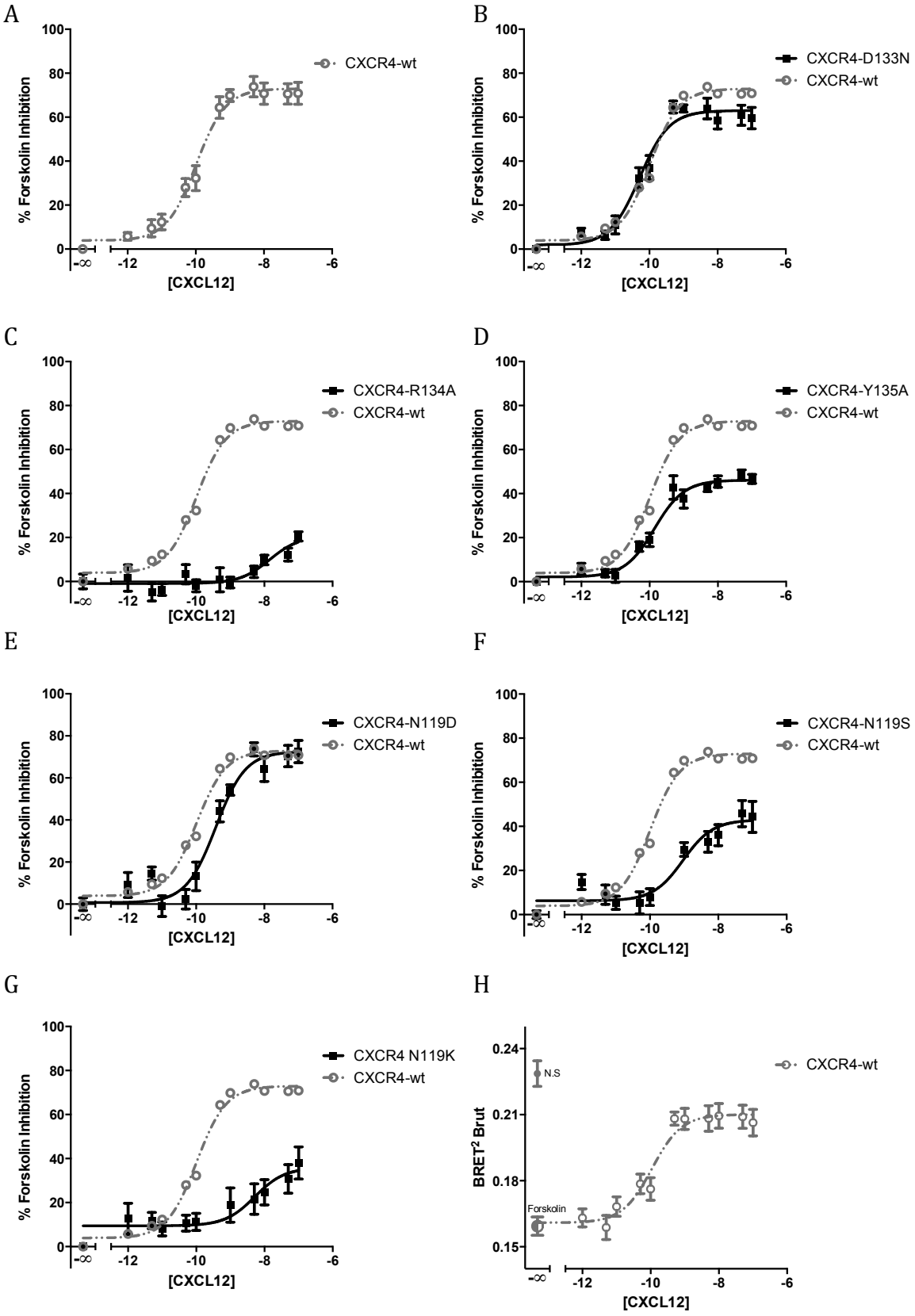
A
B
C
D
E
F
G
H
% Forskolin Inhibition
[CXCL12]
CXCR4-wt
CXCR4-D133N
CXCR4-R134A
CXCR4-Y135A
CXCR4-N119D
CXCR4-N119S
CXCR4 N119K
BRET² Brut
N.S
Forskolin

Figure 15. Gαi activity by CXCR4 mutants. Gαi activity is measured by the percentage of forskolin inhibition of each mutant. The level of cAMP is assayed by a $BRET^2$ reporter assay using GFP^{10}-Epac-Rluc3. HEK293E cells were cotransfected with the Epac plasmid and either CXCR4-myc wild-type (A) or one of its 6 mutants: D133N (B), R134A (C), Y135A (D), N119D (E), N119S (F) or N119K (G). Cells were stimulated with forskolin and CXCL12 for 10 min at room temperature prior to measurments. CXCL12 doses were varied between 10^{-5} and 10^{-12} M. The wild-type dose-response curve is shown in the background of each panel as a grey dashed line. H) The $BRET^2$ values of CXCR4 wild-type Gαi activity before normalization. N.S: Non-stimulated. Each point represents the mean ± SEM of at least three independent experiments, each conducted as triplicates.

Fig. 15H represents, as an example, non-normalized data obtained with the wild-type receptor after stimulation with CXCL12. The first point on the top left corner represents the level of $BRET^2$ without any stimulation, neither by forskolin nor CXCL12, and is estimated at 0.23 B.U (BRET Unit). Adding only 20 μM of forskolin increases the level of cAMP, and thus decreases the $BRET^2$ value to 0.16 B.U. On a logarithmic scale, the dose-response of the effect of the chemokine CXCL12 on the levels of cAMP follows a sigmoidal curve. For CXCR4 wild-type, this curve is characterized by a logEC50 of - 9.99 M that approximates to 0.102 nM, achieving a maximum inhibition of 0.21 B.U (Fig. 15A and Table I).

One important consideration in this experimental design is that CXCL12 must not be allowed to completely inverse the effect of forskolin, and the maximum value obtained when combining CXCL12 and forskolin must remain lower than the original one, before stimulation. If this is not the case, increasing CXCL12 will increase the level of the $BRET^2$ value until it attains the original non-stimulated level. Beyond this, CXCL12 will not be able to further decrease the concentration of cAMP, as this would have attained its minimum. Thus, the real effect of the higher doses of CXCL12 cannot be observed. This will translate in a left-shift of the curve and in a decrease in EC50. To avoid this situation, the forskolin dose has to be chosen carefully, at 20 μM, based on the previously published data (119). This ensured that in the experiments conducted here, CXCL12 did not completely inverse the effect of forskolin,

as the maximum $BRET^2$ value attained with CXCL12 stimulation was still lower than non stimulated condition, 0.21 and 0.23 B.U, respectively.

TABLE I. Gαi activity by CXCR4 mutants. Analysis of the Gαi activity of CXCR4, wild-type or different mutants, after fitting the data of Figure 15 with a sigmoidal curve. CI reflects the 95% confidence interval. Highlighted data indicate important results that are further discussed in the text.

Receptor	Maximum Inhibition ± CI / %	LogEC50 ± CI/ M
CXCR4-wt	73.0 ± 3.7	-9.99 ± 0.18
D133N	63.0 ± 3.3	-10.3 ± 0.19
R134A	20.6 ± 9.5	-7.85 ± 0.69
Y135A	46.1 ± 2.5	-9.86 ± 0.19
N119D	72.5 ± 5.3	-9.42 ± 0.21
N119S	43.0 ± 5.8	-9.03 ± 0.46
N119K	35.8 ± 10.0	-8.28 ± 0.72

As the level of transfection of Epac varied in each experiment, normalization was necessary. The $BRET^2$ values were normalized between 0 and 100%, where 100% was the level of the $BRET^2$ signal before adding either the forskolin or CXCL12, and 0% was the one measure after adding only forskolin.

Unfortunately, one technical limitation of this approach is, as we are normalizing the data between 0 and 100%, no basal G_α activity can be assessed. If a mutant has a constitutive intrinsic potential to activate Gαi, this will be curtained by the normalization. For these reasons, these results can only be used to make observations about the ability of a mutant to further activate the Gαi, beyond any constitutive capacity. Any inference about the intrinsic basal capacities of these mutants requires further experiments.

By comparing the different mutants to the wild-type, we found that D133N (Fig. 15B) N119D (E) followed a similar pattern. For Y135A (D), the curve has a logEC50 close to the wild-type, - 9.86, while attaining a maximum inhibition of 46.1%, compared to the 73.0%

observed with the wild-type. Although this suggests that the three mutants can activate the Gαi with the same potency and efficacy, it does not rule out the presence of any basal activity.

Only the three mutants R134A, N119S, and N119K showed distinctive patterns. The mutant R134A was found defective in its capacity to activate Gαi (C). It had a logEC50 of -7.85 M, and a maximum inhibition of 20.6%. The slight increase occurring at high doses of CXCL12 was due to other chemokine receptors, endogenous to the HEK293E, and was similar to the pattern found on non-transfected cells (84).

The mutant N119K (G) showed a pattern similar to R134A, suggesting that a mutant was unable to activate the Gαi pathway. It had a maximum inhibition of 35.8% with a logEC50 of -8.28 M. The two lower potencies associated with R134A and N119K supported their incapacity to activate Gαi. Even if this implied the inability of this mutant to activate the Gαi protein, other possibilities could explain these results. However, Berchiche et al. confirmed that the mutant was adequately expressed on the cell surface with a similar stability to the wild-type (84), and Zhang et al. had showed that its capacity to bind CXCL12 did not vary considerably from the wild-type (85).

Finally, the chemokine CXCL12 had a lower potency and efficacy in inhibiting the effect of forskolin on the mutant N119S (F). Compared to the wild-type, this mutant showed a lower maximum inhibition of 43.0% and a higher logEC50 of -9.03.

As mentioned earlier, the basal activities of these mutants could not be assayed. However, several previously published reports had determined this activity (84,85). Based on these, we know that only the mutant N119S showed a constitutive basal activity and that both N119K and R134A lacked any activity, basally or even after stimulation, thus confirming their incapacity to activate the Gαi pathway. Other experiments could be performed to complement these results and specifically study the basal Gαi activity, such as, quantifying the concentration of cellular cAMP (133). Comparing this concentration between cells transfected with different mutants would indicate if any mutant showed a lower concentration compared to the wild-type, even before stimulation, indicating a constitutive Gαi activity.

Our results are supported by previous ones (84). As discussed in the '1.7. The Conserved DRY-motif' section, Berchiche et al. have found that R134A loses its G-protein activity because of reduced GTPγS binding to the membranes containing this mutant. Also, N119S shows high basal GTPγS binding. Similarly, Zhang et al. have shown that N119S is constitutively activating the Gαi (85), which is in accordance with our results. We also showed that N119D is similar to the wild-type and that N119K is unable to activate this pathway.

As mentioned earlier, the two previous reports studying these mutants only showed the potential to activate the G-proteins in general. Here, we complete those results by explicitly studying the Gαi and showing the effects of the mutations on the latter, without ruling out the possibility of another G-protein activity present as well (60).

4.2. β-Arrestin2 Recruitment by CXCR4 Mutants

The DRY and N119 mutants have only been assayed for their G-protein activity (84,85). Moreover, no previous report has studied the importance of these residues in other CXCR4 pathways such as the β-arrestin. Here, we decided to examine the different mutants for their respective recruitment of β-arrestin2.

This was done using a $BRET^2$ assay, where the receptor, wild-type or mutant, was tagged with Rluc3 and β-arrestin2, with GFP^{10} (120). Both plasmids were transfected in HEK293E cells. The assay was designed in a dose-response model where the ligand CXCL12 concentration was varied between 10^{-6} and 10^{-11}M. The experiment was carried out in triplicate, and was repeated at least three independent times. Upon stimulation, this dose-response showed a sigmoidal curve for the CXCR4 wild-type, with a logEC50 of -7.26 (Fig. 16A and Table II) and a maximum signal of 0.086 B.N.U.

Again, similar to their Gαi activity, the mutants D133N (B), Y135A (D), and N119D (E) followed a comparable pattern to the wild-type one. This implied that the three mutants were similar to the wild-type on both pathways: Gαi and β-Arrestin2.

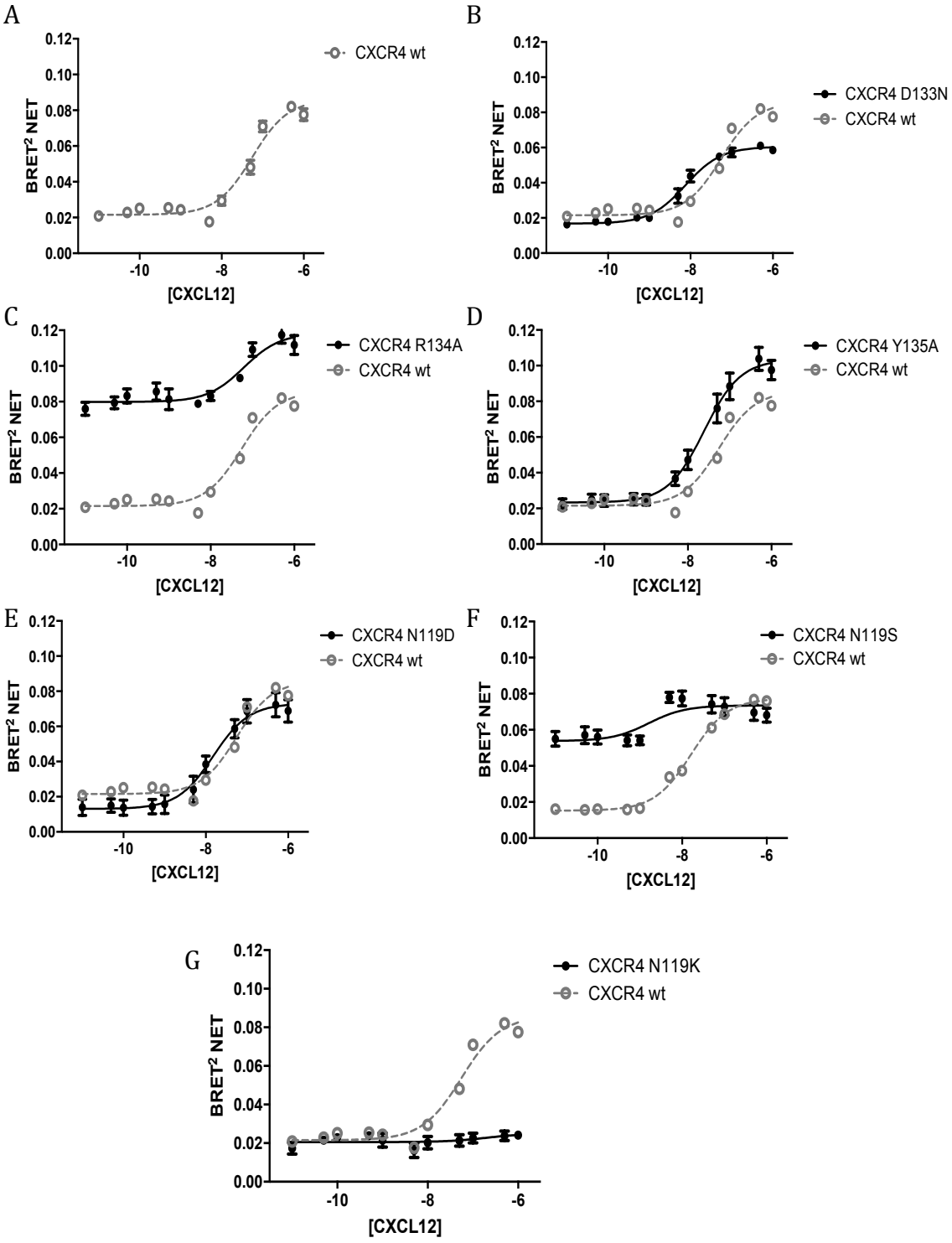
A
B
C
D
E
F
G
BRET² NET
[CXCL12]
CXCR4 wt
CXCR4 D133N
CXCR4 R134A
CXCR4 Y135A
CXCR4 N119D
CXCR4 N119S
CXCR4 N119K

Figure 16. β-arrestin2 recruitment by CXCR4 mutants using BRET^2. β-arrestin2 recruitment is measured using a BRET^2 assay. HEK293E cells were cotransfected with the β-arrestin2-GFP^{10} plasmid and either CXCR4-Rluc3 wild-type (a) or one of its 6 mutants: D133N (b), R134A (c), Y135A (d), N119D (e), N119S (f), or N119K (g). Cells were stimulated with CXCL12 for 5min at 37˚C and 10min at room temperature prior to measures. CXCL12 doses were varied between 10^{-6} and 10^{-11} M. The wild-type dose-response curve is showed in the background of each panel as a grey dashed line. Each point represents the mean ± SEM of at least three independent experiments, each conducted as triplicates.

Nevertheless, the conformation of the complex CXCR4-β-arrestin2 might not be shared between the wild-type receptor and the three mutants. Even as different BRET^2 values might indicate a different conformation, the opposite was not always true, meaning that two or more different conformations might share the same BRET^2 values. This occurs when the distance and the angle between the two BRET^2 tags remain constant.

Surprisingly, R134A had a high basal BRET^2 signal of 0.080 B.N.U even without stimulation (C). This signal was as high as the wild-type maximum stimulated one, thus implying a constitutive recruitment of β-arrestin2 to this receptor. However, stimulation with CXCL12 further increased the BRET^2 signal to a maximum of 0.118 B.N.U. As well, N119S followed a similar pattern to the R134A one, with different values (F). The curve had a basal value of 0.054 B.N.U, with a slight increase upon stimulation to reach a maximal value of 0.074 B.N.U. These high basal values observed with the two mutants R134A and N119S could reflect either constitutive recruitment to the receptor or high levels of BRET^2 donor/acceptor ratio. To exclude this latter possibility, titration assays are required.

Finally, N119K showed a basal line of 0.0206 B.N.U (G). This mutant was unresponsive to stimulation with CXCL12, showing no significant change in the BRET^2 signal. As this mutant was adequately expressed on the cell surface (84) and effectively bound to CXCL12 (85), this could be interpreted as an inability to recruit β-arrestin2. However, we could not exclude the possibility that the experimental system was not sensitive enough to detect such recruitment or that the recruitment occurred in a conformation different than the wild-type, leaving the two BRET^2 tags separated far enough to not generate a BRET signal.

TABLE II. β-arrestin2 recruitment by CXCR4 mutants using BRET^2. Analysis of the β-arrestin2 recruitment of CXCR4, wildtype or different mutants, after fitting the data of Figure 16 with a sigmoidal curve. CI indicates the 95% confidence interval. B.N.U: BRET^2 NET Unit. Highlighted data indicate important results that are further discussed in the text.

Receptor	Bottom ± CI/(B.N.U)	Top ± CI/(B.N.U)	LogEC50 ± CI/ M
CXCR4-wt	0.022 ± 0.002	0.086 ± 0.005	-7.26 ± 0.14
D133N	0.017 ± 0.002	0.061 ± 0.003	-8.12 ± 0.16
R134A	0.080 ± 0.003	0.118 ± 0.008	-7.21 ± 0.36
Y135A	0.023 ± 0.004	0.103 ± 0.007	-7.61 ± 0.21
N119D	0.013 ± 0.005	0.073 ± 0.007	-7.82 ± 0.29
N119S	0.054 ± 0.005	0.074 ± 0.004	-8.79 ± 0.68
N119K	0.021 ± 0.002	0.025 ± 0.009	N/A

The constitutive recruitment could also be confirmed using another technique, possibly a co-localization assay, with confocal microscopy (134). The distribution of β-arrestin2 between the cytoplasm, cell membrane, and intracellular compartments changes after stimulation. This assay can provide quantitative data by analyzing it with a high content imaging system like the INCell^{TM} Analyzer. The advantages of this method over the BRET^2 assay would include: (i) visualizing the β-arrestin2 distribution in the membrane or the vesicles in real time, (ii) combine the recruitment assay with receptor internalization and the trafficking data (17).The analysis of the Gαi signaling and the β-arrestin2 recruitment by these different mutants showed some discrepancies between the two pathways. Although the wild-type CXCR4 and the mutants D133N, Y135A, N119D, and N119S were all able to efficiently activate both pathways, the rest of the mutants were not. For instance, R134A showed a constitutive recruitment of β-arrestin2; nonetheless, it was not able to signal through the Gαi pathway. The mutant N119K was not able to activate either pathway.

4.3. Titrations of β-Arrestin2 Recruitment

Both R134A and N119S have high basal constitutive signals. Titration experiments would clarify if the constitutive signal observed with the mutants R134A and N119S was due to constitutive β-arrestin2 recruitment or only related to the high expression of the GFP^{10} tagged proteins. Also, it would offer an indication about the specificity of the interaction between the two proteins and how the stimulation changed their affinity ($BRET_{50}$) or the conformation of the complex ($BRET_{max}$).

As described under '3.5. Titrations Assays', the concentration of CXCR4-Rluc3, wild-type or mutants was held constant at 0.05 µg of plasmid per transfection well. However, the concentration of GFP^{10}-β-arrestin2 varied between 0.05 µg and 1.95 µg of plasmid per transfection well. After transfection, the cells were either stimulated or not, with the same saturating dose of 200 nM CXCL12, for 5 minutes, at 37˚C. These conditions were high enough to saturate β-arrestin2 recruitment (Fig. 16).

For the wild-type receptor, the $BRET^2$ signal in the function of the GFP^{10}/Rluc3 ratio followed a straight line for the non-stimulated condition (Fig. 17A). As discussed previously in the '3.8. BRET' section, this was indicative of a non-specific interaction and a signal was issued by random collisions. Stimulation with CXCL12 gave a hyperbole curve with higher $BRET^2$ values, supporting an increase in affinity and proximity between the two proteins, CXCR4 and β-arrestin2. This was indicative of a specific recruitment of β-arrestin2 to CXCR4.

The mutant R134A showed two hyperboles, one for the non-stimulated condition and one for the stimulated condition (Fig. 17B). However, the values of their $BRET_{50}$ and $BRET_{max}$ were different. This supported the proposal that R134A was constitutively recruiting β-arrestin2. CXCL12 did not change $BRET_{50}$ significantly (*p*-value = 0.26), while it increased $BRET_{max}$ (*p*-value = 0.005) (Table III). Just as $BRET_{max}$ is dependent on the conformation, $BRET_{50}$ is dependent on the affinity. This suggested a change in the conformation between the two proteins R134A and β-arrestin2, bringing the two tags closer to each other upon stimulation with CXCL12.

A: CXCR4-wt

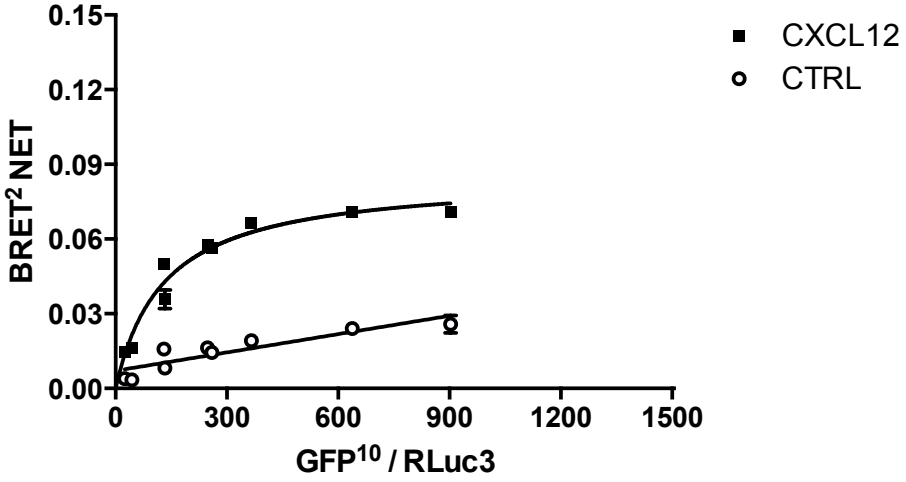

B: CXCR4-R134A

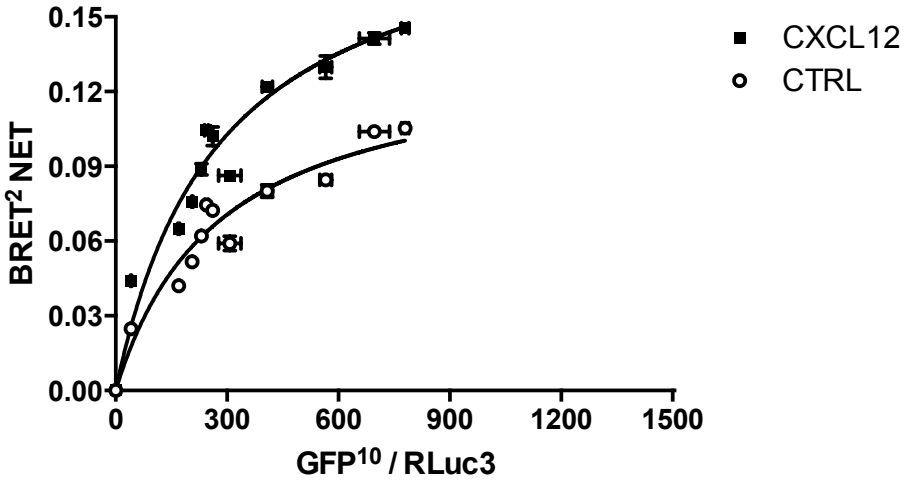

C: CXCR4-N119S

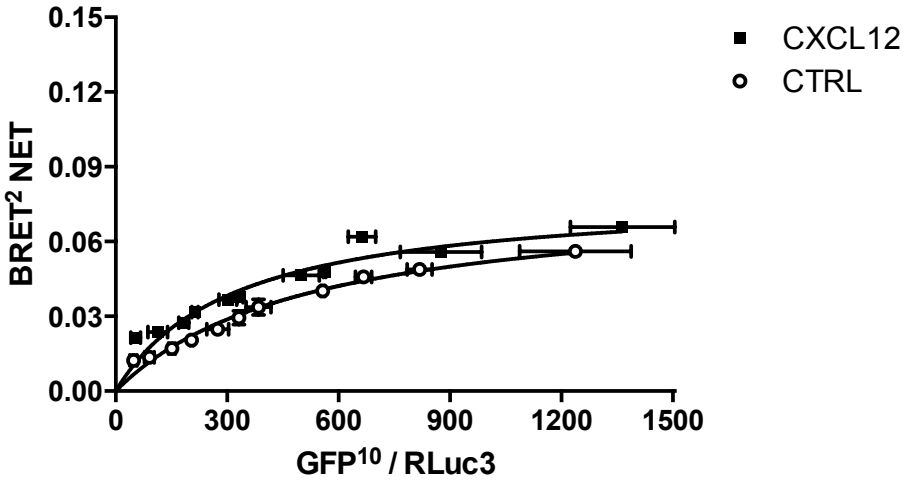

Figure 17. Titrations of β-arrestin2 recruitment by CXCR4 mutants using BRET^2. HEK293E cells were cotransfected with 0.05µg of CXCR4-Rluc3, wild-type, R134A, or N119S with a varying quantity of β-arrestin2-GFP10, between 0.05µg and 1.95µg. 48h post-transfection, cells were stimulated with a saturating dose of CXCL12, 200nM for 5min at 37˚C, and 10min at room temperature. Wild-type titration was performed once, R134A three times, and N119S twice, each conducted as triplicates. Each point represents the mean ± SEM of all performed experiments pooled together.

TABLE III. Titrations of β-arrestin2 recruitment by CXCR4 mutants. Data from Figure 17 were fitted with a hyperbola curve. CI indicates the 95% confidence interval. *P*-value reflects a comparison of the parameters between the control and stimulated conditions, using a comparison of fit test as defined by GraphPad Prism 6.0. CXCR4-wt non-stimulated condition was fitted with a linear curve. *: Significant difference. Highlighted data indicate important results that are further discussed in the text.

Treatment	$BRET_{50}$ ± CI	*p*-value	$BRET_{max}$ ± CI / B.N.U	*p*-value
CXCR4-wt				
CXCL12	131 ± 35		0.085 ± 0.007	
CXCR4-R134A				
CTRL	327 ± 96	0.26	0.146 ± 0.019	0.005 *
CXCL12	259 ± 67		0.192 ± 0.020	
CXCR4-N119S				
CTRL	556 ± 118	< 0.001 *	0.081 ± 0.009	0.57
CXCL12	308 ± 76		0.078 ± 0.008	

Furthermore, the mutant N119S showed two hyperboles, supporting the constitutive recruitment of β-arrestin2 by this mutant (Fig. 17C). However, $BRET_{50}$ decreased (*p*-value < 0.001) and $BRET_{max}$ did not change significantly (*p*-value = 0.57) (Table III). This suggested that CXCL12 increased the affinity between CXCR4-N119S and β-arrestin2.

Although the data supports a constitutive recruitment of β-arrestin2 to the two mutants, R134A and N119S, it does not mean that these mutants are constitutively active on every signaling pathway downstream of β-arrestin2, such as the ERK pathway. This recruitment may not be in a conformation capable of activating such pathways and only testing these signaling pathways can elicit whether β-arrestin2 is constitutively active on them or not.

Combined with the Gαi activity, these results confirm that N119S is a CAM on both Gαi and β-arrestin2 pathways. As well, it shows that R134A is a CIM, as it is deprived of G-protein signaling, while constitutively recruiting the β-arrestin2.

4.4. Differential Conformational Basal β-Arrestin2 Recruitment by CXCR4 Mutants

As we had two mutants that were constitutively recruiting β-arrestin2, one with a constitutive Gαi activity (N119S), and one without (R134A), we wanted to compare the modalities of β-arrestin2 recruitment between the two mutants. The modalities of the recruitment included all the properties of the interaction between the receptor and β-Arrestin2, such as: The affinity and distance between the two proteins, the dynamics and the kinetics of the interaction, and the conformation of the complex. Here only two of these parameters are being compared between the two mutants: The relative affinity and the distance/ conformation between the receptor and the β-arrestin2.

This was accomplished by performing titrations similar to the ones described earlier, while keeping the cells non stimulated. The basal activity of the wild-type receptor and the two mutants were compared. While these conditions are shown in Fig. 17, we could not compare the three receptors back then, as each panel presented there was done separately, and we were obligated to change the BRET reader between the experiments, leading to differences in sensitivity. For this reason, the wild-type and the two mutants were done here in parallel, ensuring better control between the three receptors. Only the curve of N119S was shared, however, with Fig. 17C, as that whole panel was done in parallel with Fig. 18.

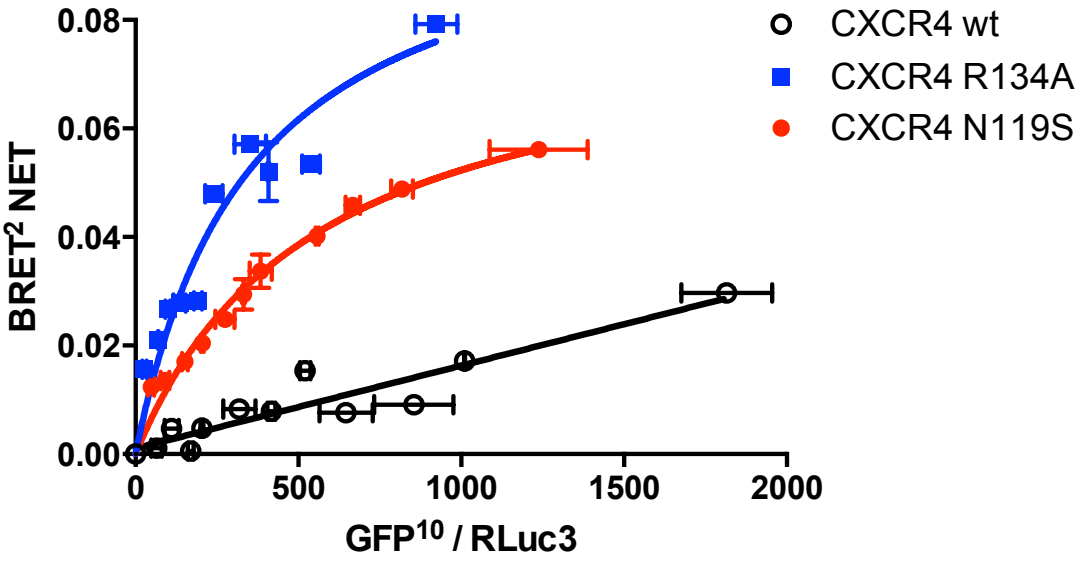

Figure 18. Titrations of basal β-arrestin2 recruitment by CXCR4 mutants using BRET^2. β-arrestin2 recruitment is measured using a BRET^2 assay. HEK293E cells were cotransfected with 0.05µg of CXCR4-Rluc3, wild-type, R134A, or N119S with a varying quantity of β-arrestin2-GFP10, between 0.05µg and 1.95µg. 48h post-transfection, BRET^2 measures were taken. Each point represents the mean ± SEM of at least two independent experiments, pooled together, each conducted as triplicates.

TABLE IV. Analysis of titrations of basal β-arrestin2 recruitment by CXCR4 mutants. Data from Figure 18 were fitted with a hyperbola curve. CI indicates the 95% confidence interval. *P*-value reflects a comparison of the parameters between the two mutants R134 and N119S, using a comparison of fit test as defined by GraphPad Prism 6.0. CXCR4-wt non-stimulated condition was fitted with a linear curve. *: Significant difference. Highlighted data indicate important results that are further discussed in the text.

Receptor	$BRET_{50}$ ± CI	*p*-value	$BRET_{max}$ ± CI / B.N.U	*p*-value
CXCR4-R134A	352 ± 123	0.040 *	0.105 ± 0.176	0.025 *
CXCR4-N119S	556 ± 118		0.081 ± 0.009	

The CXCR4-WT followed a straight line, indicative of non-specific, non-saturable random collisions (Fig. 18), while the two mutants showed a hyperbolic saturation curve, similar to what was observed in Fig. 17. However, these two hyperboles had different parameters. R134A showed a lower $BRET_{50}$, indicative of a higher affinity for β-arrestin2 recruitment (*p*-value = 0.040), and a higher $BRET_{max}$ (*p*-value = 0.025) (Table IV), indicating different conformations.

This data indicates that the two mutants had different modalities of basal β-arrestin2 recruitment, varying in both affinity and conformation.

As mentioned in the 'Introduction' section, the modalities of β-arrestin recruitment can vary depending on the conformation of the receptor or the phosphorylation of its C-terminal (23).These results can be interpreted as if the two mutants have different basal conformations leading to the different modalities of β-arrestin2 recruitment. Another possibility is the differential phosphorylation. CXCR4 is phosphorylated by GRKs 2, 3, 5, and 6 (12). We can hypothesize that each of the two mutants R134A and N119S adopt a constitutive conformation that is compatible with phosphorylation by different GRKs or on different residues. This will explain the difference in the β-arrestin2 recruitment modalities witnessed between the two mutants. To assess this differential phosphorylation, we can use mass spectrometry or mutate the different phosphorylation sites of the C-terminal of these mutants and observe the outcome on β-arrestin2 recruitment (14). Only mutating the sites implicated in the recruitment to each mutant will effectively alter this recruitment, giving an indication as to which of the sites are phosphorylated and by which GRK.

Depending on the conformation of its recruitment, β-arrestin can act as scaffolding for different cargos of various proteins. Among these we can find the MAPK pathway, the E3 ubiquitin ligases, or the endocytotic machinery. Differences in modalities of β-arrestin2 recruitment between the two mutants can result in differences in the recruitment of these cargos and the activation of downstream signaling pathways, or trafficking of the receptor.

4.5. Effect of Pertussis Toxin on Gαi Activity and β-Arrestin2 Recruitment

We wanted to assess whether the basal recruitment of β-arrestin2 by N119S, and R134A is dependent on the Gαi activity. To answer this question, we used pertussis toxin (PTX). PTX inhibited this pathway by ADP-ribosylating the α subunit of the heterotrimeric G-proteins of the G_i family (58).

First, we wanted to confirm the efficiency of the PTX and the conditions used to inhibit the Gαi activity. This was performed by the Epac method, with cells transfected with the wild-type CXCR4 receptor and incubated with 100 µg/L PTX at 37˚C, for 20 hours, prior to stimulation. Stimulation was conducted with saturating doses of 20 µM of forskolin alone or combined with 100 nM CXCL12. The data were pooled from three independent experiments conducted in triplicates.

As expected, the forskolin pre-stimulation decreased the $BRET^2$ signal by increasing the cAMP level (Fig. 19A). This effect was significant with a decrease from 0.18 to 0.14 B.N.U (*p*-value = 0.004) (Table V). The stimulation of CXCL12 on top of the forskolin did not change the level of cAMP, and gave a $BRET^2$ signal of 0.14 (*p*-value > 0.99). This confirmed the efficiency of the PTX, as it inhibited the activation of Gαi by the wild-type CXCR4, after stimulation with its agonist CXCL12. Next, we assessed the effect of PTX on β-arrestin2 recruitment. We performed all conditions in the presence of PTX. The cells were transfected with β-arrestin2-GFP^{10} and one of the receptors, CXCR4-WT, R134A or N119S. The $BRET^2$ levels were measured after stimulation with either the vehicle or 100 nM CXCL12.

One interesting observation is that the two mutants R134A and N119S maintained their high basal signal after the addition of PTX, at 0.073 and 0.057 B.N.U, respectively (Fig. 19B). Both these values are significantly different from the basal wild-type recruitment (*p*-value < 0.001 for R134A, and 0.004 for N119S) (Table VI). This suggests that both mutants constitutively recruit β-arrestin2 even after inhibition of the Gαi pathway by PTX. This supports that β-arrestin2 recruitment by these mutants is independent of the Gαi pathway.

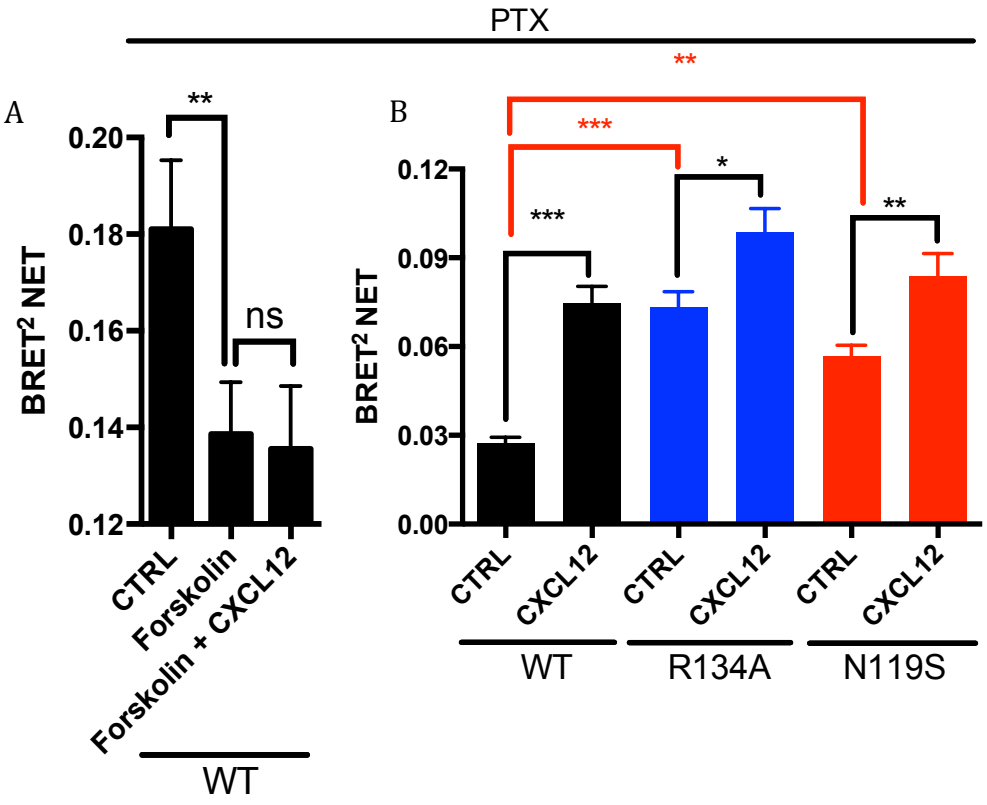

Figure 19. Effect of pertussis toxin on Gαi activity and β-arrestin2 recruitment. HEK293E cells were incubated with 100µg/L PTX at 37˚C, for 20h prior to stimulation in both panels A and B. **A)** Gαi activity is measured by a BRET^2 reporter assay using GFP^{10}-Epac-Rluc3. HEK293E cells were cotransfected with the Epac plasmid and CXCR4-myc wild-type. Cells were stimulated for 10 min at room temperature prior to measurment with forskolin alone or in combination with 200nM CXCL12. **B)** β-arrestin2 recruitment is measured using a BRET^2 assay. HEK293E cells were cotransfected with the β-arrestin2-GFP^{10} plasmid and either CXCR4-Rluc3 wild-type or one of its two mutants: R134A or N119S. Prior to measurements, cells were stimulated for 5min at 37˚C and 10 min at room temperature with vehicle or 200nM CXCL12. These experiments did not directly assess the role of PTX by comparing each condition in its presence and absence; rather, they assessed the ability of CXCL12 and the mutants to further recruit β-Arrestin2. Each column represents the mean ± SEM of at least three independent experiments, each conducted in triplicate. Data were analyzed for significance difference using 1-way ANOVA with Dunnett multiple comparisons. * $p \leq 0.05$, ** $p \leq 0.01$, *** $p \leq 0.001$, ns: Not Significant.

TABLE V. Effect of pertussis toxin on Gαi activity. Analysis of the data presented in Figure 19.A. SEM represents the standard error of the mean. Data were analyzed for significance difference using 1-way ANOVA with Dunnett multiple comparisons. *P*-values indicate the significance of the difference between each condition and the forskolin one. *: Significant difference. Highlighted data indicate important results that are further discussed in the text.

Treatment	$BRET^2$ NET ± SEM/(B.N.U)	*p*-value
CTRL	0.181 ± 0.014	0.004 *
Forskolin	0.139 ± 0.011	
Forskolin + CXCL12	0.136 ± 0.013	> 0.99

TABLE VI. Effect of pertussis toxin on β-arrestin2 recruitment. Analysis of the data presented in Figure 19.B. SEM represents the standard error of the mean. Data were analyzed for significance difference using 1-way ANOVA with Dunnett multiple comparisons. The basal activity of each mutant was compared to the wildtype, and the *p*-value indicates the significance of this difference. *: Significant difference. Highlighted data indicate important results that are further discussed in the text.

CXCR4-wt vs. CXCR4-R134A	< 0.001 *
CXCR4-wt vs. CXCR4-N119S	0.004 *

However, with this experimental design, where each condition is not done in the presence and absence of PTX in parallel, we cannot rule out the possible role of Gαi in the recruitment of β-arrestin2. This means that it is possible that the recruitment of β-arrestin contains two components, one that is independent of the Gαi and that is responsible for the constitutive recruitment observed here in the presence of PTX, and the other component is dependent on the Gαi, and studying the effect of adding PTX on each mutant would help elucidate its presence.

Subsequently, we assessed the effect of stimulating the three receptors with CXCL12 while blocking the Gαi with PTX. This ligand demonstrated an agonist effect on the wild-type receptor, increasing the β-arrestin2 recruitment to it, and raising the signal significantly from 0.027 to 0.075 B.N.U (*p*-value < 0.001) (Fig. 19B and Table VII). This supported the evidence that the recruitment of β-arrestin2 to the wild-type is independent of the Gαi pathway, as it occurs even after blocking this latter. Similar results were observed with the two mutants, R134A and N119S. However, we did not assess whether the increase of signal on the mutants after stimulation with CXCL12 was due to an increase in the affinity or to a conformational change.

In conclusion, these results imply that the two mutants have a constitutive β-arrestin2 recruitment that is independent of their Gαi activity.

TABLE VII. Effect of pertussis toxin on β-arrestin2 recruitment. Analysis of the data presented in Figure 19.B. SEM represents the standard error of the mean. Data were analyzed for significance difference using 1-way ANOVA with Dunnett multiple comparisons. For each mutant, the CXCL12 stimulation was compared to the non-stimulated one, and the *p*-value indicates the significance of this difference. *: Significant difference. B.N.U: $BRET^2$ NET Unit. Highlighted data indicate important results that are further discussed in the text.

Ligand	**$BRET^2$ Net ± SEM / B.N.U**	***p*-value**
CXCR4-wt		
CTRL	0.027 ± 0.002	
CXCL12	0.075 ± 0.006	< 0.001 *
CXCR4-R134A		
CTRL	0.073 ± 0.005	
CXCL12	0.098 ± 0.008	0.016 *
CXCR4-N119S		
CTRL	0.057 ± 0.004	
CXCL12	0.084 ± 0.008	0.009 *

4.6. Localization of the CXCR4 Mutants

As discussed earlier, both signaling pathways are involved in directing the receptor to the specific cellular organelles. Different signaling patterns lead to differential phosphorylation and ubiquitination of the receptor, directing it to the clathrin-coated vesicles, endosomes or lysosomes. As the CXCR4 mutants described here differ in their signaling pattern, both on the Gαi pathway and β-arrestin2 recruitment, we wanted to assess the effect of these mutations on receptor trafficking and localization.

We performed real-time imaging of live HEK293E cells using spinning disk confocal microscopy, where HEK293E, transfected with CXCR4-YFP, wild-type or one of its mutants, were imaged.

First, the cells transfected with the wild-type were incubated with 200 nM CXCL12 and filmed before stimulation, and for one hour and fifteen minutes after stimulation. A control condition was conducted in parallel, where the cells were incubated with the vehicle.

Incubation with CXCL12 led to the redistribution of the wild-type CXCR4 to large, round-shaped, intracellular vesicles, while maintaining the diffuse membranous distribution (Movie.1). This was used as a control of the efficiency of the system, and to ensure that the cells were maintained alive during the imaging process.

Even though this experiment does not demonstrate the origin of these vesicles, it is plausible to suggest that they arise from the internalization of the receptor.

Secondly, cells transfected with the different mutants have been imaged alive, while being maintained in a steady state, without any stimulation. This experiment has been repeated twice, and a representative image of each mutant is shown in Fig. 20. It is important to keep in mind that this is a pilot experiment and it should not be over-interpreted. Quantification is important to determine the percentage of cells showing the observed pattern of each mutant. As sufficient cells have not been imaged, we cannot perform these quantifications.

CXCR4-Wildtype

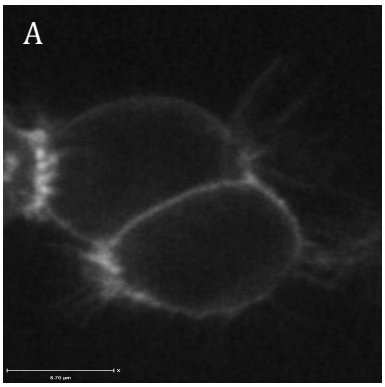

CXCR4-D133N

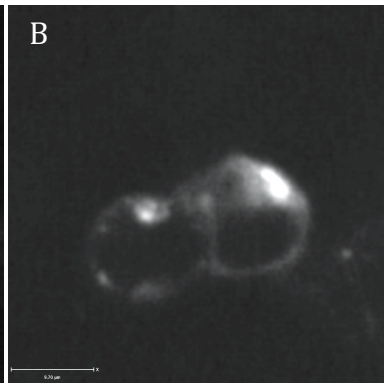

CXCR4-R134A

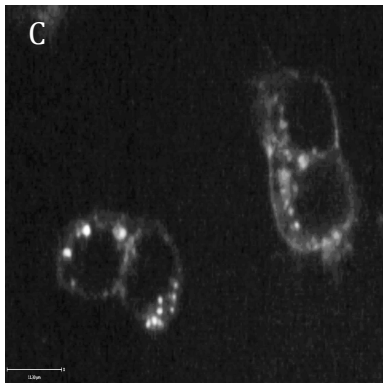

CXCR4-Y135A

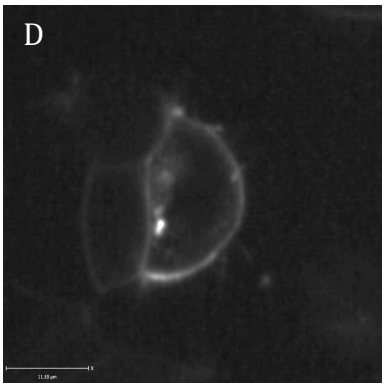

CXCR4-N119D

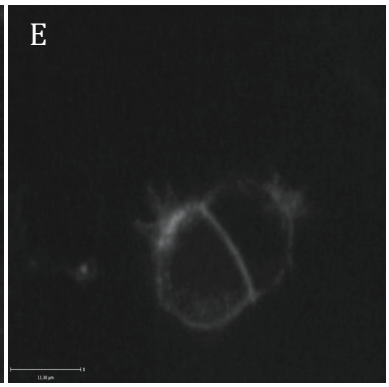

CXCR4-N119S

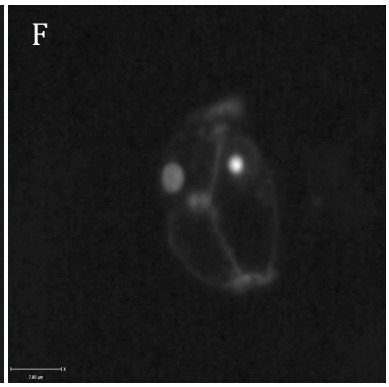

CXCR4-N119K

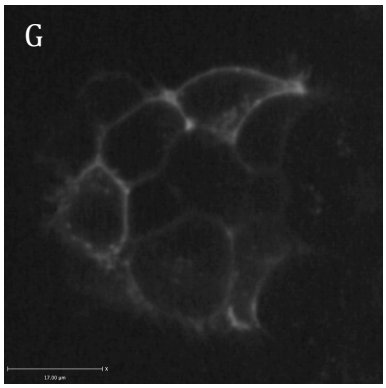

Figure 20. Localization of the CXCR4 mutants by confocal microscopy. HEK293E cells were transfected with 1µg of CXCR4-YFP, wild-type or mutants, in a pcDNA3 plasmid 48h before imaging. After 24h, cells were transferred to 8-well chambered coverglass dishes. Live cell imaging of transfected cells was performed without stimulation at 37°C and 5% CO_2 using an Ultra view Vox spinning disc confocal system, and an Orca-R2 CCD camera. This was combined to a Leica DMI6000B inverted microscope equipped with a motorized piezo-electric stage, and using a scanning unit CSU-X1. Volocity 5 software was used for image acquisition, quantitation, and analysis. Imaging was performed using a Plan Apo 40x (0.85 NA) air objective and a camera binning of 2x2. The YFP tag is observed at 488nm.

Two mutants, D133N (B) and N119S (F) showed an important intracellular concentration, while maintaining their surface expression. The origin of this intracellular pool could not be verified as it might be the consequence of constitutive internalization of the surface receptor, newly synthesized receptors being trafficked to the surface or even a concentrated intracellular pool unable to be delivered adequately to the surface. The singularity of this compartment per cell supports that these mutants are locked along the exocytosis pathway (Golgi apparatus, rough endoplasmic reticulum…).

Surprisingly, the mutant R134A showed a different localization (C). While its distribution was diffuse, it was mainly seen in round-shaped vesicles, while maintaining surface expression comparable to the wild-type (84). The appearance of vesicles observed in the R134A mutant was similar to those seen after stimulation of the wild-type receptor with CXCL12 (Movie.1), suggesting a possible constitutive internalization of R134A to the endosomal vesicles. Nevertheless, we cannot exclude the possibility that they are accumulating after synthesis due to overexpression. Although the round shape of these vesicles cannot give indications of the nature of these structures (early/late endosomes, or lysosomes…), it excludes the multivesicular bodies (MVB) as a possible destination, as they have a more distinct appearance (135).

The internalization described here is not the effect of any ligand, as the mutants are imaged without stimulation. However, it represents the spontaneous internalization of these

mutants, as they have basal conformations different from the wild-type receptor, allowing them to constitutively recruit β-arrestin2, and possibly the endocytic machinery.

The most important and striking difference was observed between R134A and N119S. As both mutants constitutively recruited β-arrestin2, a similar trafficking pattern would be expected. However, R134A was localized on several round-shaped, hollow intracellular vesicles, and N119S on a unique intracellular pool. The differences in number and shape of these vesicles between R134A and N119S might suggest trafficking of the receptor to different organelles. This means that the conformation of the two CXCR4 mutants drives them to various stages along the endocytic pathway, leading to the observable effects.

While it may seem plausible to suggest that the differences in modalities of β-arrestin2 recruitment between the two mutants led to their different localization, a causal link cannot be established. Although we suggest here that the biased trafficking of CXCR4 arises at the endocytosis level, other possibilities cannot be excluded. The differences may arise later, either through direction to separate compartments or through a biased recycling to the cell surface. The intracellular trafficking of the receptor is the result of the equilibrium between two opposed processes: Endocytosis and recycling. A difference in the recycling can also explain these results. It is possible that both conformations induce receptor endocytosis with the same dynamics, showing no biased difference at this level of receptor trafficking. On the other hand, one conformation might have an adverse effect on recycling of the receptor leading to a pseudo-increase of the endocytosis of CXCR4.

This data represents a pilot experiment that indicates the possibility of the biased trafficking of CXCR4, depending on the mutant conformation. Other experiments should be done to further assess this possibility. First, using immunofluorescence we can try to identify the nature of the round-shaped vesicles. Different stages of endosomes implicate different proteins, such as the Lamp proteins in the lysosomes, or the different Rabs observed in varying stages of endosomes. Targeting those with fluorescent antibodies, while visualizing the mutant receptors with their YFP tag, would assess any co-localization of a mutant with a specific endosomal protein, leading to the identification of these vesicles. The identity of these structures might be different between the two mutants, R134A and N119S; thus providing

support to our hypothesis that different β-arrestin2 modalities induce biased trafficking of this receptor.

The concept of biased trafficking has not been assessed in detail so far. This report provides possible support for this notion, while the molecular determinants of this bias remain to be studied. As discussed in the introduction, trafficking and signaling are closely related. The main prospect of this domain is to improve the comprehension of GPCRs trafficking and signaling for better-targeted drug development.

4.7. Effect of AMD3100 and TC14012 on Gαi Signaling

The two synthetic CXCR4 ligands, AMD3100 and TC14012 were thoroughly investigated for their effects on the G-proteins. The previous study of Zhang et al. implied that AMD3100 is a partial agonist on G-signaling, while TC14012 is an inverse agonist on this pathway. However, as described in the introduction, both ligands have only been studied for their capacities to recruit GTPγS, to induce calcium entry, and to activate the transcription of a reporter gene (85). These three pathways are shared among all G-proteins and are thus not specific to Gαi signaling. Due to the clinical importance of AMD3100, a thorough understanding of its signaling effects is primordial.

We used the Epac system described above to assess Gαi activation. The HEK293E cells were transfected with the Epac reporter plasmid, combined with one of the following: pcDNA3 (empty plasmid as a control), CXCR4-Wt, CXCR4-R134A or CXCR4-N119S. Only these two mutants were chosen as they showed distinct patterns from the wild-type, while still demonstrating a capacity to activate at least one of the two pathways of interest. The cells were again pre-stimulated with forskolin, followed by stimulation with one of the three ligands. This was done with one saturating dose of each ligand: 100 nM of CXCL12, 1 µM of AMD3100 or 1 µM of TC14012. This experiment was repeated thrice, independently. Unfortunately, we were obligated to replace the machine between these three experiments. Using a new machine, different levels of $BRET^2$ were observed due to differences in sensitivity. However, the change induced by each ligand was reproducible three times.

For this reason, the data were normalized to the forskolin condition. The difference in BRET^2 induced by the forskolin alone was normalized to 100%, and the effect of the other ligands was compared to that the forskolin.

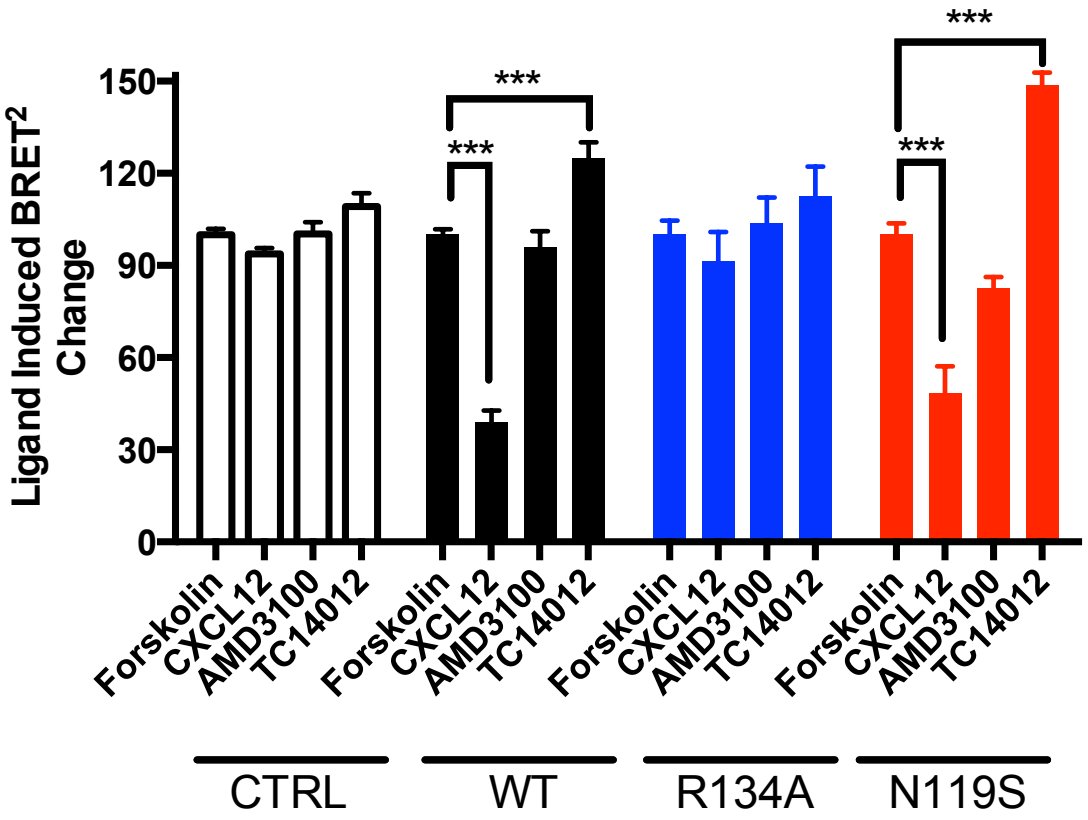

Figure 21. Effect of AMD3100 and TC14012 on Gαi. Gαi activity is measured by the percentage of forskolin inhibition of each receptor. The level of cAMP is assayed by a BRET^2 reporter assay using GFP^{10}-Epac-Rluc3. HEK293E cells were cotransfected with the Epac plasmid and either pcDNA3 (CTRL), CXCR4-myc wild-type or one of its two mutants: R134A or N119S. Prior to analysis, cells were stimulated for 10 min at room temperature with forskolin alone or combined with one of the following ligands: 200nM CXCL12, 1µM AMD3100, or 1µM TC14012. Each column represents the mean ± SEM of at least three independent experiments, each conducted in triplicate. Data were analyzed for significance difference using 1-way ANOVA with Dunnett multiple comparisons. * $p \leq 0.05$, ** $p \leq 0.01$, *** $p \leq 0.001$.

TABLE VIII. Effect of AMD3100 and TC14012 on Gαi activity. Analysis of the data presented in Figure 21. SEM represents the standard error of the mean. Data were analyzed for significance difference using 1-way ANOVA with Dunnett multiple comparisons. For each mutant, the forskolin stimulation was compared to each condition, and the *p*-value indicates the significance of this difference. *: Significant difference. Highlighted data indicate important results that are further discussed in the text.

Ligand	Ligand induced BRET^2 change ± SEM / %	*p*-value
CTRL		
Forskolin	100 ± 2	
CXCL12	94 ± 2	0.40
AMD3100	100 ± 4	> 0.99
TC14012	109 ± 4	0.13
CXCR4-wt		
Forskolin	100 ± 2	
CXCL12	39 ± 4	< 0.001 *
AMD3100	96 ± 5	0.86
TC14012	125 ± 5	< 0.001 *
CXCR4-R134A		
Forskolin	100 ± 5	
CXCL12	91 ± 10	0.78
AMD3100	104 ± 8	0.97
TC14012	113 ± 10	0.57
CXCR4-N119S		
Forskolin	100 ± 4	
CXCL12	48 ± 9	< 0.001 *
AMD3100	83 ± 4	0.12
TC14012	149 ± 4	< 0.001 *

The control condition, shown in Fig. 21, consisted of cells transfected with only the Epac reporter, without any receptor. It aimed to ensure that any changes induced by the ligands were specific to the transfected receptor and not to any endogenous ones. Without a transfected receptor, the three ligands, CXCL12, AMD3100, and TC14012 did not have any significant effect on the $BRET^2$ signal after pre-stimulation with forskolin.

For cells transfected with the CXCR4-wt plasmid, CXCL12 reduced the $BRET^2$ change induced by forskolin to 39% (p-value < 0.001) (Table VIII), confirming its agonist effect on the Gαi pathway. However, AMD3100 showed no significant effect (p-value = 0.927). On the other hand, TC14012 was able to increase the $BRET^2$ change induced by forskolin up to 125%, by increasing the concentration of the cellular cAMP (p-value < 0.001). This increase implied that there was a decrease in the basal activity of CXCR4-wt on the Gαi pathway and supported the proposal that TC14012 was an inverse agonist on this signaling pathway.

The mutant R134A showed no Gαi activity in Fig. 15C. This was supported here, where even stimulation with CXCL12 did not change the $BRET^2$ signal. Also, both ligands, AMD3100 and TC14012 had no significant effect on the cAMP levels, which implied the incapacity of R134A to activate this pathway (Fig. 21 and Table VIII).

Finally N119S, a mutant constitutively active on the Gαi pathway (Fig. 15F) was tested here with the three ligands. Even with a high basal activity N119S was able to further activate this pathway and decrease the levels of cAMP after stimulation with CXCL12. This agonist reduced the forskolin-induced change in $BRET^2$ to 48% (p-value < 0.001). AMD3100 showed a slight reduction in the $BRET^2$ change, decreasing it to 83%, although the significance could not be established (p-value = 0.12).

AMD3100 had no significant effect on this pathway with any of the receptors. This is in contradiction with what Zhang et al. have suggested. They state that AMD3100 is a partial agonist on the Gαi pathway. This difference between their results and ours can be due to a lesser sensitivity in our system of study. However, another possibility can explain this difference, where AMD3100 is a partial agonist on a G-protein different from the Gαi. As Gαi is not activated, AMD3100 would not affect the $BRET^2$ levels of the Epac experiment.

However, the stimulation with AMD3100 partially activates a different Gα subunit, leading to recruitment of GTPγS, reporter gene transcription, and calcium entry, the three effects of AMD3100 observed by Zhang et al. (85). Some other experiments can help elucidate whether this hypothesis is true, such as, repeating the experiments conducted by Zhang in the presence of a PTX. As PTX inhibits Gαi, if AMD3100 exhibits a partial agonist effect in the presence of this toxin it will confirm that its effect is independent of Gαi and that it occurs through a different G-protein, such as, Gαq/11 (59-61) or Gα12/13 (60,62).

On the other hand, TC14012, similar to the wild-type receptor, was able to further increase the $BRET^2$ change. Nonetheless, this change was more important with N1119S for an increase of up to 149% (p-value < 0.001) (Table VIII). An increased $BRET^2$ change signified a further decrease in Gαi signaling. This would not be possible unless N119S had a higher basal activity to begin with, which provided further support to the constitutive Gαi signaling of this mutant. These results were in accordance with Zhang et al. (85), and provided support that the inverse agonism effects exhibited by TC14012 and observed by Zhang were indeed induced through the Gαi pathway.

In conclusion, we can extrapolate that CXCL12 is an agonist on the Gαi pathway, showing activity on both the wild-type receptor and N119S mutant. The effect of AMD3100 was not significant on Gαi signaling through any of the three receptors. Finally, TC14012 demonstrated an inverse agonism on the wild-type and N119S, with a more pronounced effect on the latter, which was compatible with this mutant's constitutive activation of the Gαi pathway. As β-arrestin2 was the other major pathway associated with CXCR4, the next step was to determine the effect of these ligands on β-arrestin2 recruitment.

4.8. Effect of AMD3100 and TC14012 on β-Arrestin2 Recruitment

With the development of the biased signaling concept, assuming that the effects of the ligand on Gαi and β-arrestin are always correlated is not an option anymore. To adequately study the signaling of both ligands, we should study their effect on the recruitment of β-arrestin and see if this correlates with Gαi activity. As discussed earlier, AMD3100 is a partial agonist on some G-protein signaling pathways, while TC14012 is an inverse agonist on the Gαi pathway. However, these two ligands have not been tested on their ability to recruit β-arrestin2 to CXCR4.

For recruitment of β-arrestin2, an experiment was conducted using the same method described above. The HEK293E cells were transfected with the β-arrestin2-GFP[10] plasmid and combined with one of the following: CXCR4-WT-Rluc3, CXCR4-R134A-Rluc3 or CXCR4-N119S-Rluc3. The cells were stimulated with one saturating dose of each ligand: 100 nM of CXCL12, 1 μM of AMD3100 or 1 μM of TC14012.

First, the wild-type receptor showed low basal recruitment with a $BRET^2$ level of 0.014 B.N.U (Fig. 22). This was a nonspecific BRET signal, as shown in the titrations of Fig. 17.

The $BRET^2$ value increased very significantly up to 0.050 B.N.U, upon stimulation with CXCL12 (p-value < 0.001) (Table IX). This is expected, as we know that CXCL12 is an agonist on β-Arrestin2 recruitment (Fig. 15A). Adding the ligand AMD3100 was able to counteract the effect of CXCL12, when combined with the latter (p-value < 0.001). This confirmed the antagonism effect of AMD3100 on the CXCR4 receptor, and was used as a control showing the presence of active AMD3100 in the stimulation solution. Nevertheless, AMD3100 alone was not able to recruit the β-arrestin2 to the wild-type receptor (p-value > 0.99) (Table IX). Similarly, the synthetic ligand TC14012 showed no significant effect on β-arrestin2 recruitment (p-value = 0.25). As both these ligands did not induce an effect on the recruitment to the wild-type receptor, we can exclude any agonistic effect.

A

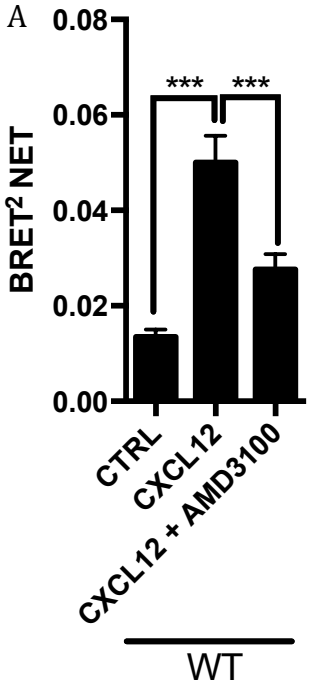
0.08
0.06
0.04
0.02
0.00
BRET2 NET
***
***
CTRL
CXCL12
CXCL12 + AMD3100
WT

B

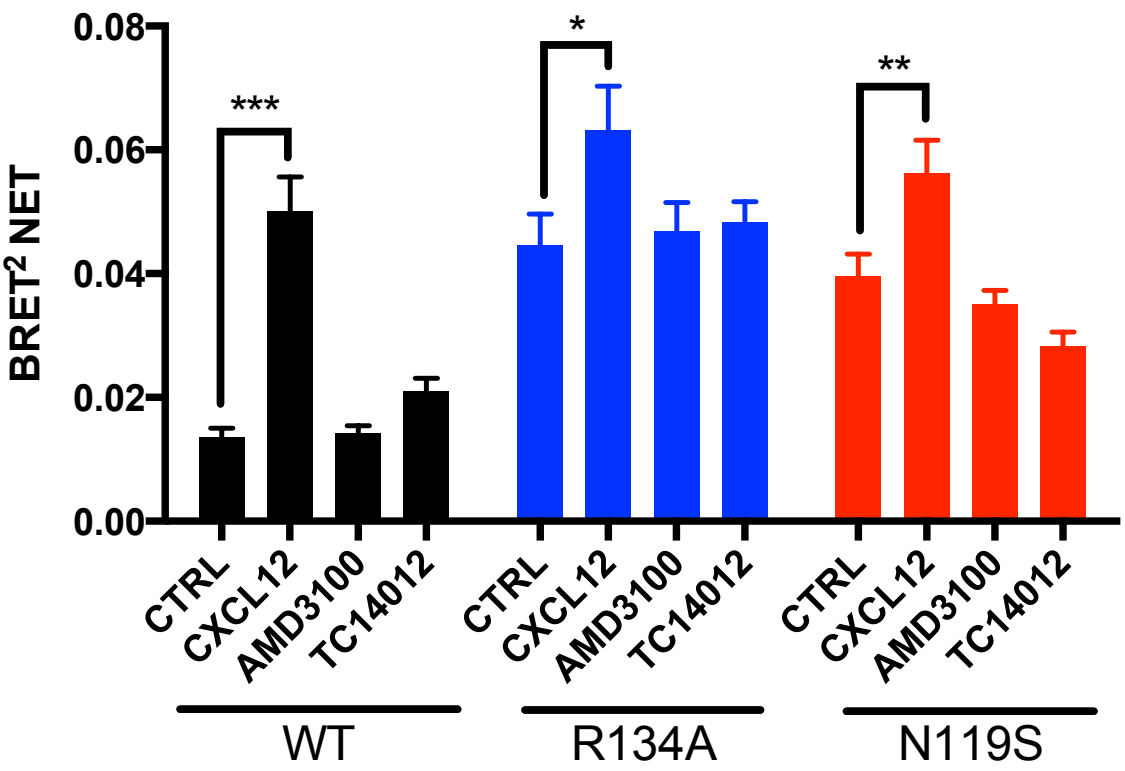
0.08
0.06
0.04
0.02
0.00
BRET2 NET
***
*
**
CTRL
CXCL12
AMD3100
TC14012
CTRL
CXCL12
AMD3100
TC14012
CTRL
CXCL12
AMD3100
TC14012
WT
R134A
N119S

Figure 22. Effect of AMD3100 and TC14012 on β-arrestin2 recruitment. β-arrestin2 recruitment is measured using a $BRET^2$ assay. HEK293E cells were co-transfected with the β-arrestin2-GFP^{10} plasmid and either CXCR4-Rluc3 wild-type or one of its two mutants: R134A or N119S. Prior to measurement, cells were stimulated for 5 min at 37˚C and 10 min at room temperature with one of the following ligands: 200nM CXCL12, 1μM AMD3100, or 1μM TC14012. **A)** The effect of AMD3100 on CXCL12 agonism is assessed. **B)** The effect of the three ligands on each of the three mutants is studied. Each column represents the mean ± SEM of at least three independent experiments, each conducted in triplicate. Data were analyzed for significance difference using 1-way ANOVA with Dunnett multiple comparisons. * $p \leq 0.05$, ** $p \leq 0.01$, *** $p \leq 0.001$.

For the mutant R134A, we observed a high basal signal 0.045 B.N.U. Stimulating the cells with CXCL12 increased the $BRET^2$ further to 0.063 B.N.U (*p*-value = 0.045). This increase was mainly due to a conformational change, rather than an increase in the recruitment of β-arrestin2, based on the titration shown in Fig. 17. Neither AMD3100 nor TC14012 showed any effect on β-arrestin2 recruitment to the R134A mutant (*p*-value = 0.98 and 0.93 respectively). The lack of an effect by these ligands could also be related to a change in the binding affinity of R134A to both ligands and binding experiments should be done to exclude this possibility.

Finally, the other constitutively β-arrestin2 recruiting mutant N119S showed a high $BRET^2$ signal of 0.040 B.N.U. In a similar manner to R134A, stimulating this mutant with CXCL12 further increased the signal to 0.056 B.N.U. (*p*-value = 0.009). However, this increase was due to an augmented affinity between CXCR4-N119S and β-arrestin2, and an increase in β-arrestin2 recruitment (Fig. 17).

Stimulating N119S with both synthetic ligands had surprising outcomes. Both AMD3100 and TC14012 decreased slightly, but not significantly, the signal down to 0.035 B.N.U (*p*-value = 0.70) and 0.028 B.N.U (*p*-value = 0.09), respectively (Table IX). However, neither ligand was able to bring down the level of recruitment to the level of a non-stimulated CXCR4-WT. With a significance level of 0.09, it is difficult to conclude the presence of an effect, or its absence.

TABLE IX. Effect of AMD3100 and TC14012 on β-arrestin2 recruitment. Analysis of the data presented in Figure 22. SEM represents the standard error of the mean. Data were analyzed for significance difference using 1-way ANOVA with Dunnett multiple comparisons. For each mutant, the control condition was compared to each stimulant, and the *p*-value indicates the significance of this difference. B.N.U: $BRET^2$ NET Unit. *: Significant difference. Highlighted data indicate important results that are further discussed in the text.

Ligand	$BRET^2$ Net ± SEM / B.N.U	*p*-value
CXCR4-wt		
CTRL	0.014 ± 0.002	
CXCL12	0.050 ± 0.006	< 0.001 *
AMD3100	0.014 ± 0.001	> 0.99
TC14012	0.021 ± 0.002	0.25
CXCR4-R134A		
CTRL	0.045 ± 0.005	
CXCL12	0.063 ± 0.007	0.045 *
AMD3100	0.047 ± 0.005	0.98
TC14012	0.048 ± 0.003	0.93
CXCR4-N119S		
CTRL	0.040 ± 0.004	
CXCL12	0.056 ± 0.005	0.009 *
AMD3100	0.035 ± 0.002	0.70
TC14012	0.028 ± 0.002	0.09

However, this decrease does not necessarily reflect a decrease in the recruitment of β-arrestin2, as the $BRET^2$ values reflect changes either in the recruitment or the conformation of the complex. To study this effect, a titration experiment must be conducted, comparing the affinity between CXCR4-N119S and β-arrestin2 and the conformation of their complex, with or without stimulation with TC14012. Also, we need to verify that TC14012 cannot further decrease the recruitment of β-arrestin2 to N119S, and whether its effect was limited by the ligand concentration.

In conclusion, we have one mutant, N119S, which is constitutively activating Gαi and recruiting β-arrestin2, and one mutant, R134A, which has a constitutive recruitment of β-arrestin2 with no detected Gαi signaling.

CXCL12, the endogenous ligand of CXCR4, is an agonist on both the Gαi and β-arrestin2 pathways. It has shown its capacity on the wild-type receptor and N119S, but not on the Gαi pathway associated with R134A, as this mutant is unable to activate this pathway.

AMD3100 antagonized the effect of CXCL12. However, by itself, it showed no effect on β-arrestin2 recruitment to any of the three receptors, the wild-type, N119S or R134A. This implies that AMD3100 is a biased G-protein partial agonist and it does not have a significant effect on the recruitment of β-arrestin2.

On the other hand, the Gαi inverse agonist TC14012 did not demonstrate a comparable inverse agonism on the recruitment of β-arrestin2. As we have two mutants constitutively recruiting β-arrestin2, N119S and R134A, TC14012 did not affect the recruitment to R134A, while it showed only a trend to decrease the $BRET^2$ signal with N119S. Nonetheless, this decrease was not significant and did not attain the basal control level. This led us to stipulate the hypothesis that TC14012 was a biased inverse agonist, showing an effect only on the Gαi pathway and its changes on β-arrestin2 recruitment were purely conformational. However, further experiments are needed to support this hypothesis, such as a dose-response of the TC14012 effect on the recruitment of β-arrestin2 to N119S and a titration experiment to differentiate between a genuine decrease in the recruitment of β-arrestin2 to N119S, and a pure conformational change.

4.9. Effect of TC14012 on β-Arrestin2 Recruitment by N119S

Next, we wanted to confirm that the effect of TC14012 on β-arrestin2 recruitment to the mutant N119S was not limited by the dose of stimulation. As we found a small, but considerable decrease of β-arrestin2 recruitment by this inverse agonist, we wanted to ensure that this effect was not minimized by the use of an insufficient dose of TC14012 to stimulate the cells with this ligand. Furthermore, we wanted to test whether this decrease was done by interfering with the affinity of the receptor to β-arrestin2 or by changing the conformation of the complex.

To answer these questions, a dose-response of the stimulation and a titration were performed. The results shown in Fig. 23 are combined from at least two independent experiments, all done in triplicate. First, we performed a dose-response experiment, where the dose of TC14012 was varied between 10^{-5} M, and 5 x 10^{-11} M. The stimulation was conducted at 37˚C, for a five minute period. The cells were transfected with β-arrestin2-GFP[10] combined with CXCR4-N119S-Rluc3.

For the mutant N119S, TC14012 was able to decrease the high basal $BRET^2$ signal from 0.076 B.N.U to 0.058 B.N.U. (Fig. 23A). This dose-response had a sigmoidal curve with a logEC50 of - 8.11, corresponding to 7.76 nM. This was in accordance with what we had observed in the previous figure. However, as discussed earlier in the '3.8. BRET' section, this decrease could be either due to a net decrease in the recruitment or to a conformational change of the complex, and only a titration experiment would help differentiate between these two options. As the dose of TC14012 used in Figure 22 was 1 μM, it exceeded the EC50 by over 100 times. As we can see in Figure 23.A, this dose is placed high in the plateau attained with TC14012, confirming that the dose used previously was sufficient to illustrate the maximum possible response.

To examine whether the change in the $BRET^2$ signal of β-arrestin2 recruitment was a change in conformation or affinity, a titration experiment was conducted. The conditions of transfection were similar to the ones demonstrated in Fig. 17. The cells were either stimulated with 1 μM of TC14012 for five minutes at 37˚C or not.

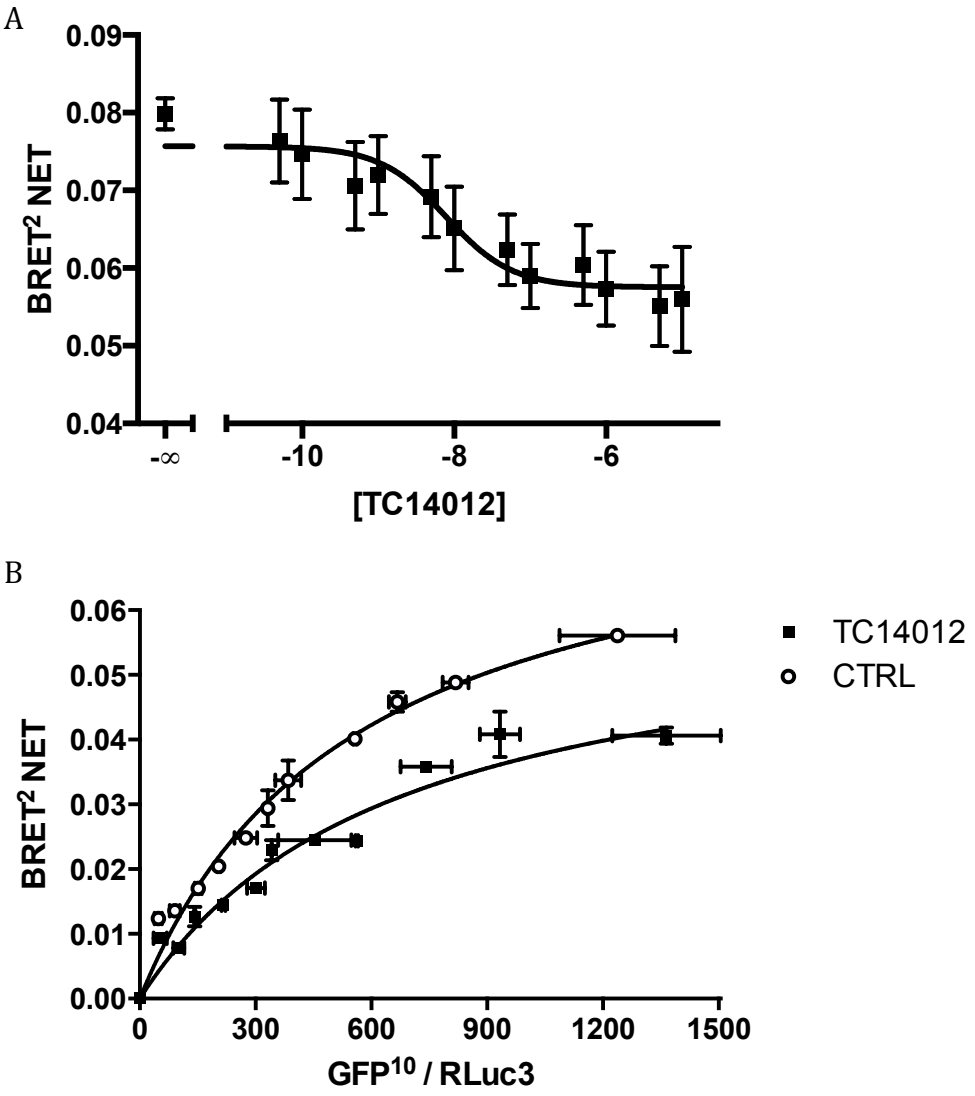

Figure 23. Effect of TC14012 on β-arrestin2 recruitment by N119S. HEK293E cells were cotransfected with the β-arrestin2-GFP^{10} plasmid and CXCR4-N119S-Rluc3. **A)** Dose response of TC14012. Cells were stimulated with TC14012 for 5 min at 37˚C prior to measurment. TC14012 doses were varied between 10^{-5} and $5X10^{-11}$ M. **B)** Titrations of β-arrestin2 recruitment by CXCR4-N119S. HEK293E cells were cotransfected with 0.05µg of CXCR4-N119S with a varying quantity of β-arrestin2-GFP10, between 0.05µg and 1.95µg. 48h post-transfection, cells were stimulated with a saturating dose of 1µM TC14012 for 5 min at 37˚C. Each point represents the mean ± SEM of at least two independent experiments, pooled together, each conducted as triplicates.

Table X. Titrations of the effect of TC14012 on β-arrestin2 recruitment by N119S. Analysis of the data presented in Figure 23.B after fitting it with a hyperbole curve. CI represents the 95% confidence interval. *P*-value indicates the significance of the difference of each parameter between the two conditions. B.N.U: $BRET^2$ NET Unit. *: Significant difference. Highlighted data indicate important results that are further discussed in the text.

Treatment	$BRET_{50}$ ± CI	*p*-value	$BRET_{max}$ ± CI / B.N.U	*p*-value
CTRL	556 ± 118	0.35	0.081 ± 0.009	0.008 *
TC14012	663 ± 206		0.062 ± 0.010	

Both titrations followed a hyperbole curve irrespective of whether N119S was stimulated with TC14012 or not, indicating a specific constitutive interaction, even in the presence of TC14012 (Fig. 23B). Comparing the two curves, we found that between the two, $BRET_{50}$ did not vary significantly (*p*-value = 0.35), while $BRET_{max}$ was significantly different and lower in TC14012 stimulation (*p*-value = 0.008) (Table X). $BRET_{50}$ is related to the affinity between the two proteins, CXCR4 and β-arrestin2. As TC14012 did not affect the $BRET_{50}$, it suggests that TC14012 did not change the affinity and the level of β-arrestin2 recruitment remained the same. On the other hand, $BRET_{max}$ depends on the distance and the angle between the two BRET tags. The decrease in $BRET_{max}$ suggests that the conformation of the complex N119S-β-arrestin2 was different, upon stimulation with TC14012 and that this ligand induced a conformation change.

These titration experiments support our hypothesis that TC14012 does not exhibit an effect on the recruitment of β-arrestin2 to CXCR4; and that the slight decrease in signal observed earlier is mainly due to a conformational change. In conclusion, we have found that TC14012 is a Gαi biased inverse agonist, without displaying a similar activity on the recruitment of β-arrestin2**.**

5. DISCUSSION

5.1. Overview

Our knowledge of the activation of GPCRs evolves daily with the increasing amount of experimental data. The theoretical models also evolve to accommodate these findings. First, the old model stated that a receptor can exist in a limited number of conformations, flipping between active and inactive forms. This model was unable to explain the variation of signaling pathways activated by the same receptor depending on the ligand used (93).

On the other hand, the biased signaling model offers a better explanation by proposing the concept that a receptor can change its conformation between an infinite number of conformations. Each conformation is associated with a different level of activity in the several signaling pathways associated with this receptor (93).

The importance of biased signaling in the therapeutic field is tremendous. As stated earlier, more than 30% of the prescribed drugs act on GPCRs (4). It may be beneficial for the treatment of several pathologies to activate or inhibit only one pathway associated with the targeted receptor and not the others (96) as we have thoroughly discussed in the '1.11. Functional Selectivity' section. In the study conducted here, we aimed to understand the relation between the Gαi and β-arrestin2 signaling by CXCR4 and to test whether one pathway is dependent on the other.

To be able to study this, we developed mutants of CXCR4 to look for receptors capable of constitutively activating one pathway or the other. The mutant panel used here was chosen carefully, targeting the DRY motif as well as the conserved asparagine N3.35. All these mutants were equally expressed on the cell membrane (84).

For each mutant, we tried to assess its activity on two key signaling pathways of CXCR4: Gαi, studied by Epac and recruitment of β-Arrestin2 assessed by $BRET^2$.

No previous report has effectively studied the Gαi signaling of these mutants. All former results are related to the G-proteins in general without targeting the Gαi pathway specifically. This study completes previous investigations and provides a link between the DRY, N119 mutants and the Gαi pathway. As well, it studies the role of these conserved residues in the recruitment of β-arrestin2.

Using the mutant panel, we assayed the signaling of two synthetic ligands AMD3100 and TC14012. The effect of these ligands had only been shown on the capacity to activate G-proteins. Here, we wanted to study their detailed effect on two specific pathways, the Gαi and β-arrestin2.

5.2. N3.35: N119

The asparagine N3.35 in TMIII is conserved in receptors of the CXC chemokines (85). This residue is situated at position 119 in CXCR4, where it was believed to act as a switch in rhodopsin activation (136). Zhang et al have demonstrated that the N119 mutants used here are able to bind effectively to CXCL12 at a level comparable to the wild-type receptor (85).

To summarize, taking into account the two pathways, Gαi and β-arrestin2, we found the mutant N119D showing a pattern similar to the wild-type receptor, while N119K showed no activity on either pathway. Finally, the mutant N119S was known for its constitutive activation of the Gαi pathway (84,85). This activity could not be verified due to the limitation of this method to assess the basal activity of the receptors. However, Zhang et al. have shown that the constitutive GTPγS recruitment to membranes of CHO human cells expressing N119S is sensitive to PTX (85) which confirms the constitutive activity of this mutant on the Gαi pathway specifically. As well, the Gαi inverse agonist, TC14012, had the capacity to significantly decrease the activation of the Gαi pathway through N119S supporting a high basal Gαi activity of this mutant.

Unexpectedly, N119S exhibited high $BRET^2$ signal and recruitment of β-arrestin2 in the absence of stimulation. Titration assays have confirmed the constitutive recruitment of β-arrestin2 to this mutant. This constitutive β-arrestin activity of a CXCR4 mutant is entirely

novel. Stimulating N119S with CXCL12 increased the $BRET^2$ signal by affecting the affinity of β-arrestin2 to N119S without changing the complex conformation.

According to the literature, N119S is a confirmed CAM on the Gαi pathway (85). Here we show that this mutant is a CAM on the β-arrestin2 pathway as well. Usually, mutants that are constitutively recruiting β-arrestin, are found uncoupled from G-protein signaling, and constitutively desensitized (83). Here however, N119S was constitutively recruiting the β-arrestin2 while maintaining its constitutive Gαi activity.

Other receptors displayed a similar pattern upon mutating the conserved asparagine. Auger-Messier et al. demonstrated the importance of this amino acid in the angiotensin II receptor, AT1R (137). The mutants N111A and N111G showed a constitutive Gαq activity leading to stimulation of Phospholipase C (PLC), while N111Q and N111W lost their capacities to activate this pathway.

In CXCR4, mutating this asparagine residue to different amino acids led to either a constitutively active mutant on both Gαi and β-arrestin2 (N119S) or a mutant inactive in both (N119K). This demonstrates the importance of this residue and its implication in the signaling of the receptor CXCR4 through both pathways.

5.3. The DRY Motif

The DRY motif had been widely described for its implication in β-arrestin recruitment in several GPCRs (83). Situated at the beginning of the second intracellular loop, this motif was highly conserved among different GPCR families (19,138).

Here, we found that D133N, and Y135A followed a pattern similar to the wild-type, in respect to both pathways: Gαi and β-arrestin2. On the other hand, mutating arginine in the DRY motif to an alanine showed no detectable Gαi activity. R134A exhibited high $BRET^2$ signal and recruitment, even in the absence of stimulation, which suggests constitutive recruitment of β-arrestin2 as confirmed by titration assays. Stimulation with CXCL12

increased the BRET^2 signal by affecting the conformation of the complex β-arrestin2-R134A, without changing the affinity between the two.

While N119S was previously described as a Gαi CAM, no CXCR4 mutant has been known to be a CIM. The latter is a mutant which constitutively recruits β-arrestin, leading to the deprivation of activity on the Gαi pathway (83) and R134A fulfills this description. This new finding fills the gap, by identifying R134A as the first Gαi CIM for the CXCR4 receptor.

Mutating the aspartic acid residue (D 3.49) in different GPCRs leads to different consequences. As the interaction between the arginine and the aspartic acid keeps the receptor in an inactive conformation, mutating the latter generates a constitutively active mutant (CAM) in some receptors (82). These receptors have been classified as the P1-type. This is the case for rhodopsin (139) and V_2R (140).

On the other hand, mutations of the arginine R 3.50 display different patterns of signaling. This mutation disrupts the activity of some GPCRs, generating a CIM that have lost the potential to activate the G-proteins (82). Receptors that follow this pattern have been grouped as the P2-type. Among these receptors, we can find CCR5 (141) and α_{2A}-AR (142). Although these receptors are not able to activate the Gα proteins they might maintain the capacity to signal through other pathways.

Using these results, we could confirm that CXCR4 belongs to the P2-type with regard to its DRY motif. Like other P2-type receptors, mutating the aspartate 3.49 (D133) produced mutants that were not constitutively activating the Gα-proteins, while mutating the arginine 3.50 (R134) led to a CIM. Also, we illustrated that this R134A mutant was not deprived of activity, but rather it was constitutively recruiting β-arrestin2.

Similar results were observed by others regarding different chemokine receptors. Mutating the Arginine residue in the DRY motif of the CCR5 chemokine receptor (R126N) abolished the activation of G proteins (141). Nevertheless, this mutant displayed a higher basal phosphorylation of the C-terminus as well as constitutive β-arrestin recruitment and endocytosis. Wilbanks et al. studied the arginine mutants for several receptors such the α1B-

adrenoceptor (α_{1B}-AR) (143), and the $AT_{1A}R$. Both receptors showed a constitutive desensitization and endocytosis associated with the basal recruitment of β-arrestin. They explained the loss of Gα activity by this constitutive desensitization. As well, they have even suggested this constitutive desensitization to be universal for all GPCRs. This report confirms this hypothesis for CXCR4 and further supports its possible validity among chemokine receptors (83).

Some naturally occurring arginine mutants deprived of Gα signaling were perceived in endocrine pathologies. Not surprisingly, endocrine signaling is primordial for the biological functioning of the human body and disturbance of this signaling leads to pathological states and interferes with multiple organ systems. Additional studies on the implicated receptors and the sequencing of their genes has led to the discovery of Arg 3.50 mutants, such as in nephrogenic diabetes insipidus (144). This syndrome is associated with loss of water through the kidneys as they become non-responsive to stimulation by antidiuretic hormone. This hormone increases reabsorption of water in collecting ducts by signaling through vasopressin type II receptor (V2R) (83,144). The naturally occurring mutation R137H in V2R led to a receptor uncoupled from the G-proteins which constitutively recruited β-arrestin and localized mainly onto endosomes (145). This CIM mutant was unable to adequately signal after stimulation with antidiuretic hormone, which leads to the symptoms associated with the diabetes insipidus syndrome.

5.4. β-Arrestin2 Recruitment Modalities

β-arrestin recruitment depends on two factors and divergence in either was shown to modulate the recruitment. These two factors were the conformation of the activated receptor and the phosphorylation of its C-terminal. It had been postulated for several GPCRs that this phosphorylation generates a barcode that regulates the conformation of β-arrestin recruitment and its functioning (24). This was established for various GPCRs, such as AT1-R (146) and β_2-AR (100). GRK2 and GRK3 phosphorylation led to the recruitment of β-arrestins and endocytosis of the receptor. However, phosphorylation by GRK5 and GRK6 activated the signaling pathways ERK1/2.

Zimmerman et al. studied the effect of different β-arrestin modalities in the signaling of AT1R (23). They have used several AngII analogs to suggest that the concept of functional selectivity extends beyond G-protein and β-arrestin responses. Biased signaling also occurred within the level of β-arrestin responses, where different β-arrestin conformations led to distinct biological functions.

All used analogs induced the recruitment of β-arrestin to AT1R, measured by a BRET assay. As well, they were able to translocate a fluorescent-tagged β-arrestin2 to the endosomes and form complexes of AT1R and β-arrestin2 on these vesicles. A double-brilliance β-arrestin was used to study the conformation of this recruitment. β-arrestin was positioned between the two BRET tags, similar to Epac in our study (147). The BRET signal measured in this assay would depend on the distance and the conformation between the two BRET tags, and thus it reflects the conformation of the recruited β-arrestin. Stimulating HEK293 cells with the different analogs demonstrated that they induced different conformations of β-arrestin.

The differences between the analogs also included the avidity between β-arrestin and AT1R on endosomes (23). This was assayed using fluorescence recovery after photobleaching (FRAP). This avidity reflects the stability of the AT1R-β-arrestin complex and it correlated well with the activation of ERK1/2. Ligands that were able to form more stable complexes on endosomes led to the arrangement of more stable MAPK scaffolds, increasing the efficiency of the activation of this signaling pathway.

As described earlier, two factors can explain the differences in β-arrestin recruitment: conformation of the receptor and its phosphorylation. Zimmerman et al. suggested that these different conformational rearrangements were the result of distinct AT1R conformations induced by the different analogs, as well as specific GRKs phosphorylation (23). Knockdown of GRK6 affected the various analogs differently in respect to the recruitment of β-arrestin and its conformation. This led them to propose that these analogs induced differential phosphorylation of AT1R by GRK6, which led to the differences in the conformation of β-arrestin recruitment.

These differences in β-arrestin conformation translated into different biological outcomes. The most important difference was observed between AngII and one of its analogs called DVG on rat aortic vascular smooth muscle cells (VSMCs). In these live cells, the conformation of β-arrestin induced by the two analogs was distinct. While both ligands

induced cell proliferation in a β-arrestin dependent manner, only AngII was able to promote migration which suggests that the different conformation of β-arrestin induced by DVG is not an efficient scaffold for the proteins implicated in chemotaxis.

Similar to the AT1R receptor described by Zimmerman et al., we have shown here that the two mutants constitutively recruiting β-arrestin2, R134A, and N119S had different modalities of recruitment. Two parameters were looked into, namely the relative affinity of each receptor for the β-arrestin2 protein and the conformation of the complex formed by each receptor and this protein. By performing a titration assay, we found that these two recruitments differed in both parameters, suggesting different modalities of β-arrestin2 recruitment. The next step would be to study whether a differential phosphorylation of the C-terminus of the two mutants is the molecular basis of the differences in modalities. As well, we should assay if these different β-arrestin conformations will promote different biological outcomes.

5.5. Trafficking of CXCR4 Mutants

The imaging of CXCR4 shows a variety of localization differences. Although the wild-type receptor and the mutants Y135A, N119D and N119K shared a predominantly membranous expression the other mutants did not. On the other hand, the two mutants constitutively recruiting β-arrestin2 differed in their localization pattern. N119S was found in a single cellular pool, compatible with the endoplasmic reticulum or the Golgi apparatus, while R134A was found on hollow circular structures compatible with endocytic vesicles. This remains a pilot experiment and thus should not be over-interpreted.

Accumulating data suggest that signaling and trafficking are interrelated by several scaffolding molecules (23). β-arrestin plays a central role in the internalization of GPCRs by recruiting and orchestrating all the actors of internalization, such as the deubiquitinases and the Rab endocytic machinery. Any difference in the modalities of its recruitment may be associated with differences in GPCRs' trafficking. The two mutants, R134A and N119S, displayed differences in the modalities of this recruitment in Fig. 9, which can explain the differences in their trafficking.

Wilbanks et al. studied the trafficking of the DRY mutants in both α_{1B}-AR, and $AT_{1A}R$ (83). The arginine mutants of both receptors were CIM, deprived of G-protein coupling and constitutively recruited the β-arrestin. For traffic experiments, GFP tagged receptors were used, similar to the ones used here. Stimulating the wild-type receptor induced its internalization to endocytic vesicles. The arginine mutants however were found constitutively on similar vesicles. This intracellular localization was reversed using the inverse agonist phentolamine.

As we discussed in the '1.3. Trafficking' section, GPCRs follow one of two patterns of trafficking, class A or B. After internalization, class A receptors are mostly recycled to the cell surface, while class B receptors are directed to degradation. The molecular basis of these two patterns depends on the affinity to the β-arrestins — whether it is transient or more stable (18,22). In class A receptors, β-arrestins are transiently recruited to the activated receptor. Once in the endosome, the receptor detaches quickly from its β-arrestin which facilitates its recycling. On the other hand, class B receptors form stable complexes with β-arrestins, even on the endosomes, which slow down their recycling and direct them towards degradation (83).

As α_{1B}-AR belongs to the class A receptors, the stimulated wild-type induced the translocation of β-arrestin to the plasma membrane. On the other hand, $AT_{1A}R$ is a member of class B, and stimulating it with an agonist led to recruitment of β-arrestin on the endocytic vesicles. Interestingly, both CIM mutants followed the pattern of their respective stimulated wildtype (83).

5.6. β-Arrestin2 Independent of G-Proteins Coupling

As described under the functional selectivity section 'Introduction 1.11', a ligand can act as an agonist on a signaling pathway without affecting the others. Here, we wanted to verify if the recruitment of β-arrestin2 to CXCR4 is dependent on the activation of the Gαi protein.

First, the R134A mutant showed a constitutive recruitment of β-arrestin2 with no apparent Gαi activity, indicating that the latter was not required for efficient β-arrestin2 recruitment.

Second, we used PTX as a way of modulating the Gαi activity. PTX inhibits this pathway by ADP-ribosylating the C-terminus of the α subunit of the heterotrimeric G-proteins of the Gαi family (58). This modification leads to its complete inhibition. As we inhibited the Gαi activity, we assayed its effect on β-arrestin2 recruitment. In the presence of PTX the basal recruitment of the two mutants R13A and N119S was maintained, showing that both had a constitutive β-arrestin2 recruitment independent of their Gαi activity. As well, stimulation with CXCL12 was able to recruit β-arrestin2 even when Gαi is inhibited by PTX.

Other studies have reported similar findings. The chemokine receptor CCR2 has shown partial β-arrestin2 recruitment and endocytosis that are PTX-resistant, implying that they are independent of the Gαi activity (25,148). However the role of other G-proteins cannot be excluded as we know that CCR2 can activate Gαq, Gα14, and Gα16 (149,150). Similarly, β-arrestin2 may be triggered by another Gα activated by CXCR4, and that this recruitment depended on this subunit.

These results suggest that agonist-mediated β-arrestin2 recruitment requires conformation changes of CXCR4 that are independent of G-protein activity.

5.7. AMD3100 vs TC14012

The two synthetic CXCR4 ligands, AMD3100 and TC14012 have not been previously studied for their effect on Gαi or β-arrestin2 activities.

Here we have shown that AMD3100 is an antagonist on both pathways. It did not activate the Gαi pathway as previously claimed by Zhang. AMD3100 might have a possible effect on a different G-protein, distinct from the Gαi one. This suggests that Plerixafor is a biased partial agonist on a G-protein that remains to be identified, which has no effect on Gαi or β-arrestin2.

Although the TC14012 ligand has been suggested to be an inverse agonist (85), the published data examined only the G-protein signaling. After elucidation of the biased ligands principle for several GPCRs (91), the inverse agonism of TC14012 had to be stated

specifically in respect to a particular pathway. Here, we investigated the effect of this ligand on the mutants, thus illustrating its impact on the Gαi and a non G-protein pathway; the β-arrestin2 one. TC14012 revealed to be a biased inverse agonist on the Gαi pathway. It did not decrease the recruitment of β-arrestin2 but induced a slight conformational change of the CXCR4-β-arrestin2 complex.

AMD3100 or Plerixafor has been approved for use in the US (126) and EU (151) for autologous stem-cell transplantation (152). AMD-3100 was suggested to be a weak agonist on the G-protein pathway of CXCR4 (85). This activity might explain some of the Plerixafor side effects. By weakly activating CXCR4, the most widely expressed chemokine receptor on cancer cells (72), Plerixafor leads to the mobilization of tumor cells and contamination of the peripheral blood leading to subsequent relapse after autotransplantation with the contaminated stem cells (127,128).

Accumulating evidence suggests that inverse agonists are more clinically efficient than the antagonists (153). The data illustrated here show that TC14012 is an inverse agonist on the Gαi pathway and this will possibly offer a solution to the side effects of Plerixafor. While having the same effect as AMD3100 of blocking the binding of CXCL12, TC14012 might be more convenient. This ligand will further reduce any basal Gαi activity, without affecting β-arrestin2 recruitment. This work supports the development of TC14012 for stem cell mobilization trials.

6. CONCLUSION

In conclusion, we have assayed different CXCR4 mutants on both pathways: Gαi and β-arrestin2, using different BRET techniques. Two interesting mutants were found, N119S and R134A. N119S, a previously described constitutively active mutant (CAM), is constitutively active on both pathways. On the other hand, R134A is a newly identified, constitutively inactive mutant (CIM) that is deprived of G-protein signaling, while constitutively recruiting β-arrestin2. Both mutants differed in their β-arrestin2 recruitment modalities, showing different affinities and conformations. Also, the results of a pilot experiment suggest that the two mutants showed different cellular localizations while maintaining their surface expression. N119S was found in a single intracellular pool and R134A on several hollow circle-shaped structures.

Targeting these mutants with PTX, an inhibitor of the Gαi activation, showed efficient blocking of the Gαi pathway. However, β-arrestin2 recruitment induced by CXCL12 was maintained, as well as the constitutive recruitment shown by the two mutants R134A and N119S. This endorsed the fact that β-arrestin2 recruitment was independent of the Gαi activation by CXCR4.

Finally, two synthetic ligands of CXCR4, AMD3100 and TC14012 were tested on their β-arrestin2 recruitment. Both ligands had only been tested on the Gαi pathway. AMD3100 or Plerixafor was a clinically approved drug used for stem cell transplantation. It was known to be a partial agonist on the G-proteins and was found to be an antagonist on both Gαi and β-arrestin2 recruitment. On the other hand, TC14012, which was a G-protein inverse agonist, was found to be an inverse agonist on Gαi specifically and an antagonist on β-arrestin2 recruitment. AMD3100 induced some considerable side effects due to its partial agonism on the Gα. Therefore, TC14012 might offer an alternative that is more suitable and efficient, with fewer side effects than AMD3100.

7. PERSPECTIVES

The results presented here support that CXCR4 mutants showed different modalities of recruitment of β-arrestin2 and suggest that this differential recruitment might have led to differential trafficking. Two major points need to be studied in further detail, the molecular basis of these different conformations and the biological outcomes resulting from the differences. GRKs play an important role in generating the bar code for the specific conformation of recruitment of β-arrestin. The C-terminal phosphorylation of the two mutants, as well as their ubiquitination should be assessed to illustrate the biochemical differences leading to their differential trafficking.

While our results suggest that the differences in modalities are translated in differences in trafficking, the basal localization of these mutants should be identified. This could be performed using immunofluorescence studies to identify the main structures in which these mutants are present. Besides trafficking, several downstream biological outcomes could be studied, such as the effect of the β-arrestin conformation on chemotaxis or cell survival.

As well, we suggested here that AMD3100 or Plerixafor is a partial agonist on a G-protein different from Gαi. This remains to be validated by other experiments and the different Gα subunit remains to be identified.

Finally, while we suggest here that TC14012 might potentially be superior to Plerixafor as it is an inverse agonist on the Gαi pathway, several aspects remain to be examined, such as its biological functions and its pharmacological parameters. We should test the capacity of this ligand to mobilize hematopoietic stem cells and inhibit the migration of metastatic cancer cells expressing CXCR4.

8. REFERENCES

1. Luttrell LM. Reviews in molecular biology and biotechnology: transmembrane signaling by G protein-coupled receptors. Mol. Biotechnol. 2008 Jul.;39(3):239–264.

2. King N, Hittinger CT, Carroll SB. Evolution of key cell signaling and adhesion protein families predates animal origins. Science. 2003 Jul. 18;301(5631):361–363.

3. Thompson MD, Cole DEC, Jose PA. Pharmacogenomics of G protein-coupled receptor signaling: insights from health and disease. Methods Mol. Biol. 2008;448:77–107.

4. Overington JP, Al-Lazikani B, Hopkins AL. How many drug targets are there? Nat Rev Drug Discov. 2006 Dec.;5(12):993–996.

5. Müller G. Towards 3D structures of G protein-coupled receptors: a multidisciplinary approach. Curr. Med. Chem. 2000 Sep.;7(9):861–888.

6. Schiöth HB, Fredriksson R. The GRAFS classification system of G-protein coupled receptors in comparative perspective. Gen. Comp. Endocrinol. 2005 May 15;142(1-2):94–101.

7. Neer EJ. Heterotrimeric G proteins: organizers of transmembrane signals. Cell. 1995 Jan. 27;80(2):249–257.

8. Arshavsky VY, Lamb TD, Pugh EN. G proteins and phototransduction. Annu. Rev. Physiol. 2002;64:153–187.

9. Perry SJ, Baillie GS, Kohout TA, McPhee I, Magiera MM, Ang KL, et al. Targeting of cyclic AMP degradation to beta 2-adrenergic receptors by beta-arrestins. Science. 2002 Oct. 25;298(5594):834–836.

10. Kurose H. Galpha12 and Galpha13 as key regulatory mediator in signal transduction. Life Sci. 2003 Dec. 5;74(2-3):155–161.

11. Oldham WM, Hamm HE. Structural basis of function in heterotrimeric G proteins. Q. Rev. Biophys. 2006 May;39(2):117–166.

12. Cheng ZJ, Zhao J, Sun Y, Hu W, Wu YL, Cen B, et al. beta-arrestin differentially regulates the chemokine receptor CXCR4-mediated signaling and receptor internalization, and this implicates multiple interaction sites between beta-arrestin and CXCR4. J. Biol. Chem. 2000 Jan. 28;275(4):2479–2485.

13. Kohout TA, Lefkowitz RJ. Regulation of G protein-coupled receptor kinases and arrestins during receptor desensitization. Mol. Pharmacol. 2003 Jan.;63(1):9–18.

14. Busillo JM, Armando S, Sengupta R, Meucci O, Bouvier M, Benovic JL. Site-specific phosphorylation of CXCR4 is dynamically regulated by multiple kinases and results in differential modulation of CXCR4 signaling. J. Biol. Chem. 2010 Mar. 5;285(10):7805–7817.

15. Ren X-R, Reiter E, Ahn S, Kim J, Chen W, Lefkowitz RJ. Different G protein-coupled receptor kinases govern G protein and beta-arrestin-mediated signaling of V2 vasopressin receptor. Proc. Natl. Acad. Sci. U.S.A. 2005 Feb. 1;102(5):1448–1453.

16. Shenoy SK, Drake MT, Nelson CD, Houtz DA, Xiao K, Madabushi S, et al. beta-arrestin-dependent, G protein-independent ERK1/2 activation by the beta2 adrenergic receptor. J. Biol. Chem. 2006 Jan. 13;281(2):1261–1273.

17. Zhang R, Xie X. Tools for GPCR drug discovery. Acta Pharmacol. Sin. 2012 Mar.;33(3):372–384.

18. Kendall RT, Luttrell LM. Diversity in arrestin function. Cell. Mol. Life Sci. 2009 Sep.;66(18):2953–2973.

19. Ferguson SS. Evolving concepts in G protein-coupled receptor endocytosis: the role in receptor desensitization and signaling. Pharmacol. Rev. 2001 Mar.;53(1):1–24.

20. Lefkowitz RJ, Rajagopal K, Whalen EJ. New roles for beta-arrestins in cell signaling: not just for seven-transmembrane receptors. Mol. Cell. 2006 Dec. 8;24(5):643–652.

21. De Lean A, Stadel JM, Lefkowitz RJ. A ternary complex model explains the agonist-specific binding properties of the adenylate cyclase-coupled beta-adrenergic receptor. J. Biol. Chem. 1980 Aug. 10;255(15):7108–7117.

22. DeWire SM, Ahn S, Lefkowitz RJ, Shenoy SK. Beta-arrestins and cell signaling. Annu. Rev. Physiol. 2007;69:483–510.

23. Zimmerman B, Beautrait A, Aguila B, Charles R, Escher E, Claing A, et al. Differential β-arrestin-dependent conformational signaling and cellular responses revealed by angiotensin analogs. Sci Signal. 2012 Apr. 24;5(221):ra33.

24. Reiter E, Ahn S, Shukla AK, Lefkowitz RJ. Molecular mechanism of β-arrestin-biased agonism at seven-transmembrane receptors. Annu. Rev. Pharmacol. Toxicol. 2012;52:179–197.

25. Berchiche YA. Étude de la relation entre les conformations et la signalisation des 7TMRs. Université de Montréal; 2010.

26. Shenoy SK, Barak LS, Xiao K, Ahn S, Berthouze M, Shukla AK, et al. Ubiquitination of beta-arrestin links seven-transmembrane receptor endocytosis and ERK activation. J. Biol. Chem. 2007 Oct. 5;282(40):29549–29562.

27. Shenoy SK, Xiao K, Venkataramanan V, Snyder PM, Freedman NJ, Weissman AM. Nedd4 mediates agonist-dependent ubiquitination, lysosomal targeting, and degradation of the beta2-adrenergic receptor. J. Biol. Chem. 2008 Aug. 8;283(32):22166–22176.

28. Oakley RH, Laporte SA, Holt JA, Caron MG, Barak LS. Differential affinities of visual arrestin, beta arrestin1, and beta arrestin2 for G protein-coupled receptors delineate two major classes of receptors. J. Biol. Chem. 2000 Jun. 2;275(22):17201–17210.

29. Shenoy SK, Lefkowitz RJ. Receptor-specific ubiquitination of beta-arrestin directs assembly and targeting of seven-transmembrane receptor signalosomes. J. Biol. Chem. 2005 Apr. 15;280(15):15315–15324.

30. Krueger KM, Daaka Y, Pitcher JA, Lefkowitz RJ. The role of sequestration in G protein-coupled receptor resensitization. Regulation of beta2-adrenergic receptor dephosphorylation by vesicular acidification. J. Biol. Chem. 1997 Jan. 3;272(1):5–8.

31. Shenoy SK. Seven-transmembrane receptors and ubiquitination. Circ. Res. 2007 Apr. 27;100(8):1142–1154.

32. Shenoy SK, McDonald PH, Kohout TA, Lefkowitz RJ. Regulation of receptor fate by ubiquitination of activated beta 2-adrenergic receptor and beta-arrestin. Science. 2001 Nov. 9;294(5545):1307–1313.

33. Martin NP, Lefkowitz RJ, Shenoy SK.

Regulation of V2 vasopressin receptor degradation by agonist-promoted ubiquitination. J. Biol. Chem. 2003 Nov. 14;278(46):45954–45959.

34. Hicke L. Protein regulation by monoubiquitin. Nat. Rev. Mol. Cell Biol. 2001 Mar.;2(3):195–201.

35. Haglund K, Sigismund S, Polo S, Szymkiewicz I, Di Fiore PP, Dikic I. Multiple monoubiquitination of RTKs is sufficient for their endocytosis and degradation. Nat. Cell Biol. 2003 May;5(5):461–466.

36. Urbé S, McCullough J, Row P, Prior IA, Welchman R, Clague MJ. Control of growth factor receptor dynamics by reversible ubiquitination. Biochem. Soc. Trans. 2006 Nov.;34(Pt 5):754–756.

37. Marchese A, Paing MM, Temple BRS, Trejo J. G protein-coupled receptor sorting to endosomes and lysosomes. Annu. Rev. Pharmacol. Toxicol. 2008;48:601–629.

38. Luttrell LM, Lefkowitz RJ. The role of beta-arrestins in the termination and transduction of G-protein-coupled receptor signals. J. Cell. Sci. 2002 Feb. 1;115(Pt 3):455–465.

39. Gravel S. Évaluation de l'effet des antagonistes synthétiques du récepteur de chimiokine CXCR4 sur CXCR7. Université de Montréal; 2010.

40. Murphy PM, Baggiolini M, Charo IF, Hébert CA, Horuk R, Matsushima K, et al. International union of pharmacology. XXII. Nomenclature for chemokine receptors. Pharmacol. Rev. 2000 Mar.;52(1):145–176.

41. Proudfoot AEI, Power CA, Schwarz MK. Anti-chemokine small molecule drugs: a promising future? Expert Opin Investig Drugs. 2010 Mar.;19(3):345–355.

42. Horuk R. Chemokine receptors. Cytokine Growth Factor Rev. 2001 Dec.;12(4):313–335.

43. Vanhoutte PM, Humphrey P, Spedding M. NC-IUPHAR recommendations for nomenclature of receptors. The IUPHAR Compendium of Receptor Characterization and Classification. Burlington Press, Foxton, Cambridge, UK. 1998 Jun. 19;:31–33.

44. Allen SJ, Crown SE, Handel TM. Chemokine: receptor structure, interactions, and antagonism. Annu. Rev. Immunol. 2007;25:787–820.

45. Townson DH, Liptak AR. Chemokines in the corpus luteum: implications of leukocyte chemotaxis. Reprod. Biol. Endocrinol. 2003 Nov. 10;1:94.

46. Lomize AL, Pogozheva ID, Mosberg HI. Structural organization of G-protein-coupled receptors. J. Comput. Aided Mol. Des. 1999 Jul.;13(4):325–353.

47. Van Coillie E, Van Damme J, Opdenakker G. The MCP/eotaxin subfamily of CC chemokines. Cytokine Growth Factor Rev. 1999 Mar.;10(1):61–86.

48. Busillo JM, Benovic JL. Regulation of CXCR4 signaling. Biochim. Biophys. Acta. 2007 Apr.;1768(4):952–963.

49. Décaillot FM, Kazmi MA, Lin Y, Ray-Saha S, Sakmar TP, Sachdev P. CXCR7/CXCR4 heterodimer constitutively recruits beta-arrestin to enhance cell migration. J. Biol. Chem. 2011 Sep. 16;286(37):32188–32197.

50. Peled A, Petit I, Kollet O, Magid M, Ponomaryov T, Byk T, et al. Dependence of human stem cell engraftment and repopulation of NOD/SCID mice on CXCR4. Science. 1999 Feb. 5;283(5403):845–848.

51. Alkhatib G. The biology of CCR5 and CXCR4. Curr Opin HIV AIDS. 2009 Mar.;4(2):96–103.

52. Crump MP, Gong JH, Loetscher P, Rajarathnam K, Amara A, Arenzana-Seisdedos F, et al. Solution structure and basis for functional activity of stromal cell-derived factor-1; dissociation of CXCR4 activation from binding and inhibition of HIV-1. EMBO J. 1997 Dec. 1;16(23):6996–7007.

53. Kofuku Y, Yoshiura C, Ueda T, Terasawa H, Hirai T, Tominaga S, et al. Structural basis of the interaction between chemokine stromal cell-derived factor-1/CXCL12 and its G-protein-coupled receptor CXCR4. J. Biol. Chem. 2009 Dec. 11;284(50):35240–35250.

54. Veldkamp CT, Ziarek JJ, Su J, Basnet H, Lennertz R, Weiner JJ, et al. Monomeric structure of the cardioprotective chemokine SDF-1/CXCL12. Protein Sci. 2009 Jul.;18(7):1359–1369.

55. Veldkamp CT, Seibert C, Peterson FC, la Cruz De NB, Haugner JC, Basnet H, et al. Structural basis of CXCR4 sulfotyrosine recognition by the chemokine SDF-1/CXCL12. Sci Signal. 2008;1(37):ra4.

56. Kucia M, Jankowski K, Reca R, Wysoczynski M, Bandura L, Allendorf DJ, et al. CXCR4-SDF-1 signalling, locomotion, chemotaxis and adhesion. J. Mol. Histol. 2004 Mar.;35(3):233–245.

57. Vicente-Manzanares M, Cabrero JR, Rey M, Pérez-Martínez M, Ursa A, Itoh K, et al. A role for the Rho-p160 Rho coiled-coil kinase axis in the chemokine stromal cell-derived factor-1alpha-induced lymphocyte actomyosin and microtubular organization and chemotaxis. J. Immunol. 2002 Jan. 1;168(1):400–410.

58. Katada T, Tamura M, Ui M. The A protomer of islet-activating protein, pertussis toxin, as an active peptide catalyzing ADP-ribosylation of a membrane protein. Arch. Biochem. Biophys. 1983 Jul. 1;224(1):290–298.

59. Soede RD, Wijnands YM, Kamp M, van der Valk MA, Roos E. Gi and Gq/11 proteins are involved in dissemination of myeloid leukemia cells to the liver and spleen, whereas bone marrow colonization involves Gq/11 but not Gi. Blood. 2000 Jul. 15;96(2):691–698.

60. Twery EN, Raper JA. SDF1-induced antagonism of axonal repulsion requires multiple G-protein coupled signaling components that work in parallel. PLoS ONE. 2011;6(4):e18896.

61. Maghazachi AA. Role of the heterotrimeric G proteins in stromal-derived factor-1alpha-induced natural killer cell chemotaxis and calcium mobilization. Biochem. Biophys. Res. Commun. 1997 Jul. 18;236(2):270–274.

62. Tan W, Martin D, Gutkind JS. The Galpha13-Rho signaling axis is required for SDF-1-induced migration through CXCR4. J. Biol. Chem. 2006 Dec. 22;281(51):39542–39549.

63. Sun Y, Cheng Z, Ma L, Pei G. Beta-arrestin2 is critically involved in CXCR4-mediated chemotaxis, and this is mediated by its enhancement of p38 MAPK activation. J. Biol. Chem. 2002 Dec. 20;277(51):49212–49219.

64. Teicher BA, Fricker SP. CXCL12 (SDF-1)/CXCR4 pathway in cancer. Clin. Cancer Res. 2010 Jun. 1;16(11):2927–2931.

65. Voermans C, Kooi ML, Rodenhuis S, van der Lelie H, van der Schoot CE, Gerritsen WR. In vitro migratory capacity of CD34+ cells is related to hematopoietic recovery after autologous stem cell transplantation. Blood. 2001 Feb. 1;97(3):799–804.

66. Miller RJ, Banisadr G, Bhattacharyya BJ. CXCR4 signaling in the regulation of stem cell migration and development. J. Neuroimmunol. 2008 Jul. 31;198(1-2):31–38.

67. Chute JP. Stem cell homing. Curr. Opin. Hematol. 2006 Nov.;13(6):399–406.

68. Cottler-Fox MH, Lapidot T, Petit I, Kollet O, DiPersio JF, Link D, et al. Stem cell mobilization. Hematology Am Soc Hematol Educ Program. 2003;:419–437.

69. Lapidot T, Dar A, Kollet O. How do stem cells find their way home? Blood. 2005 Sep. 15;106(6):1901–1910.

70. Calvi LM, Adams GB, Weibrecht KW, Weber JM, Olson DP, Knight MC, et al. Osteoblastic cells regulate the haematopoietic stem cell niche. Nature. 2003 Oct. 23;425(6960):841–846.

71. Lapidot T. Mechanism of human stem cell migration and repopulation of NOD/SCID and B2mnull NOD/SCID mice. The role of SDF-1/CXCR4 interactions. Ann. N. Y. Acad. Sci. 2001 Jun.;938:83–95.

72. Fulton AM. The chemokine receptors CXCR4 and CXCR3 in cancer. Curr Oncol Rep. 2009 Mar.;11(2):125–131.

73. Müller A, Homey B, Soto H, Ge N, Catron D, Buchanan ME, et al. Involvement of chemokine receptors in breast cancer metastasis. Nature. 2001 Mar. 1;410(6824):50–56.

74. Holman DW, Klein RS, Ransohoff RM. The blood-brain barrier, chemokines and multiple sclerosis. Biochim. Biophys. Acta. 2011 Feb.;1812(2):220–230.

75. Murphy PM. Chemokines and the molecular basis of cancer metastasis. N. Engl. J. Med. 2001 Sep. 13;345(11):833–835.

76. Chambers AF, Groom AC, MacDonald IC. Dissemination and growth of cancer cells in metastatic sites. Nat. Rev. Cancer. 2002 Aug.;2(8):563–572.

77. Burger M, Glodek A, Hartmann T, Schmitt-Gräff A, Silberstein LE, Fujii N, et al. Functional expression of CXCR4 (CD184) on small-cell lung cancer cells mediates migration, integrin activation, and adhesion to stromal cells. Oncogene. 2003 Nov. 6;22(50):8093–8101.

78. Bruce J, Carter DC, Fraser J. Patterns of recurrent disease in breast cancer. Lancet. 1970 Feb. 28;1(7644):433–435.

79. Jensen A-SM, Sparre-Ulrich AH, Davis-Poynter N, Rosenkilde MM. Structural Diversity in Conserved Regions Like the DRY-Motif among Viral 7TM Receptors-A Consequence of Evolutionary Pressure? Adv Virol. 2012;2012:231813.

80. Rasmussen SGF, DeVree BT, Zou Y, Kruse AC, Chung KY, Kobilka TS, et al. Crystal structure of the β2 adrenergic receptor-Gs protein complex. Nature. 2011 Sep. 29;477(7366):549–555.

81. Mirzadegan T, Benkö G, Filipek S, Palczewski K. Sequence analyses of G-protein-coupled receptors: similarities to rhodopsin. Biochemistry. 2003 Mar. 18;42(10):2759–2767.

82. Rovati GE, Capra V, Neubig RR. The highly conserved DRY motif of class A G protein-coupled receptors: beyond the ground

state. Mol. Pharmacol. 2007 Apr.;71(4):959–964.

83. Wilbanks AM, Laporte SA, Bohn LM, Barak LS, Caron MG. Apparent loss-of-function mutant GPCRs revealed as constitutively desensitized receptors. Biochemistry. 2002 Oct. 8;41(40):11981–11989.

84. Berchiche YA, Chow KY, Lagane B, Leduc M, Percherancier Y, Fujii N, et al. Direct assessment of CXCR4 mutant conformations reveals complex link between receptor structure and G(alpha)(i) activation. J. Biol. Chem. 2007 Feb. 23;282(8):5111–5115.

85. Zhang W-B, Navenot J-M, Haribabu B, Tamamura H, Hiramatu K, Omagari A, et al. A point mutation that confers constitutive activity to CXCR4 reveals that T140 is an inverse agonist and that AMD3100 and ALX40-4C are weak partial agonists. J. Biol. Chem. 2002 Jul. 5;277(27):24515–24521.

86. Kenakin T. A Pharmacology Primer. Academic Press; 2010.

87. Neubig RR, Spedding M, Kenakin T, Christopoulos A, International Union of Pharmacology Committee on Receptor Nomenclature and Drug Classification. International Union of Pharmacology Committee on Receptor Nomenclature and Drug Classification. XXXVIII. Update on terms and symbols in quantitative pharmacology. Pharmacol. Rev. 2003 Dec.;55(4):597–606.

88. Kenakin T. Efficacy as a vector: the relative prevalence and paucity of inverse agonism. Mol. Pharmacol. 2004 Jan.;65(1):2–11.

89. Gilchrist A, Blackmer T. G-protein-coupled receptor pharmacology: examining the edges between theory and proof. Curr Opin Drug Discov Devel. 2007 Jul.;10(4):446–451.

90. Costa T, Cotecchia S. Historical review: Negative efficacy and the constitutive activity of G-protein-coupled receptors. Trends Pharmacol. Sci. 2005 Dec.;26(12):618–624.

91. Goupil E, Laporte SA, Hébert TE. Functional selectivity in GPCR signaling: understanding the full spectrum of receptor conformations. Mini Rev Med Chem. 2012 Aug.;12(9):817–830.

92. Galandrin S, Bouvier M. Distinct signaling profiles of beta1 and beta2 adrenergic receptor ligands toward adenylyl cyclase and mitogen-activated protein kinase reveals the pluridimensionality of efficacy. Mol. Pharmacol. 2006 Nov.;70(5):1575–1584.

93. Kenakin T. Functional selectivity and biased receptor signaling. J. Pharmacol. Exp. Ther. 2011 Feb.;336(2):296–302.

94. Wei H, Ahn S, Shenoy SK, Karnik SS, Hunyady L, Luttrell LM, et al. Independent beta-arrestin 2 and G protein-mediated pathways for angiotensin II activation of extracellular signal-regulated kinases 1 and 2. Proc. Natl. Acad. Sci. U.S.A. 2003 Sep. 16;100(19):10782–10787.

95. Galandrin S, Oligny-Longpré G, Bonin H, Ogawa K, Galés C, Bouvier M. Conformational rearrangements and signaling cascades involved in ligand-biased mitogen-activated protein kinase signaling through the beta1-adrenergic receptor. Mol. Pharmacol. 2008 Jul.;74(1):162–172.

96. Kenakin T. The potential for selective pharmacological therapies through biased receptor signaling. BMC Pharmacol Toxicol. 2012;13:3.

97. Bohn LM, Lefkowitz RJ, Gainetdinov RR, Peppel K, Caron MG, Lin FT. Enhanced morphine analgesia in mice lacking beta-arrestin 2. Science. 1999 Dec. 24;286(5449):2495–2498.

98. Groer CE, Tidgewell K, Moyer RA, Harding WW, Rothman RB, Prisinzano TE, et al. An opioid agonist that does not induce mu-opioid receptor--arrestin interactions or receptor internalization. Mol. Pharmacol. 2007 Feb.;71(2):549–557.

99. Violin JD, DeWire SM, Yamashita D, Rominger DH, Nguyen L, Schiller K, et al. Selectively engaging β-arrestins at the angiotensin II type 1 receptor reduces blood pressure and increases cardiac performance. J. Pharmacol. Exp. Ther. 2010 Dec.;335(3):572–579.

100. Nobles KN, Xiao K, Ahn S, Shukla AK, Lam CM, Rajagopal S, et al. Distinct phosphorylation sites on the β(2)-adrenergic receptor establish a barcode that encodes differential functions of β-arrestin. Sci Signal. 2011 Aug. 9;4(185):ra51.

101. Keating GM. Plerixafor: a review of its use in stem-cell mobilization in patients with lymphoma or multiple myeloma. Drugs. 2011 Aug. 20;71(12):1623–1647.

102. De Clercq E, Yamamoto N, Pauwels R, Balzarini J, Witvrouw M, De Vreese K, et al. Highly potent and selective inhibition of human immunodeficiency virus by the bicyclam derivative JM3100. Antimicrob. Agents Chemother. 1994 Apr.;38(4):668–674.

103. De Vreese K, Van Nerum I, Vermeire K, Anné J, De Clercq E. Sensitivity of human immunodeficiency virus to bicyclam derivatives is influenced by the three-dimensional structure of gp120. Antimicrob. Agents Chemother. 1997 Dec.;41(12):2616–2620.

104. Hendrix CW, Flexner C, MacFarland RT, Giandomenico C, Fuchs EJ, Redpath E, et al. Pharmacokinetics and safety of AMD-3100, a novel antagonist of the CXCR-4 chemokine receptor, in human volunteers. Antimicrob. Agents Chemother. 2000 Jun.;44(6):1667–1673.

105. Liles WC, Broxmeyer HE, Rodger E, Wood B, Hübel K, Cooper S, et al. Mobilization of hematopoietic progenitor cells in healthy volunteers by AMD3100, a CXCR4 antagonist. Blood. 2003 Oct. 15;102(8):2728–2730.

106. Fruehauf S, Seeger T, Maier P, Li L, Weinhardt S, Laufs S, et al. The CXCR4 antagonist AMD3100 releases a subset of G-CSF-primed peripheral blood progenitor cells with specific gene expression characteristics. Exp. Hematol. 2006 Aug.;34(8):1052–1059.

107. De Clercq E. The AMD3100 story: the path to the discovery of a stem cell mobilizer (Mozobil). Biochem. Pharmacol. 2009 Jun. 1;77(11):1655–1664.

108. Calandra G, McCarty J, McGuirk J, Tricot G, Crocker S-A, Badel K, et al. AMD3100 plus G-CSF can successfully mobilize CD34+ cells from non-Hodgkin"s lymphoma, Hodgkin"s disease and multiple myeloma patients previously failing mobilization with chemotherapy and/or cytokine treatment: compassionate use data. Bone Marrow Transplant. 2008 Feb.;41(4):331–338.

109. Welschinger R, Liedtke F, Basnett J, Pena Dela A, Juarez JG, Bradstock KF, et al. Plerixafor (AMD3100) induces prolonged mobilization of acute lymphoblastic leukemia cells and increases the proportion of cycling

cells in the blood in mice. Exp. Hematol. 2013 Mar.;41(3):293–302.e1.

110. Uy GL, Rettig MP, Motabi IH, McFarland K, Trinkaus KM, Hladnik LM, et al. A phase 1/2 study of chemosensitization with the CXCR4 antagonist plerixafor in relapsed or refractory acute myeloid leukemia. Blood. 2012 Apr. 26;119(17):3917–3924.

111. Tamamura H, Omagari A, Hiramatsu K, Gotoh K, Kanamoto T, Xu Y, et al. Development of specific CXCR4 inhibitors possessing high selectivity indexes as well as complete stability in serum based on an anti-HIV peptide T140. Bioorg. Med. Chem. Lett. 2001 Jul. 23;11(14):1897–1902.

112. Dong S, Rogan SC, Roth BL. Directed molecular evolution of DREADDs: a generic approach to creating next-generation RASSLs. Nat Protoc. 2010 Mar.;5(3):561–573.

113. Nakashima H, Masuda M, Murakami T, Koyanagi Y, Matsumoto A, Fujii N, et al. Anti-human immunodeficiency virus activity of a novel synthetic peptide, T22 ([Tyr-5,12, Lys-7]polyphemusin II): a possible inhibitor of virus-cell fusion. Antimicrob. Agents Chemother. 1992 Jun.;36(6):1249–1255.

114. Tamamura H, Xu Y, Hattori T, Zhang X, Arakaki R, Kanbara K, et al. A low-molecular-weight inhibitor against the chemokine receptor CXCR4: a strong anti-HIV peptide T140. Biochem. Biophys. Res. Commun. 1998 Dec. 30;253(3):877–882.

115. Tamamura H, Fujii N. The therapeutic potential of CXCR4 antagonists in the treatment of HIV infection, cancer metastasis and rheumatoid arthritis. Expert Opin. Ther. Targets. 2005 Dec.;9(6):1267–1282.

116. Murakami T, Nakajima T, Koyanagi Y, Tachibana K, Fujii N, Tamamura H, et al. A small molecule CXCR4 inhibitor that blocks T cell line-tropic HIV-1 infection. J. Exp. Med. 1997 Oct. 20;186(8):1389–1393.

117. Tamamura H, Hiramatsu K, Mizumoto M, Ueda S, Kusano S, Terakubo S, et al. Enhancement of the T140-based pharmacophores leads to the development of more potent and bio-stable CXCR4 antagonists. Org. Biomol. Chem. 2003 Nov. 7;1(21):3663–3669.

118. Tamamura H, Hori A, Kanzaki N, Hiramatsu K, Mizumoto M, Nakashima H, et al. T140 analogs as CXCR4 antagonists identified as anti-metastatic agents in the treatment of breast cancer. FEBS Lett. 2003 Aug. 28;550(1-3):79–83.

119. Leduc M, Breton B, Galés C, Le Gouill C, Bouvier M, Chemtob S, et al. Functional selectivity of natural and synthetic prostaglandin EP4 receptor ligands. J. Pharmacol. Exp. Ther. 2009 Oct.;331(1):297–307.

120. Achour L, Kamal M, Jockers R, Marullo S. Using quantitative BRET to assess G protein-coupled receptor homo- and heterodimerization. Methods Mol. Biol. 2011;756:183–200.

121. Kechad A, Jananji S, Ruella Y, Hickson GRX. Anillin acts as a bifunctional linker coordinating midbody ring biogenesis during cytokinesis. Curr. Biol. 2012 Feb. 7;22(3):197–203.

122. Galés C, Van Durm JJJ, Schaak S, Pontier S, Percherancier Y, Audet M, et al. Probing the activation-promoted structural rearrangements in preassembled receptor-G protein complexes. Nat. Struct. Mol. Biol. 2006 Sep.;13(9):778–786.

123. Galés C, Rebois RV, Hogue M, Trieu P,

Breit A, Hébert TE, et al. Real-time monitoring of receptor and G-protein interactions in living cells. Nat. Methods. 2005 Mar.;2(3):177–184.

124. Bouvier M. Oligomerization of G-protein-coupled transmitter receptors. Nat. Rev. Neurosci. 2001 Apr.;2(4):274–286.

125. Loening AM, Fenn TD, Wu AM, Gambhir SS. Consensus guided mutagenesis of Renilla luciferase yields enhanced stability and light output. Protein Eng. Des. Sel. 2006 Sep.;19(9):391–400.

126. Brave M, Farrell A, Ching Lin S, Ocheltree T, Pope Miksinski S, Lee S-L, et al. FDA review summary: Mozobil in combination with granulocyte colony-stimulating factor to mobilize hematopoietic stem cells to the peripheral blood for collection and subsequent autologous transplantation. Oncology. 2010;78(3-4):282–288.

127. Kopp HG, Yildirim S, Weisel KC, Kanz L, Vogel W. Contamination of autologous peripheral blood progenitor cell grafts predicts overall survival after high-dose chemotherapy in multiple myeloma. J. Cancer Res. Clin. Oncol. 2009 Apr.;135(4):637–642.

128. Gorin N-C, Labopin M, Blaise D, Reiffers J, Meloni G, Michallet M, et al. Higher incidence of relapse with peripheral blood rather than marrow as a source of stem cells in adults with acute myelocytic leukemia autografted during the first remission. J. Clin. Oncol. 2009 Aug. 20;27(24):3987–3993.

129. Mercier J-F, Salahpour A, Angers S, Breit A, Bouvier M. Quantitative assessment of beta 1- and beta 2-adrenergic receptor homo- and heterodimerization by bioluminescence resonance energy transfer. J. Biol. Chem. 2002 Nov. 22;277(47):44925–44931.

130. Ayoub MA, Pfleger KDG. Recent advances in bioluminescence resonance energy transfer technologies to study GPCR heteromerization. Curr Opin Pharmacol. 2010 Feb.;10(1):44–52.

131. Ponsioen B, Zhao J, Riedl J, Zwartkruis F, van der Krogt G, Zaccolo M, et al. Detecting cAMP-induced Epac activation by fluorescence resonance energy transfer: Epac as a novel cAMP indicator. EMBO Rep. 2004 Dec.;5(12):1176–1180.

132. Bhat SV, Dohadwalla AN, Bajwa BS, Dadkar NK, Dornauer H, de Souza NJ. The antihypertensive and positive inotropic diterpene forskolin: effects of structural modifications on its activity. J. Med. Chem. 1983 Apr.;26(4):486–492.

133. Dong C, Li C, Wu G. Regulation of α(2B)-adrenergic receptor-mediated extracellular signal-regulated kinase 1/2 (ERK1/2) activation by ADP-ribosylation factor 1. J. Biol. Chem. 2011 Dec. 16;286(50):43361–43369.

134. Oakley RH, Hudson CC, Sjaastad MD, Loomis CR. The ligand-independent translocation assay: an enabling technology for screening orphan G protein-coupled receptors by arrestin recruitment. Meth. Enzymol. 2006;414:50–63.

135. Katzmann DJ, Odorizzi G, Emr SD. Receptor downregulation and multivesicular-body sorting. Nat. Rev. Mol. Cell Biol. 2002 Dec.;3(12):893–905.

136. Palczewski K, Kumasaka T, Hori T, Behnke CA, Motoshima H, Fox BA, et al. Crystal structure of rhodopsin: A G protein-coupled receptor. Science. 2000 Aug. 4;289(5480):739–745.

137. Auger-Messier M, Clement M, Lanctot PM, Leclerc PC, Leduc R, Escher E, et al. The constitutively active N111G-AT1 receptor for angiotensin II maintains a high affinity conformation despite being uncoupled from its cognate G protein Gq/11alpha. Endocrinology. 2003 Dec.;144(12):5277–5284.

138. Lefkowitz RJ. G protein-coupled receptors. III. New roles for receptor kinases and beta-arrestins in receptor signaling and desensitization. J. Biol. Chem. 1998 Jul. 24;273(30):18677–18680.

139. Franke RR, Sakmar TP, Graham RM, Khorana HG. Structure and function in rhodopsin. Studies of the interaction between the rhodopsin cytoplasmic domain and transducin. J. Biol. Chem. 1992 Jul. 25;267(21):14767–14774.

140. Morin D, Cotte N, Balestre MN, Mouillac B, Manning M, Breton C, et al. The D136A mutation of the V2 vasopressin receptor induces a constitutive activity which permits discrimination between antagonists with partial agonist and inverse agonist activities. FEBS Lett. 1998 Dec. 28;441(3):470–475.

141. Lagane B, Ballet S, Planchenault T, Balabanian K, Le Poul E, Blanpain C, et al. Mutation of the DRY motif reveals different structural requirements for the CC chemokine receptor 5-mediated signaling and receptor endocytosis. Mol. Pharmacol. 2005 Jun.;67(6):1966–1976.

142. Chung DA, Wade SM, Fowler CB, Woods DD, Abada PB, Mosberg HI, et al. Mutagenesis and peptide analysis of the DRY motif in the alpha2A adrenergic receptor: evidence for alternate mechanisms in G protein-coupled receptors. Biochem. Biophys. Res. Commun. 2002 May 17;293(4):1233–1241.

143. Scheer A, Costa T, Fanelli F, De Benedetti PG, Mhaouty-Kodja S, Abuin L, et al. Mutational analysis of the highly conserved arginine within the Glu/Asp-Arg-Tyr motif of the alpha(1b)-adrenergic receptor: effects on receptor isomerization and activation. Mol. Pharmacol. 2000 Feb.;57(2):219–231.

144. Rosenthal W, Antaramian A, Gilbert S, Birnbaumer M. Nephrogenic diabetes insipidus. A V2 vasopressin receptor unable to stimulate adenylyl cyclase. J. Biol. Chem. 1993 Jun. 25;268(18):13030–13033.

145. Barak LS, Oakley RH, Laporte SA, Caron MG. Constitutive arrestin-mediated desensitization of a human vasopressin receptor mutant associated with nephrogenic diabetes insipidus. Proc. Natl. Acad. Sci. U.S.A. 2001 Jan. 2;98(1):93–98.

146. Kim J, Ahn S, Ren X-R, Whalen EJ, Reiter E, Wei H, et al. Functional antagonism of different G protein-coupled receptor kinases for beta-arrestin-mediated angiotensin II receptor signaling. Proc. Natl. Acad. Sci. U.S.A. 2005 Feb. 1;102(5):1442–1447.

147. Charest PG, Terrillon S, Bouvier M. Monitoring agonist-promoted conformational changes of beta-arrestin in living cells by intramolecular BRET. EMBO Rep. 2005 Apr.;6(4):334–340.

148. García Lopez MA, Aguado Martínez A, Lamaze C, Martínez-A C, Fischer T. Inhibition of dynamin prevents CCL2-mediated endocytosis of CCR2 and activation of ERK1/2. Cell. Signal. 2009 Dec.;21(12):1748–1757.

149. Tian Y, Lee MMK, Yung LY, Allen RA, Slocombe PM, Twomey BM, et al. Differential involvement of Galpha16 in CC

chemokine-induced stimulation of phospholipase Cbeta, ERK, and chemotaxis. Cell. Signal. 2008 Jun.;20(6):1179–1189.

150. Kuang Y, Wu Y, Jiang H, Wu D. Selective G protein coupling by C-C chemokine receptors. J. Biol. Chem. 1996 Feb. 23;271(8):3975–3978.

151. Duarte RF, Shaw BE, Marín P, Kottaridis P, Ortiz M, Morante C, et al. Plerixafor plus granulocyte CSF can mobilize hematopoietic stem cells from multiple myeloma and lymphoma patients failing previous mobilization attempts: EU compassionate use data. Bone Marrow Transplant. 2011 Jan.;46(1):52–58.

152. Vose JM, Ho AD, Coiffier B, Corradini P, Khouri I, Sureda A, et al. Advances in mobilization for the optimization of autologous stem cell transplantation. Leuk. Lymphoma. 2009 Sep.;50(9):1412–1421.

153. Parra S, Bond RA. Inverse agonism: from curiosity to accepted dogma, but is it clinically relevant? Curr Opin Pharmacol. 2007 Apr.;7(2):146–150.